

UNCLASSIFIED

AD NUMBER

AD859275

LIMITATION CHANGES

TO:

Approved for public release; distribution is unlimited.

FROM:

Distribution authorized to U.S. Gov't. agencies and their contractors;
Administrative/Operational Use; JUN 1969. Other requests shall be referred to Army Aviation Materiel Labs., Fort Eustis, VA.

AUTHORITY

AMRDL ltr 23 Jun 1971

THIS PAGE IS UNCLASSIFIED

AD 859275

AD

USAALABS TECHNICAL REPORT 69-36

CONVERTIBLE FAN/SHAFT ENGINES INCORPORATING VARIABLE-PITCH FAN ROTORS

81

Dennis P. Edkins

June 1969

U. S. ARMY AVIATION MATERIEL LABORATORIES
FORT EUSTIS, VIRGINIA

CONTRACT DAAJ02-68-C-0054
GENERAL ELECTRIC COMPANY
WEST LYNN, MASSACHUSETTS



121



DEPARTMENT OF THE ARMY
U. S. ARMY AVIATION MATERIEL LABORATORIES
FORT EUSTIS VIRGINIA 23604

The research described herein was conducted by the General Electric Company under U. S. Army Contract DAAJ02-68-C-0054. This contract was carried out under the technical management of the U. S. Army Aviation Materiel Laboratories, Propulsion Division.

The report presents an evaluation of the convertible fan/shaft engine incorporating variable-pitch fan rotors as it may relate to future V/STOL propulsion systems.

This Command concurs with the conclusions and recommendations herein.

Task 1G162203D14415
Contract DAAJ02-68-C-0054
USAAVLABS Technical Report 69-36
June 1969

CONVERTIBLE FAN/SHAFT ENGINES
INCORPORATING
VARIABLE-PITCH FAN ROTORS

Final Report

By

Denis P. Edkins

Prepared by

**Aircraft Engine Technical Division, Aircraft Engine Group
General Electric Company
Lynn, Massachusetts**

for

**U. S. ARMY AVIATION MATERIEL LABORATORIES
FORT EUSTIS, VIRGINIA**

This document is subject to special export controls
and each transmittal to foreign governments or foreign
nationals may be made only with prior approval of US Army
Aviation Materiel Laboratories, Fort Eustis, Virginia 23604

SUMMARY

In July 1968, the United States Army Aviation Materiel Laboratories (USAAVLABS) awarded the Aircraft Engine Group, General Electric Company, a contract for preliminary design study of a convertible fan/shaft engine using a variable-pitch fan rotor as the key feature defining the method of achieving convertibility. The study was primarily directed toward the mechanical, aerodynamic and control system aspects of a dual-rotor high-bypass turbofan engine in which the ability to reduce fan blade pitch angle permits fan thrust to be reduced to a low value and shaft power to be provided by the low-pressure rotor for takeoff of a helicopter rotor type vehicle.

The study included the use of analytical methods to predict the fan's aerodynamic performance over the range of blade pitch angles from maximum (normal fan operation) to minimum (operation as a shaft engine); the dynamic simulation on a digital computer of the complete engine/control/rotor system for prediction and definition of the control system; and the preliminary mechanical design for the mechanism required to change fan blade pitch. The results of these three basic studies were then integrated into a complete engine preliminary design, with relatively small emphasis on the gas generator and low-pressure turbine portions of the engine. Two basic engine layouts were studied with equal emphasis: one having a drive shaft at approximately right angles to the engine centerline, with a bevel gear immediately aft of the fan rotor, and the second with a straight forward or aft drive shaft, requiring no gears but necessitating an S-shaped inlet for the more likely forward drive version.

The design requirements were for 2000 HP/engine at 6000 ft, 95° F, and 3500 lb thrust/engine at 400 knots S. L. The latter proved to be the sizing condition for the engine. The final cycle had a bypass ratio of 5.5, a fan pressure ratio of 1.44, an overall pressure ratio of 22.35, and a turbine inlet temperature of 2200° F. During shaft power operation, the fan supercharge pressure ratio is estimated at 1.29 and the "bypass ratio" at .12, with the fan running at 80% of the speed selected as maximum in the fan mode. The fan's and gas generator's exhaust areas are then 2.4 and 139% respectively of their fan mode areas. Fan parasitic power is 394 HP or 11.8% of the maximum power available at 80% speed.

A novel method was devised for fan blade retention, which permits rotation for pitch changing but involves almost pure rolling motion between the surfaces carrying the blade centrifugal load. The conventional approach, as used in variable pitch propellers (that of thrust bearings), is not feasible for the fan because of higher loads and reduced space at the blade hub. Satisfactory control and system dynamics were shown to be possible with the control mode developed.

FOREWORD

This report on convertible fan/shaft engines is submitted by the Aircraft Engine Group, General Electric Company, as required by Contract DAAJ02-68-C-0054, Task 1G162203D14415.

This seven-month study was conducted for the U. S. Army Aviation Materiel Laboratories, Fort Eustis, Virginia, under the technical cognizance of Mr. Michael Seery of the Propulsion Division. Principal Aircraft Engine Group personnel associated with the program were Messrs. A. C. Bryans, W. H. Clark, D. P. Edkins, R. C. Hickok, and N. J. Klomps.

TABLE OF CONTENTS

| | <u>Page</u> |
|------------------------------------|-------------|
| SUMMARY | iii |
| FOREWORD | v |
| LIST OF ILLUSTRATIONS | viii |
| LIST OF TABLES | xi |
| LIST OF SYMBOLS | xii |
| INTRODUCTION AND BACKGROUND | 1 |
| STATEMENT OF THE PROBLEM | 3 |
| CYCLE ANALYSIS | 6 |
| FAN AERODYNAMIC DESIGN | 28 |
| FAN MECHANICAL DESIGN | 43 |
| CONTROL MODE ANALYSIS | 56 |
| ENGINE PRELIMINARY DESIGN | 77 |
| RISK AREAS | 92 |
| CONCLUSIONS | 94 |
| RECOMMENDATIONS | 95 |
| LITERATURE CITED | 98 |
| APPENDIX | |
| Engine Performance Data | 99 |
| DISTRIBUTION | 103 |

LIST OF ILLUSTRATIONS

| <u>Figure</u> | | <u>Page</u> |
|---------------|--|-------------|
| 1 | Station Diagram | xv |
| 2 | Schematic of Variable-Pitch Fan Convertible Engine | 2 |
| 3 | Sample Time Share Computer Output | 6 |
| 4 | Effect of Pressure Ratio on Engine Performance | 7 |
| 5 | Parametric Cycle Data | 8 |
| 6 | Parametric Cycle Data | 9 |
| 7 | Cooling Flow Assumptions | 11 |
| 8 | Effect of Fan Speed and Supercharge on Shaft Power | 14 |
| 9 | Composite Aircraft Power Requirements and Availability | 15 |
| 10 | Thrust Modulation Versus Nozzle Area | 18 |
| 11 | Ungeared Engine Inlet Installation | 19 |
| 12 | Bypass Migration Schematic | 22 |
| 13 | Approximate Bypass Ratio/Core Inlet Mass Flow Ratio Relationship (Engine A) | 25 |
| 14 | Approximate Bypass Ratio/Core Inlet Mass Flow Ratio Relationship (Engine B) | 26 |
| 15 | Fan Flow Versus Rotor Restagger | 30 |
| 16 | Fan Blade Row Settings, Normal Pitch | 31 |
| 17 | Fan Blade Row Settings, Minimum Pitch | 32 |
| 18 | Incidence Versus Percentage Blade Height at Design and Restaggered Conditions | 33 |
| 19 | Incidence Versus Percentage Blade Height at Design and Restaggered Conditions | 34 |
| 20 | Incidence Versus Percentage Blade Height at Design and Restaggered Conditions | 35 |

| <u>Figure</u> | | <u>Page</u> |
|---------------|---|-------------|
| 21 | Total Pressure-Loss Coefficient Versus Percentage Blade Height | 36 |
| 22 | Stream Functions, Maximum Restagger | 37 |
| 23 | Stream Functions, Normal Pitch | 38 |
| 24 | Preliminary Design of Fan Rotor | 45 |
| 25 | Model of Variable-Pitch Principle | 47 |
| 26 | Geometric Surfaces of Blade Mechanism | 48 |
| 27 | Primary Structural Features of Blades and Disks | 49 |
| 28 | Blade Synchronizing Details | 51 |
| 29 | Blade Counterweight Details | 52 |
| 30 | Tip and Root Leakage Prevention Details | 53 |
| 31 | Blade Tip Antifretting Pad | 55 |
| 32 | Fan/Shft Engine Control Functional Block Diagram | 57 |
| 33 | Fan/Shft Engine Control System | 58 |
| 34 | Time History, Shaft to Fan Conversion, Rotor Vertical | 59 |
| 35 | Time History, Shaft to Fan Conversion, Rotor Horizontal | 62 |
| 36 | Time History, Fan to Shaft Conversion, Rotor Vertical | 65 |
| 37 | Time History, Fan to Shaft Conversion, Rotor Horizontal | 68 |
| 38 | Engine Control Scheduled Parameters | 72 |
| 39 | Computer Simulation, Control System | 74 |
| 40 | Computer Simulation, Engine Dynamics | 75 |
| 41 | Computer Simulation, Fan | 76 |
| 42 | Cross Section, Geared Engine | 79 |

| <u>Figure</u> | | <u>Page</u> |
|---------------|--|-------------|
| 43 | Cross Section, Ungeared Engine | 81 |
| 44 | Alternate Method of Pressurizing Actuators | 83 |
| 45 | Preliminary Installation Drawing, Geared Engine . . . | 85 |
| 46 | Preliminary Installation Drawing, Ungeared Engine . . | 87 |
| 47 | Sand Trajectories in Convertible Engine Fan | 91 |
| 48 | Rig, Test, Pitch Mechanism | 97 |

LIST OF TABLES

| <u>Table</u> | | <u>Page</u> |
|--------------|--|-------------|
| I | Cycle Parametric Assumptions | 10 |
| II | Preliminary Engine Performance | 16 |
| III | Sample Calculation of Transition Power Requirements | 20 |
| IV | Bypass Ratio Versus Spacing Parameter | 27 |
| V | Fan Aerodynamic Design Parameters | 39 |
| VI | Fan Design Point Performance Data - Rotor (26 Blades - Double Circular Arc) | 40 |
| VII | Fan Design Point Performance Data - Stator (38 Blades - 65 Series) | 41 |
| VIII | Fan Design Point Performance Data - Fixed Stator (38 Blades - 65 Series) | 42 |

LIST OF SYMBOLS

| | |
|---|---|
| A | area, sq ft |
| BSFC | specific fuel consumption, lb fuel/hr/SHP |
| F | thrust, lb |
| GW | gross weight, lb |
| H | core inlet height, in. |
| Δh | specific enthalpy, BTU/lb |
| ΔH | enthalpy, BTU |
| I | moment of inertia, lb-ft-sec ² |
| K | constant |
| L | length between leading edge of splitter and trailing edge of fan exit guide vane, in. |
| M | Mach number |
| N_1 | gas generator speed, RPM |
| N_2 | fan speed, RPM |
| $N/\sqrt{\theta}$ | corrected speed, RPM |
| n | number of stages |
| P | pressure, psi |
| $\Delta P_0/P_{23}^*$ | percent loss of pressure in fan exhaust duct |
| $\Delta P_B/P_3$ | percent loss of pressure in combustor |
| $\Delta P_E/P_{23}$ | tailpipe loss |
| $\Delta P_L/P_{23}$ | percent loss of pressure between fan and compressor |
| PR_C | compressor pressure ratio, P_3/P_{2C} |
| PR_F | fan pressure ratio, P_{23}/P_2 |
| $\Delta P_T/P_5$ | interturbine duct loss |
| PLA | power lever angle γ of maximum |
| Q | torque, ft-lb |
| RNI | Reynolds Number Index, non-dimensional |
| I/S | integrating operator |

• See Figure 1. Station Diagram, for definition of subscript numbers.

| | |
|-------------------|---|
| SFC | specific fuel consumption, lb fuel/hr/lb thrust |
| SHP | shaft horsepower |
| SLA | set lever angle (max N_2), $\% N_2$ |
| TLA | transition lever angle |
| T | temperature, °R |
| t | time, sec |
| V | airspeed, knots |
| W | airflow, lb/sec |
| W_{cool} | turbine cooling air, lb/sec |
| W_f | fuel flow, lb/hr |
| $W/\theta/\delta$ | corrected flow, lb/sec |
| α | rotor axis angle |
| β | bypass ratio |
| γ | ratio of specific heats, non-dimensional |
| δ | pressure, psi/14.7 (non-dimensional) |
| η | efficiency, $\%$ |
| α | temperature, °R/518.7 (non-dimensional) |
| λ | fan angle, $\%$ |
| ψ | stream function |
| ω | angular velocity, radians/sec |
| $\dot{\omega}$ | angular acceleration, radians/sec ² |

Subscripts

| | |
|------|-----------------------|
| C | compressor |
| F, f | fan |
| G | guarantee |
| g | gas generator |
| HPT | high-pressure turbine |
| I | inlet |
| L | shaft load |
| LPT | low-pressure turbine |

| | |
|----------|------------------------|
| N | net |
| P | primary |
| R | rotor |
| S | stagnation |
| T | turbine |
| Z | axial direction |

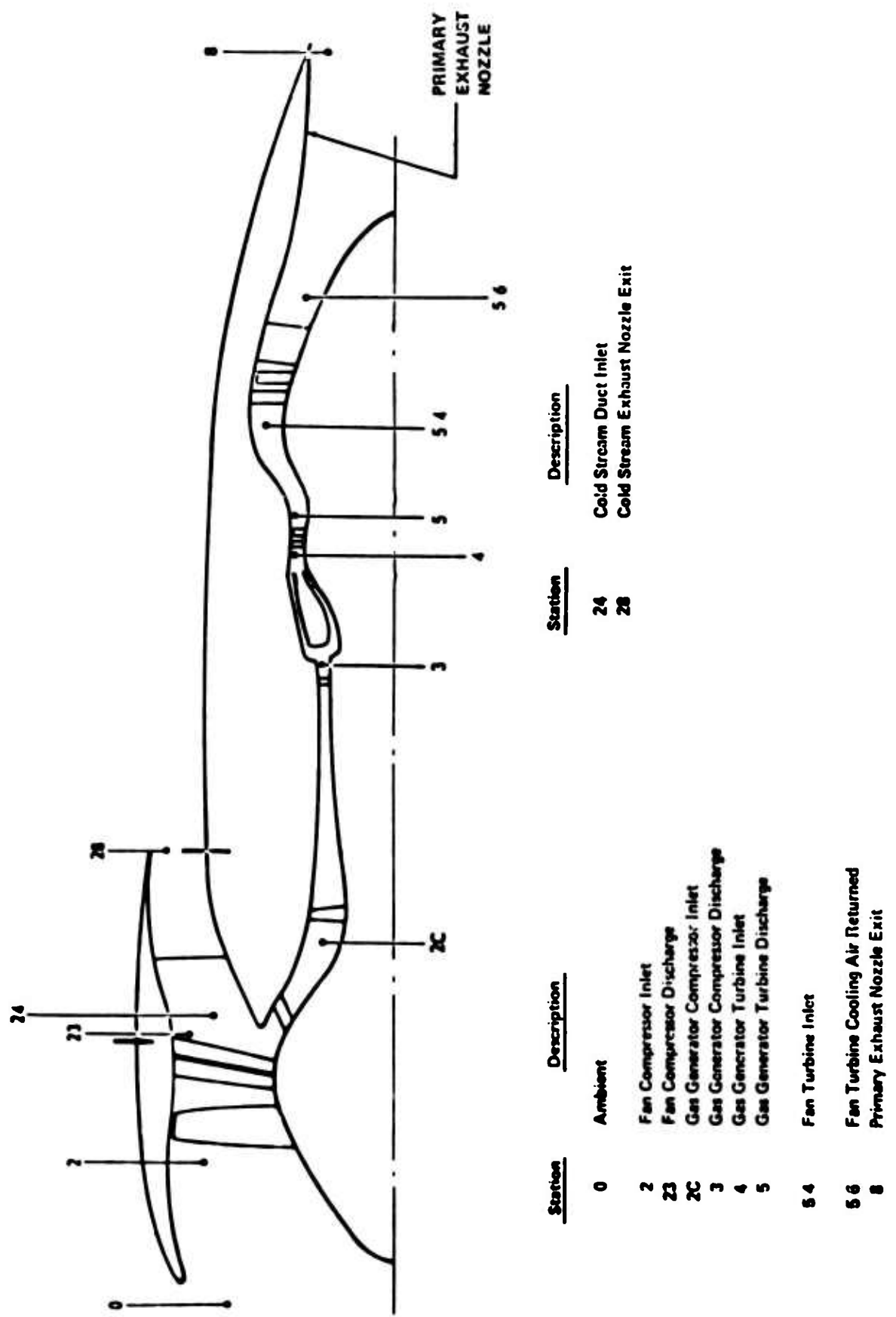


Figure 1. Station Diagram.

BLANK PAGE

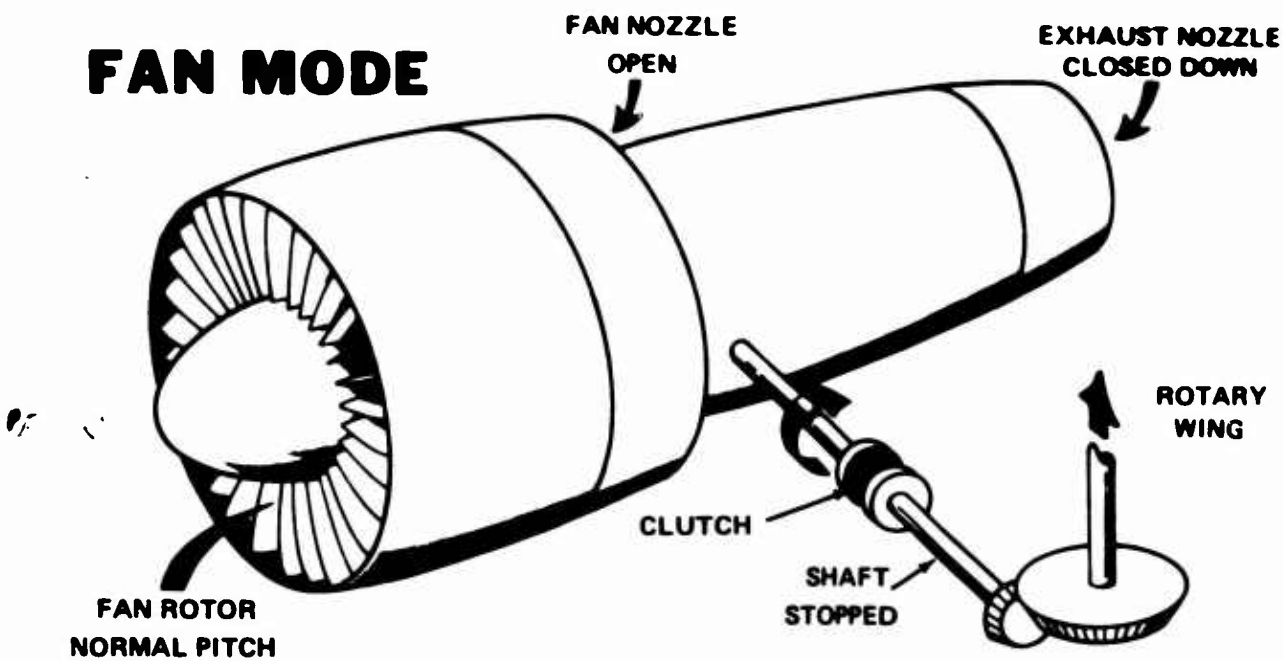
INTRODUCTION AND BACKGROUND

The U. S. Army is currently sponsoring and conducting studies on advanced V STOL systems which retain the well-known advantages and developed technology of rotary wing aircraft while obviating their drawback of inefficient forward flight and undesirable or even unacceptable flight speed limitations. These systems embody unloaded or retracted rotary wings and hence require a thrust-type propulsion system, preferably a high bypass turbofan, for cruise flight, with the same power plant system used in both the shaft and fan modes. Previous studies (1,2) have covered the broader aspects of convertible aircraft and engines; the current study is one of several aimed at arriving at one or more preferred propulsion systems. A self-explanatory schematic of the variable-pitch concept is shown in Figure 1.

It should be noted that some propulsion systems do not require specific study since they are already known state of the art thus, a convertible engine based on tip-turbine-driven cruise fans, gas diverter valves, and separate free-power turbines could be put together using technology already flight tested in the XV-5A aircraft. Reference 2 recommended closed variable fan stators plus a fan disconnect clutch as the key features of the convertible propulsion system. The fan portion of this system is the subject of a hardware test program under U.S.AAVLABS contract.

The subject study examines a related system where the fan disconnect clutch might be eliminated because the parasitic power is estimated to be lower when the fan rotor blades rather than the stators are moved into reduced pitch. This involves increased difficulty and risk in the fan mechanical design; possible increased risk in the fan aerodynamic design, depending ultimately on comparative test results; and somewhat different control system requirements.

FAN MODE



SHAFT MODE

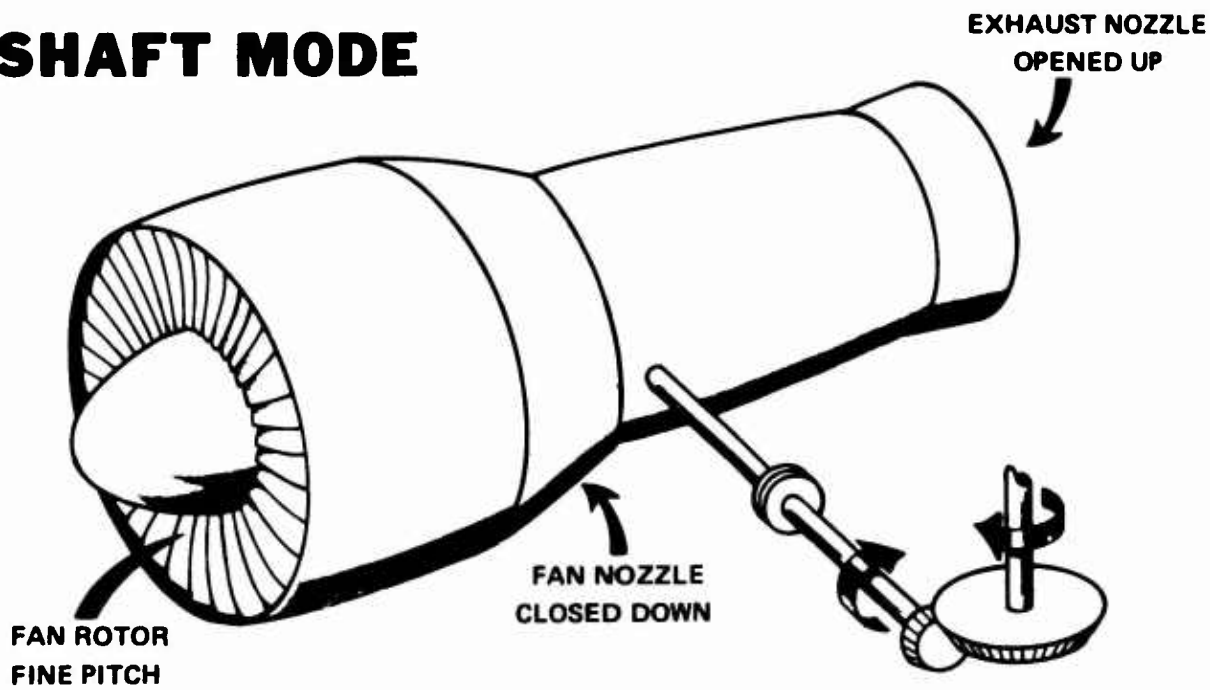


Figure 2. Schematic of Variable-Pitch Fan Convertible Engine.

STATEMENT OF THE PROBLEM

The problems associated with design and development of a variable pitch fan/shaft propulsion system are readily identified

1. Mechanical design of the variable pitch mechanism
2. Aerodynamic design and prediction of off-design (reduced pitch) aerodynamic characteristics of the fan and fan exit flow behavior
3. Control mode and engine/aircraft interface

MECHANICAL DESIGN OF THE VARIABLE-PITCH MECHANISM

Variable-pitch propeller blades are fully developed devices and at first sight, it might seem that this technology could be applied directly to a variable pitch fan blade. However, this is not so for the following reasons

- The tip speed of typical fans is appreciably higher, typically 1300 ft/sec vs 800 ft/sec in a propeller. Consequently, the centrifugal load on the blade attachment is much higher, for the area available.
- The space available for the blade attachment, which also has to provide relatively low friction rotation for pitch change, is much less because of the vastly increased blade solidity. For instance, the fan rotor in this report has 24 blades, whereas the typical propeller has 4 blades.

Simple calculations show that the largest ball thrust bearings for blade attachment that can be squeezed in are overloaded by a factor of at least 5:1. There is also the problem of providing simultaneous actuation of the fan blades. This can be expected to be relatively straightforward although obviously more complicated than in propellers.

AERODYNAMIC DESIGN OF THE FAN

The problems in this area may be categorised as:

- Behavior of the flow in the rotor as blade angle is reduced. The blockage in the flow path changes both in overall magnitude and in radial distribution. Bypass flow is greatly reduced, resulting in large radial flow components. A related problem is that of devising a suitable mathematical representation of the flow at reduced blade angles.
- Flow in the region of the splitter between the bypass and compressor ducts. Because of the radial components, the local flow near the splitter will exhibit appreciable migration of the stagnation point and stagnation streamline. Some flow separation in this region may occur unless design features are provided to prevent it.

- Angle variation of the flow entering the fan exit stator as the fan blade angle goes from design point to maximum closure. This angle variation is beyond the range capability of a fixed stator but may be within that of a stator system utilizing variable vanes.
- Prediction of the fan efficiency as the blades are closed. Once this is known, the parasitic fan power may be computed.

CONTROL MODE AND ENGINE/AIRCRAFT INTERFACE

The problems here are only in the transition flight region (≈ 140 knots flight speed), where the rotary wing has to be unloaded or brought up to speed at low load. Thus varying amounts of shaft power have to be provided, along with enough forward thrust to balance aircraft drag, itself varying because of rotary wing drag and other drag elements such as induced drag. The various phases of the transition, such as occur during fan pitch change, exhaust nozzle area change, clutch deployment, rotor acceleration, speed reset, and so on, require analysis.

The control/engine/rotor system has to be stable under various conditions of transition from one engine mode to the other, such as interruption or modification by the pilot of the normal transition process.

CYCLE ANALYSIS

GENERAL

The study of the convertible fan engine was started with an optimization of the thermodynamic cycle. It was found that the requirement for 3500 pounds of thrust at 400 knots sea level sized the engine; therefore, this flight condition was considered to be the design point, with shaft mode considered as off-design.

The optimization of the cycle for the variable-geometry fan consists of selecting T_4 , pressure ratio, and bypass ratio. This investigation was conducted on a time-sharing computer using an available two-spool nonmixed fan computer program³. A typical output printout is shown in Figure 3. This program is restricted to design point calculations, but through proper attention to effective nozzle pressure ratio, P_e/P_2 , ram conditions can be optimized. Many previous cycle investigations of fan engines have shown that the nozzle pressure ratio under ram conditions should approximate the static nozzle pressure ratio times the ram pressure ratio. This assumption has been confirmed by the GE 635 Computer in the final cycle selection. The assumptions used in the parametric study are shown on Table I.

SELECTION OF OVERALL PRESSURE RATIO

The effect of overall pressure ratio on engine performance was investigated using Reference 4 as a basis. The results of this study are shown in Figure 4. An examination of the results shows a loss in thrust associated with the SFC gain; therefore, a mission analysis would be required to identify a specific choice. However, it should be noted that the lower overall pressure ratios require higher fan pressure ratios - above the values selected for the variable-pitch fan design - to maintain the correct nozzle P_e/P_0 . An overall pressure ratio of ≈ 24 was selected for the remainder of the optimization study.

SELECTION OF BYPASS RATIO, T_4 and PR

To optimize the remaining cycle parameters, a series of T_4 with β combinations was run at the minimum-SFC overall pressure ratio. These two parameters combined with the nozzle pressure ratio dictate the fan/core pressure ratio split. The working optimization curves with the circled points representing a P_e/P_2 of 1.25 are shown as Figures 5 and 6. These curves show that a correctly exploited increase in T_4 improves performance. However, since this engine is designed around a new fan concept, unduly advanced turbine temperatures or fan aerodynamic loadings are not desirable. With these considerations and the working curves, a realistic selection of the cycle was completed.

4010 253.3,5.8,556,18.74
 4020 1.44,.84,.905,.99,0
 4030 16.6,.855,.905,.97,.99
 4040 .985,18400,.95,.995,1
 4045 2700
 4050 .105,.9,.1,0,0
 4060 400,14.7,.99,1,.995,.995,0
 4070 .99,.99,1,1,0
 RUN

NMIXF* 12:53 AEG WED08/07/68

T3
1481.00

| | | | | | |
|-------------------------|----------------------|------------------------|------------------------|-------------------------|-----------------------|
| T2 556.00 | T23 628.63 | W(CORR)2C 23.02 | P2C 26.18 | P3 434.52 | F/A BURNER .02042 |
| T4 2700.00 | TFF(4) 4.28 | DELTA H/T4 .0871 | T54 1860.81 | TFF(54) 21.75 | DELTA H/T54 .06323 |
| P54 74.46 | P8 22.82 | A8 124.68 | T8 1435.47 | P28 26.72 | A28 385.66 |
| VJET PRIMARY 1424.68 | V JET FAN 1083.55 | F GROSS PRI 1679.59 | F GROSS FAN 7276.06 | INLET AIRFLOW 253.30 | |
| BYPASS RATIO 5.80 | F NET PRI 897.86 | F NET FAN 2742.04 | NET THRUST 3639.90 | SFC .6732 | |

Figure 3. Sample Time Share Computer Output.

CONVERTIBLE FAN ENGINE STUDY

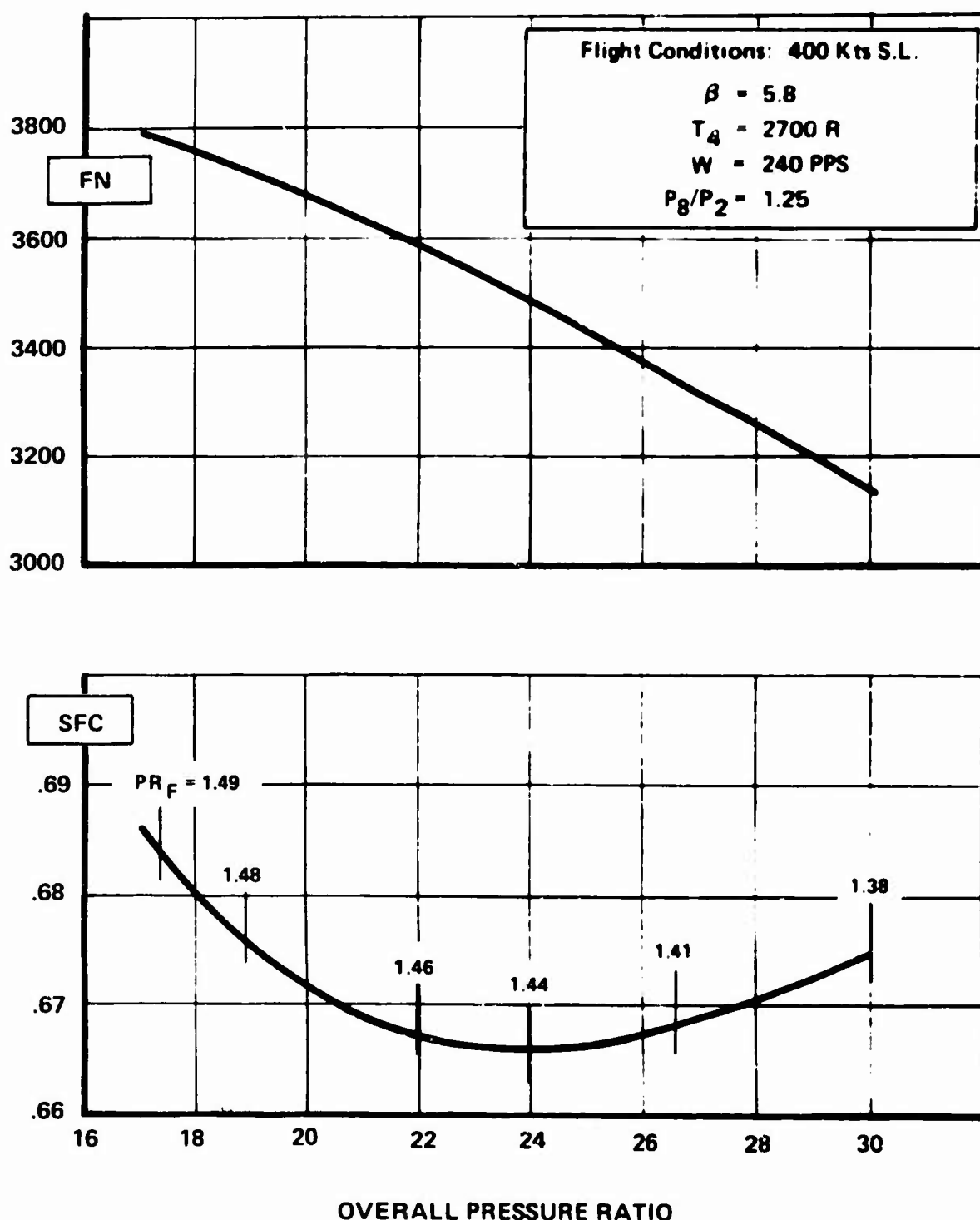


Figure 4. Effect of Pressure Ratio on Engine Performance.

• REPRESENTS $P_8/P_2 = 1.25$

A,B,C,D Lettered Points are Optimization Steps

Discussed in Text

FLIGHT CONDITION ~ 400 Kts., S.L.

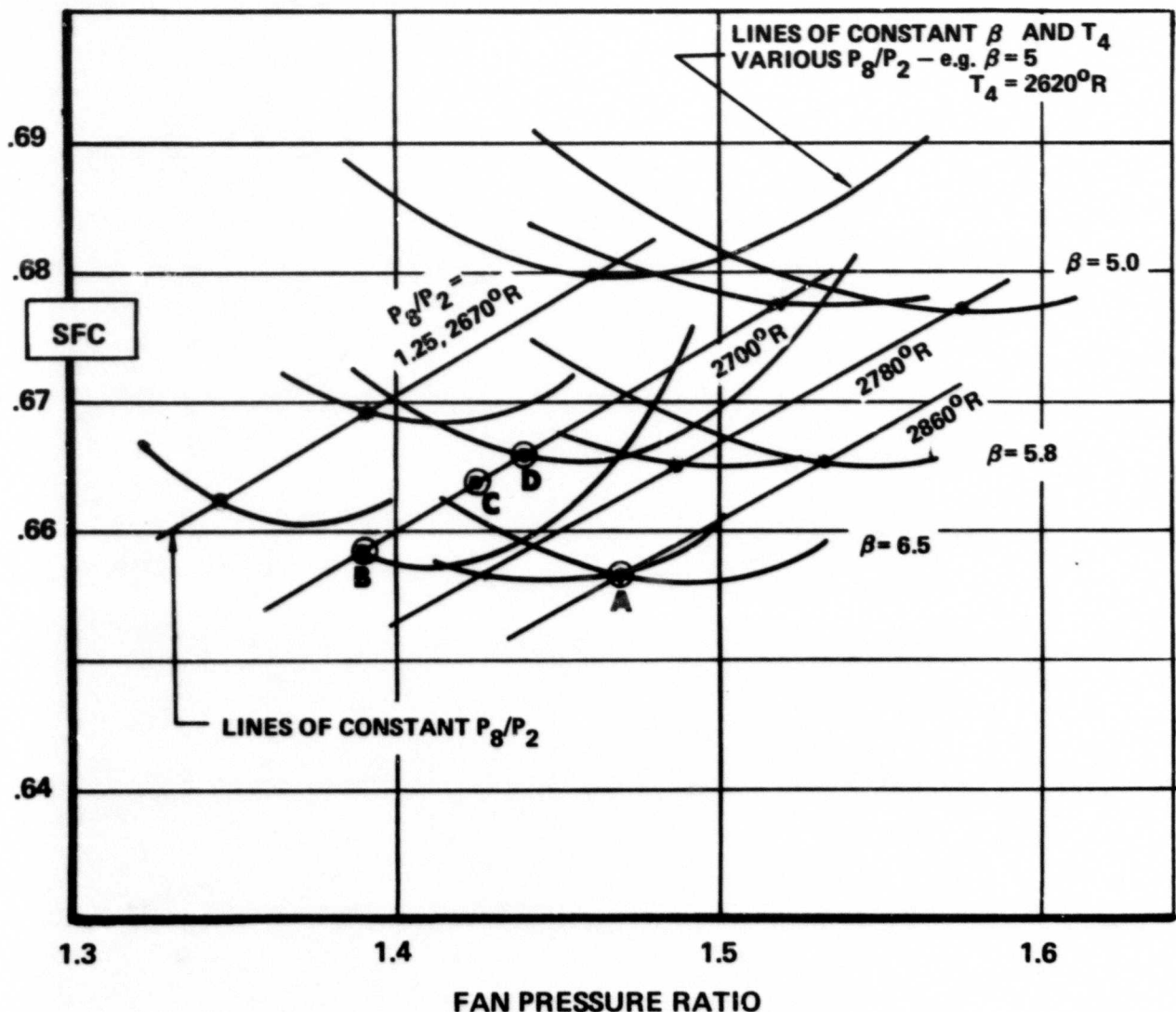


Figure 5. Parametric Cycle Data.

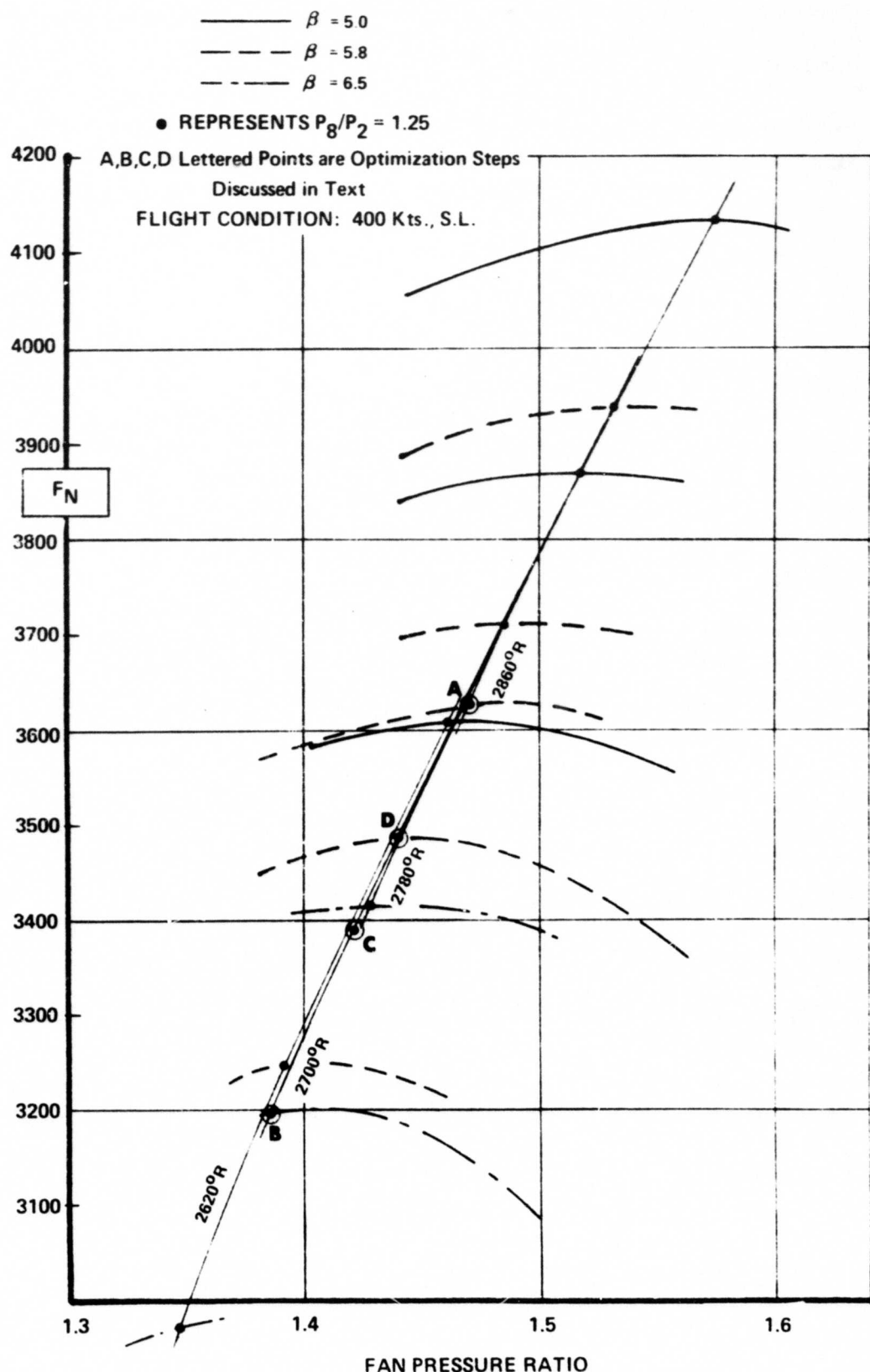


Figure 6. Parametric Cycle Data.

TABLE I. CYCLE PARAMETRIC ASSUMPTIONS

1. Inlet airflow - 240 lb/sec
2. Compressor efficiency was compatible with current General Electric high stage loading compressor technology. Above an overall pressure ratio of 24, efficiency varied with compression ratio at a constant polytropic efficiency
3. High pressure turbine efficiency - 905
4. Low pressure turbine efficiency - 905
5. Combustor efficiency - 985
6. Fuel heating value - 18400 BTU/lb
7. $\Delta P_L/P_{s3}$ 39
8. $\Delta P_o/P_{s3}$ 19
9. $\Delta P_B/P_s$ 57
10. $\Delta P_T/P_o$ 19
11. $\Delta P_E/P_o$ 19
12. P_o/R_s 1.25
13. Turbine cooling flows are extracted at the compressor discharge
14. Turbine cooling varied with T_s and T_o as shown in Figure 7
15. Cooling flows do no work in the turbine that they cool.
16. Average values of SFC, BSFC, F_N , and SHP were used throughout the optimisation. The final engine was then sized to represent the following

| | |
|-------------------------------------|-------|
| Guarantee level multiplier on SHP | 1.104 |
| Guarantee level multiplier on BSFC | 1.04 |
| Guarantee level multiplier on F_N | 1.104 |
| Guarantee level multiplier on SFC | 1.04 |

 These values are determined from numerous previous analyses of engine performance sensitivity to component variations and are appropriate to the temperature and pressure ratio levels used
17. Variable A_0 to provide for the low nozzle pressure ratio in the shaft mode

TOTAL COOLING FLOW = HIGH PRESSURE COOLING FLOW
 + LEAKAGE AND LOW PRESSURE TURBINE COOLING FLOW
 LEAKAGE AND LOW PRESSURE TURBINE = 4%

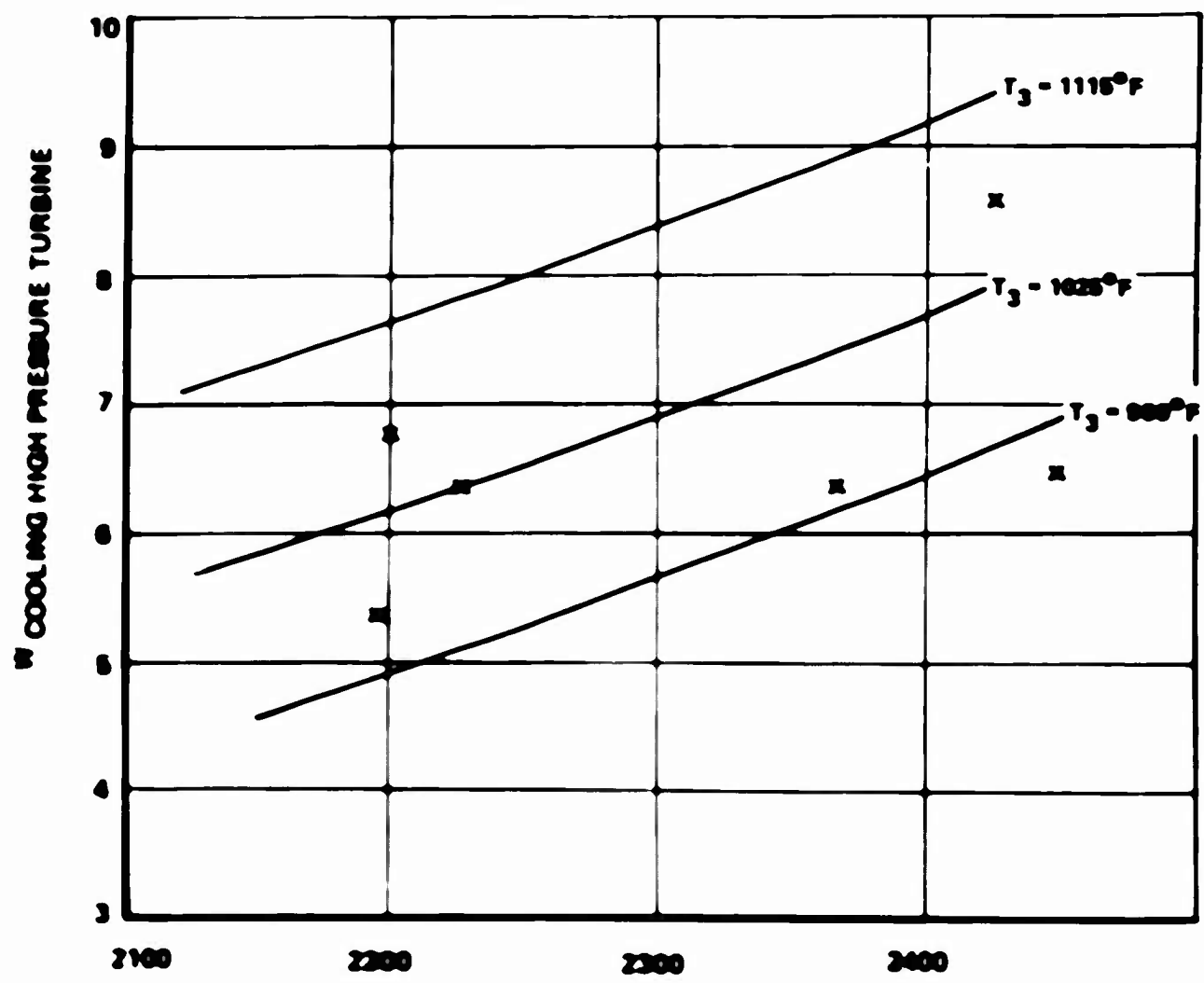


Figure 7. Cooling Flow Assumptions

Several steps of the optimization process are shown below:

Point A. Minimum SFC Point

T_4 = 2860 °R
 β = 6.5
 PR_F = 1.47
 PR_C = 16.25
SFC = .656
 F_N = 3625
 W_2 = 240 pps

Comments: This T_4 is too high, but the data provide a good basis for comparing future points.

Point B. Minimum SFC Point

T_4 = 2700 °R
 β = 6.5
 PR_F = 1.388
 PR_C = 17.25
SFC = .658
 F_N = 3200
 W_2 = 240 pps
 ΔSFC from A = + .57
 ΔF_N from A = - 11.77

Comments: Good T_4 , but high sacrifice to keep low SFC

Point C Lower Bypass Design

T_4 = 2700 °R
 β = 6
 PR_F = 1.42
 PR_C = 16.9
SFC = .6635
 F_N = 3395
 W_2 = 240 pps
 ΔSFC from A = + 1.173
 ΔF_N from A = - 6.57

Comments: Still a high loss in F_N for a small loss in SFC

Point D. Lower Bypass Design

$T_4 = 2700^{\circ}\text{R}$

$\beta = 5.8$

$\text{PR}_F = 1.44$

$\text{PR}_C = 16.6$

$\text{SFC} = .666$

$F_N = 3485$

$W_2 = 240 \text{ pps}$

$\Delta \text{SFC} \text{ from A} = + 1.57\%$

$\Delta F_N \text{ from A} = - 3.92\%$

Comments: A good preliminary selection for fan pressure ratio for the variable-geometry fan and a reasonable compromise in F_N and SFC.

The results of the study show that the 2700°R turbine with a $\beta = 5.8$ and a fan pressure ratio of 1.44 is a good compromise for performance and a normal risk mechanical design.

FINAL CYCLE

Simultaneous study of the gas generator aerodynamic design revealed that an axial-centrifugal compressor arrangement is desirable to avoid small airfoil sizes at the back of the compressor. This choice requires a deviation from the optimum shown in Figure 4 because of the characteristics of the axial-centrifugal compressor and the requirement to operate in both the fan and the shaft mode. This new cycle, which lowers overall bypass and pressure ratio, will have higher thrust per pound of air, but a slightly higher SFC than the optimum described above. However, without a mission study, the optimum cycle pressure ratio for the system cannot be determined, but it would appear that the optimum operating condition would not be at the minimum SFC point. The design point engine performance is shown in Table II, while a complete performance bulletin is included in the Appendix.

SHAFT MODE OPERATION

Due to the requirement for 400 knots at sea level, the cycle has 52% more horsepower than that required at 6000 ft, 95°F day. A portion of this margin is supplied by the fan supercharge to the core. The fan in fine pitch is operating at a 20% reduction in design speed and a large reduction in flow to eliminate fan thrust and to reduce parasitic power, while maintaining a pressure ratio of 1.29. This supercharge provides the core with an additional 24% power, which after allowing for guarantee power margin, parasitic fan power and reduced low-pressure turbine power resulting from the reduced speed, permits operation at lower T_4 . The reduced speed also provides a lower output speed in the rotary wing mode, with consequent reduction in gear ratio. Figures 8 and 9 show the shaft power breakdown. Figure 8

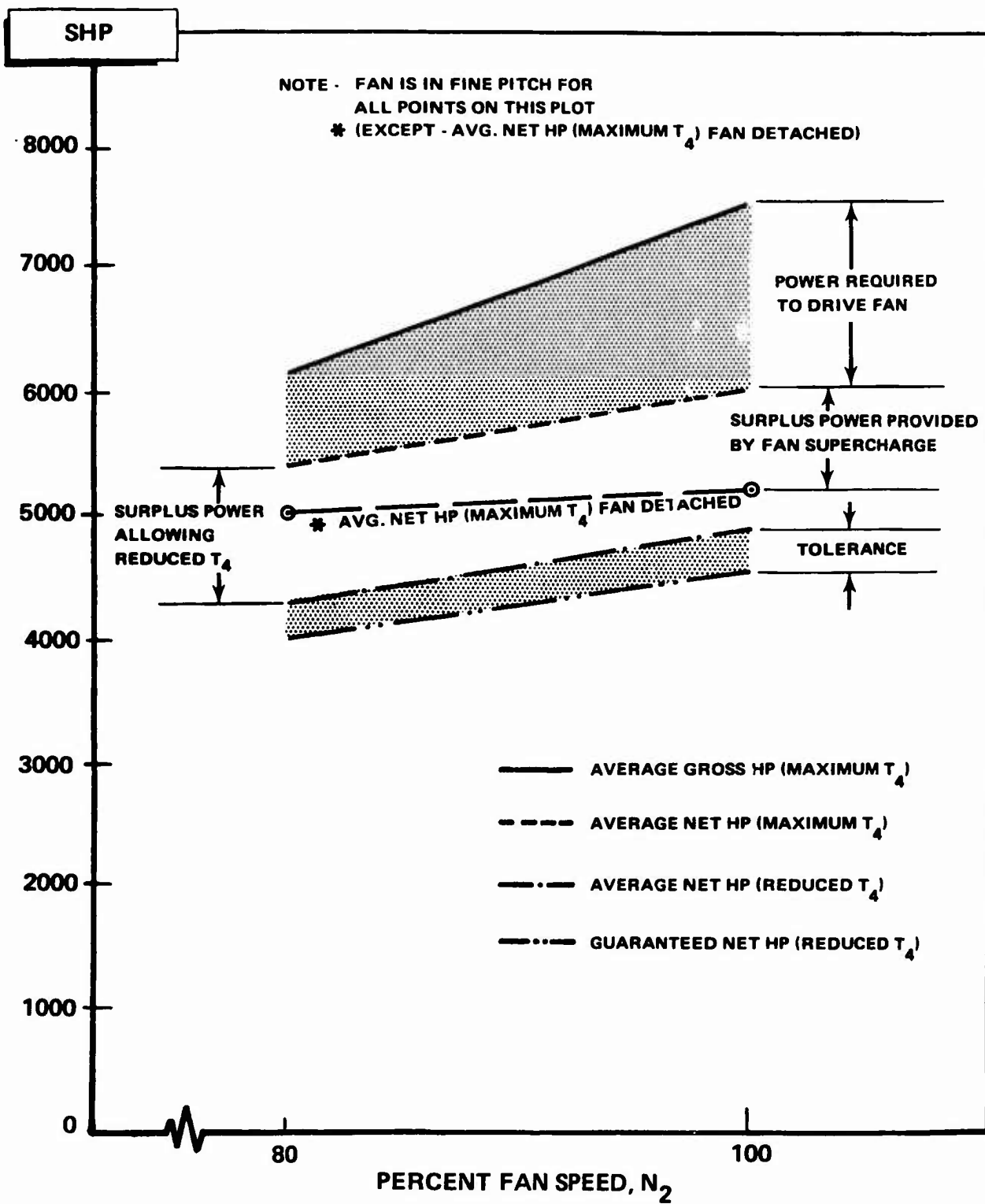


Figure 8. Effect of Fan Speed and Supercharge on Shaft Power.

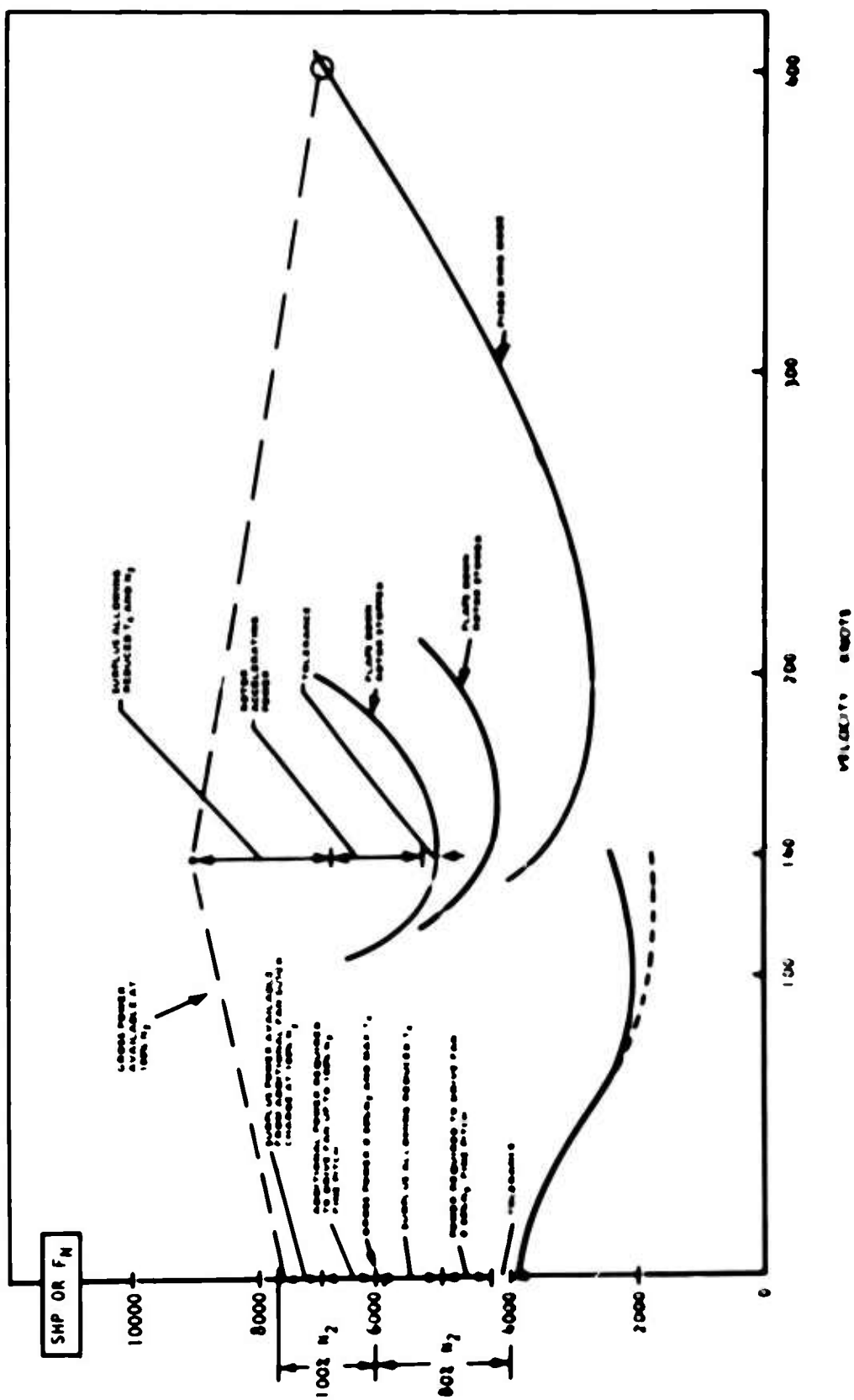


Figure 9 Commercial Aircraft Power Requirements and Availability

TABLE II. PRELIMINARY ENGINE PERFORMANCE

| Flight Condition | Cruise 400 Kts. Sea Level | Shaft Static, 6000 Ft., 95°F |
|--|------------------------------|---------------------------------|
| Total Flow (lb/sec) | 248 | 22.81 |
| Fan Pressure Ratio | 1.44 | 1.297 |
| η Fan (adiabatic) | .84 | .84 |
| Number of Fan Stages | 1 | 1 |
| Transition Duct Pressure Loss (%) | 3 | 2.2 |
| Bypass Ratio | 5.5 | .12 |
| Corrected Flow, Compressor (lb/sec) | 23.5 | 21.75 |
| η Compressor (adiabatic) | .83 | .831 |
| Number of Compressor Stages | 5 + 1 | 5 + 1 |
| Compressor Pressure Ratio | 16.0 | 14.3 |
| Overall Pressure Ratio | 22.35 | 18.14 |
| Burner Pressure Loss (%) | 4 | 4 |
| Burner Efficiency | .985 | .985 |
| Turbine Inlet Temperature (°R) | 2700 | 2455 |
| Δh Gas Generator Turbine (BTU/lb) | 240.7 | 219 |
| η Gas Generator Turbine | .905 | .905 |
| Fan Turbine Inlet Temperature (°R) | 1849 | 1665 |
| Δh Fan Turbine (BTU/lb) | 112.67 | 88 |
| η Fan Turbine | .905 | .887 |
| Exhaust Temperature (°R) | 1442 | 1342 |
| Cooling Flow (%) | 10.5 | 10.5 |
| High Pressure Spool Speed (RPM) | 26980 | 25600 |
| Low Pressure Spool Speed (RPM) | 8120 | 6496 |
| Net Thrust (lb) _G (= $F_N \times 1/1.04$) | 3500 | 475 |
| SFC _G (= SFC $\times 1.04$) | .711 | - |
| Shaft Horsepower _G (= SHP $\times 1/1.08$) | - | 2000 |
| Parasitic Horsepower | - | 394 |
| BSFC _G (= BSFC $\times 1.04$) | - | .544 |
| Exhaust Area, Gas Generator | 129.4 | 180 |
| Exhaust Area, Fan | 369.3 | 8.8 |

shows the variation of power versus N_2 , including the effect of the fan supercharge, illustrated by the hypothetical case of operation with the fan removed. Figure 9 shows the shaft power and the turbofan mode thrust versus flight speed in relation to the power and thrust requirements of the reference convertible aircraft. The upper line, of the roof-top shape, shows the gross power or thrust available and illustrates the fact that the 400-knot sea

level case sizes the engines. Since the shaft mode is not the sizing point, the shaft version of the optimum engine was the only shaft engine studied.

TRANSITION

In convertible aircraft the conversion sequence from rotary wing to fixed wing flight consists of unloading the rotor by transferring lift to the fixed wing, slowing down and stopping the rotor and finally, folding and stowing the rotor. Reconversion consists of unstowing and unfolding the rotor, acceleration of the rotor (either by aerodynamic means or by applying engine torque) and transfer of lift from the wing to the rotor. For applications where the aircraft will use a conventional horizontal helicopter rotor configuration, the engine will be required to provide rotor accelerating power as well as the 2600 pounds of thrust specified in Reference 5. A sample calculation, Table III, shows a requirement of approximately 1000 HP to accelerate the rotor to full speed in 15 seconds. Again, even with this additional power requirement, the engine has surplus power and will be operating at reduced T_4 . For the case of aircraft operating with rotors that can be accelerated through aerodynamic means, the engine will be even more over-powered in the transition mode (see Figure 9).

In discussions with airframe companies and with USAAVLABS personnel during the contract period, the point was made that thrust modulation is required during transition. This is because of variations in drag encountered as the rotor is unloaded, stopped, folded, and stowed during conversion. Two ways to accomplish this thrust variation are to modulate A_g and to run intermediate fan pitch settings. A study has been made to determine how the thrust varied with A_g . It was found that the T_4 , A_g , and speed combination necessary to provide the specified transition thrust (2600 pounds) gave such a reduced power level that it provided minimal capability for further thrust reduction. This is shown by point A on Figure 10. A possible solution would be to reduce shaft speed further, which would require a decreased A_g and increased T_4 . This higher power setting would effectively locate the 2600-pound thrust condition in a more sensitive portion of the thrust/ A_g curve, point B, which consequently allows a lower thrust capability as A_g is increased and T_4 is reduced. It appears that the capability for approximately 30% thrust decrease is possible. Intermediate fan pitch settings can also provide thrust control through reduced fan airflow. Naturally, the engine controls would be more complicated in order to handle the intermediate fan settings, but this method is completely feasible.

INSTALLATION EFFECTS

The engine can be provided with a side drive, aft drive, or front drive. The front drive for engine installations, requiring an S-shaped duct, Figure 11, is estimated to cause a 3% loss in inlet pressure at the 400-knot sea level flight condition. For the study engine, the loss is equivalent to 6.3% reduction in

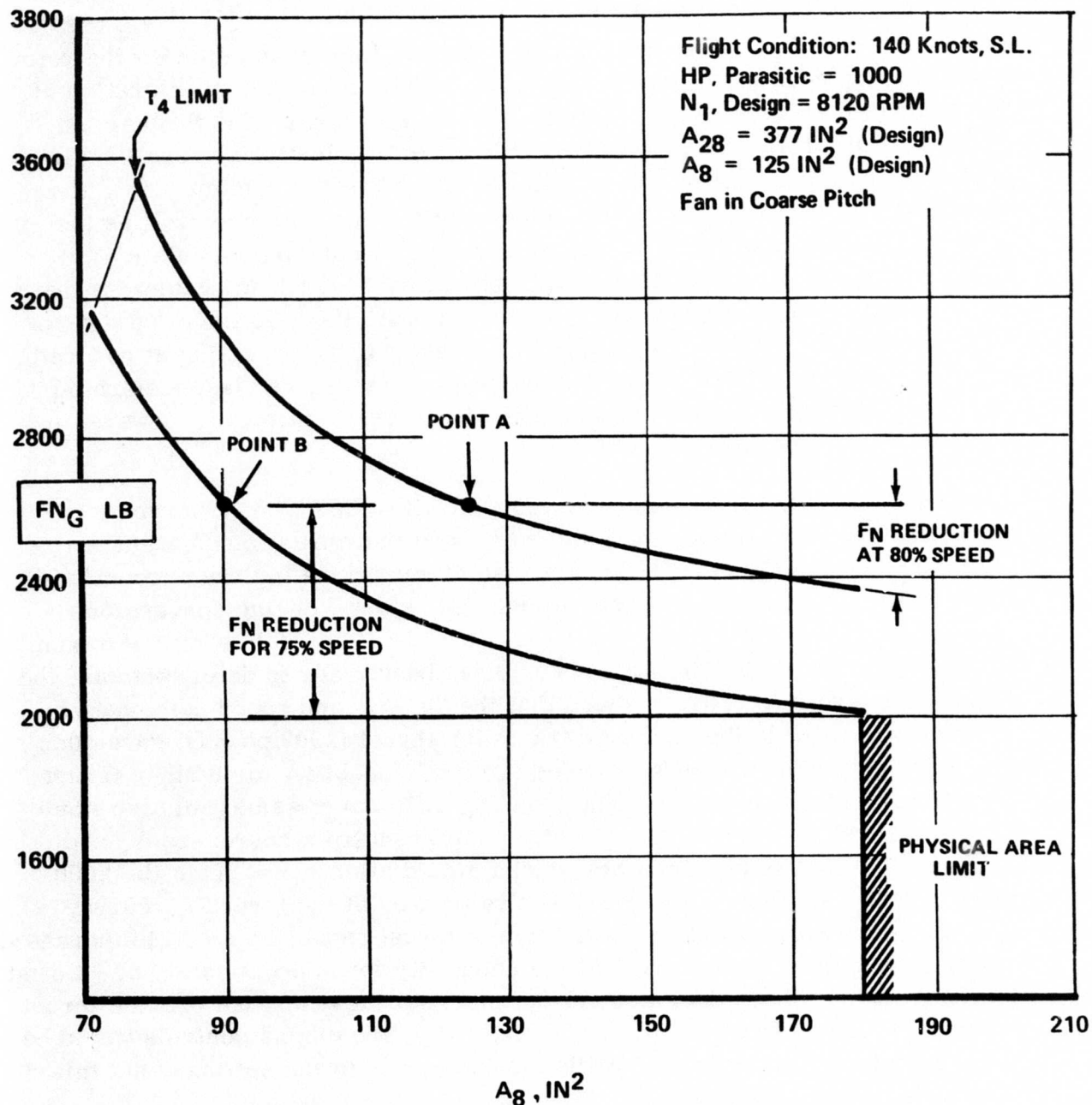


Figure 10. Thrust Modulation Versus Nozzle Area.

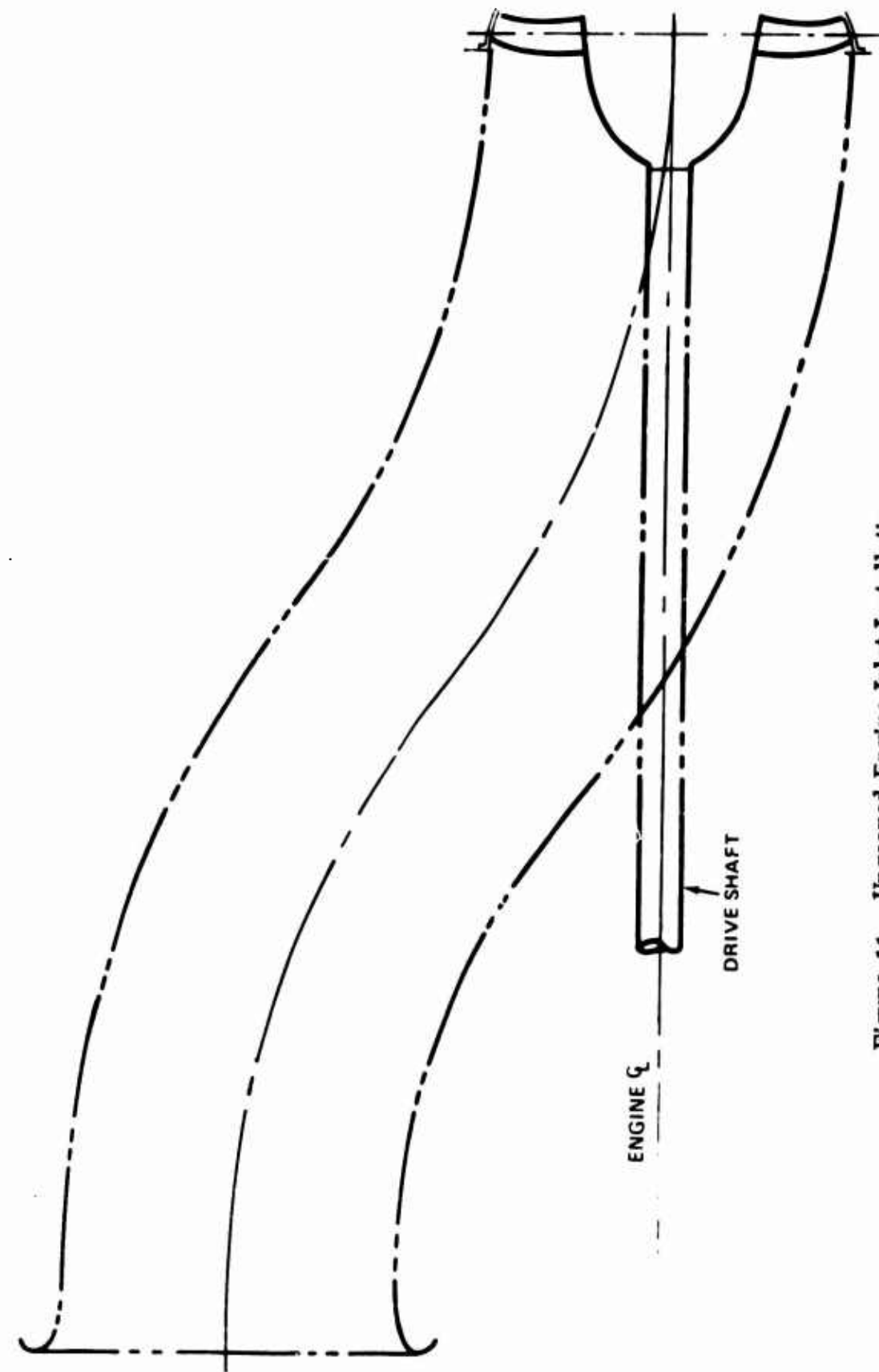


Figure 11. Ungearred Engine Inlet Installation.

F_N and 6.6% increase in SFC. This would require an engine weight flow increase of 6.3% to maintain the 3500 lb thrust and a total weight increase of 7.3%. It should be noted that the inlet size in relation to the shaft mode airflow is very large; therefore, this increase in engine size is applicable only where basic sizing is in the fan mode. If, for instance, rotor disk loading were to be increased to the point where shaft power was limiting, the difference in engine sizing between geared and ungeared installations would be negligible because inlet losses in both cases would be at the same low value.

TABLE III. SAMPLE CALCULATION OF TRANSITION POWER REQUIREMENTS

ASSUMPTIONS:

| | | |
|------------------|---|---|
| GW/SHP | = | 5 |
| GW/A | = | 15 |
| GW _R | = | .1 GW (concentrated at half the radius) |
| SHP | = | 4000 (2 engines) |
| Vel Rotor Tip | = | 650 ft/sec |
| SHP _p | = | 3 SHP (proportional to ω^3) |
| t | = | desired time to accelerate rotor = 15 to 20 sec |

CALCULATIONS:

| | | |
|-------------------|---|---|
| GW | = | 5 x 4000 = 20000 lb |
| A | = | 20000/15 = 1333.3 ft ² |
| Diag _R | = | $[1333.3 / .785]^{1/2} = 41.2$ ft |
| R _R | = | 20.6 ft |
| GW _R | = | .1 x 20000 = 2000 lb |
| I _R | = | MR ² |
| R | = | R _R /2 = 10.3 |
| I _R | = | (2000/32.2) x (10.3) ² = 6589.4 lb ft sec ² |
| ω | = | V/R = 650/20.6 = 31.55 rad/sec |
| N | = | 60/2 π x 1 = 60/2 π x 31.55 = 301.4 RPM |
| SHP _p | = | 3 x 4000 = 1200 |

$Q_{\text{required for transition}} = Q_{\text{parasit}} + Q_{\text{accelerate}}$

TABLE III - Continued

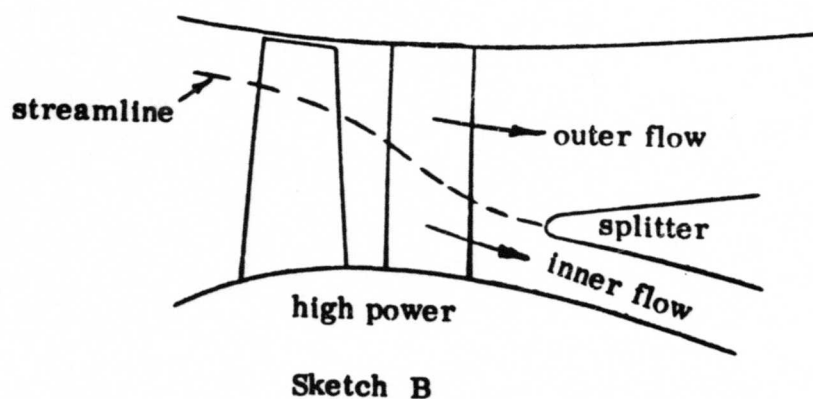
| | | | |
|------------|---|---|--|
| where | SHP_p | = | $K\omega^2$ |
| or | Q_p | = | $550 K \omega$ |
| | K | = | $1200/(31.55)^2 = 1.205$ |
| | Q_p | = | $663 \omega \text{ ft lb}$ |
| and | Q_a | = | $I \dot{\omega} = 6589.4 \dot{\omega}$ |
| and | Q_{required} | = | $SHP_T \times 550/\omega = SHP_T \times 550/31.55$ |
| | | = | $17.43 SHP_T$ |
| therefore | $6589.4 \dot{\omega} + 663 \omega = 17.43 SHP_T$ | | |
| integrate | $6589.4 \omega + 331.5 \omega^2 = 17.43 SHP_T t + K_1$ | | |
| | but at $t = 0$ $\omega = 0$, therefore $K_1 = 0$ | | |
| substitute | $\omega = 31.55 \text{ rad/sec}$, $t = 15 \text{ sec}$ | | |
| | $207895.6 + 329975.9 = 261.45 SHP_T$ | | |
| | $537871.5 = 261.45 HP_T$ | | |
| | $SHP_T = 2057 \text{ (2 engines)}$ | | |
| for | t | = | 20 sec |
| | 537871.5 | = | $348.6 SHP_T$ |
| | SHP_T | = | 1543 (2 engines) |

BYPASS MIGRATION

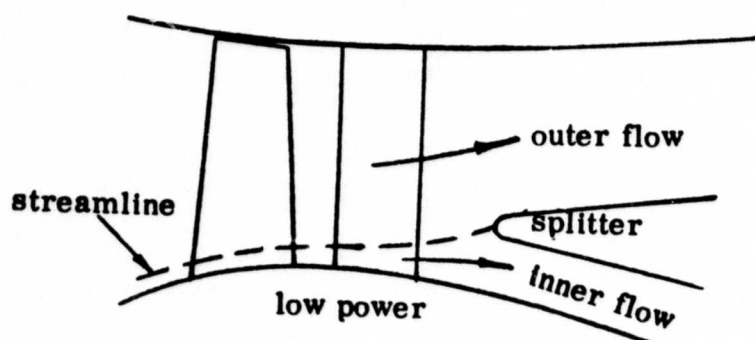
The convertible fan engine with a bypass ratio of 5.5 will have some bypass migration as in the case of any turbofan engine. But the long space between the fan and compressor for the variable-pitch mechanism should provide good migration characteristics.

The engine must contend with two types of bypass migrations, shown in Figure 12.

When the low-pressure rotor is running at high speed, with the fan in normal pitch and with the gas generator operating at low power, the bypass ratio can migrate to an extreme value about 2-1/2 times design value. Although this type of migration is common in turbofan engines operating successfully at part-power ram conditions, it could be the cause of stall at the root of the fan stator. The second migration possibility occurs when the fan is in fine pitch and the gas generator is running at high power. In this case, the gas



Sketch B



Sketch A

Figure 12. Bypass Migration Schematic.

generator is requiring most of the flow that the fan is pumping. The associated possibility of stator tip stall is not as critical because the fan thrust is not wanted, and the streamline shift is less likely to affect the gas generator because the entering flow is accelerating and thus is more stable. The possibility of physical damage at the tip due to this stall is essentially nonexistent because of the low level of energy input and because of the rugged structure of this area. In both cases, A_{28} will be varied to keep the fan on its operating line. This second mode of bypass migration is the important one to understand and analyze in the convertible engine, since the extent of migration is more severe than would be experienced in a turbofan with fixed-pitch fan blades. This mode of migration has been studied as part of the fan aero-dynamic design. Several methods are available to circumvent any problem that may be revealed. The most likely problem region is that due to high angle of attack at the splitter. The methods available are:

1. Increased radius of curvature of the splitter nose to provide greater angle-of-attack tolerance.
2. A bleed port between the fan exit duct inner wall and the compressor inlet duct, which would reduce the angle of attack.
3. Increased spacing between the stators and the splitter. This spacing is already large, as discussed in the following paragraphs.

When the gas generator is operated at reduced speed and flow while the fan is still operating at full speed and low pitch, the migration mode of Sketch B, Figure 12, is changed in the direction toward the Sketch A mode; thus the extreme case of mode B is that of takeoff power.

Bypass migration experience with both fan components and turbofan engines is available. From test data for these machines, the following observations have been made:

- The important parameters for determining the seriousness of the effects of bypass ratio migration are the spacing parameter (distance between splitter leading edge and last vane trailing edge) and the core inlet mass flow ratio (related to bypass ratio).
- For the values of spacing parameter shown in Table IV, the effects of bypass migration on fan stall are essentially negligible. The convertible fan should be especially insensitive because of the large spacing.
- Locating fan blading too near the leading edge of the splitter will result in the "inlet analogy" adverse pressure gradient and possibly separation propagation upstream into the fan blading in the hub region which may already be heavily loaded. This results in a magnified core inlet velocity profile deterioration and a loss in fan stability.

The problems that arise from bypass migration can be explained as follows: As bypass ratio increases, the core inlet mass flow decreases. A pressure gradient, as in the case of the scoop inlet, propagates upstream of the splitter lip a distance of several inlet heights. This adverse gradient causes boundary layer thickening or separation. If the blading is located too near the splitter the adverse gradient will feed upstream through the hub region. In most cases this region of the blade is already highly loaded, and the additional back pressure will initiate stall. Similarly, this can happen at the blade tip, but for the fine pitch mode this is of little importance.

A listing of typical full-scale vehicles and engines is shown in Table IV, with the convertible engine for comparison. A sampling of the data that shows the effect of spacing parameter is shown in Figures 13 and 14. Figure 13 shows the velocity profile into the core compressor for the engine as bypass ratio varies, assuming the bypass/ flow-rate variation shown. Figure 14 is the comparable curve for engine B. The major difference in the design of the two systems is the spacing parameter, .609 and 1.4 respectively. Examination of the plots will show that the profile for engine B, even though it has a more severe bypass migration, is better than the profile for engine A. For constant spacing parameter, it would be expected that a high bypass ratio machine would be more susceptible to profile distortion with core inlet mass flow rate reduction, because a greater percentage of the core flow consists of boundary layer. Engine B design bypass ratio is four times that for engine A, so that if spacing were not important, engine B should have more distortion. For the convertible fan engine, the spacing parameter for the geared and ungeared version is 3.9 and 3.0 respectively. These values are much larger than for any of the listed engines.

| | $\%N_1/\sqrt{\theta}$ | $\%N_2/\sqrt{\theta}$ | β |
|---|-----------------------|-----------------------|---------|
| △ | 100.1 | 98.6 | 1.85 |
| ◇ | 87.5 | 95.8 | 1.89 |
| □ | 82.6 | 94.5 | 2.08 |
| ○ | 38.4 | 72.7 | 3.62 |

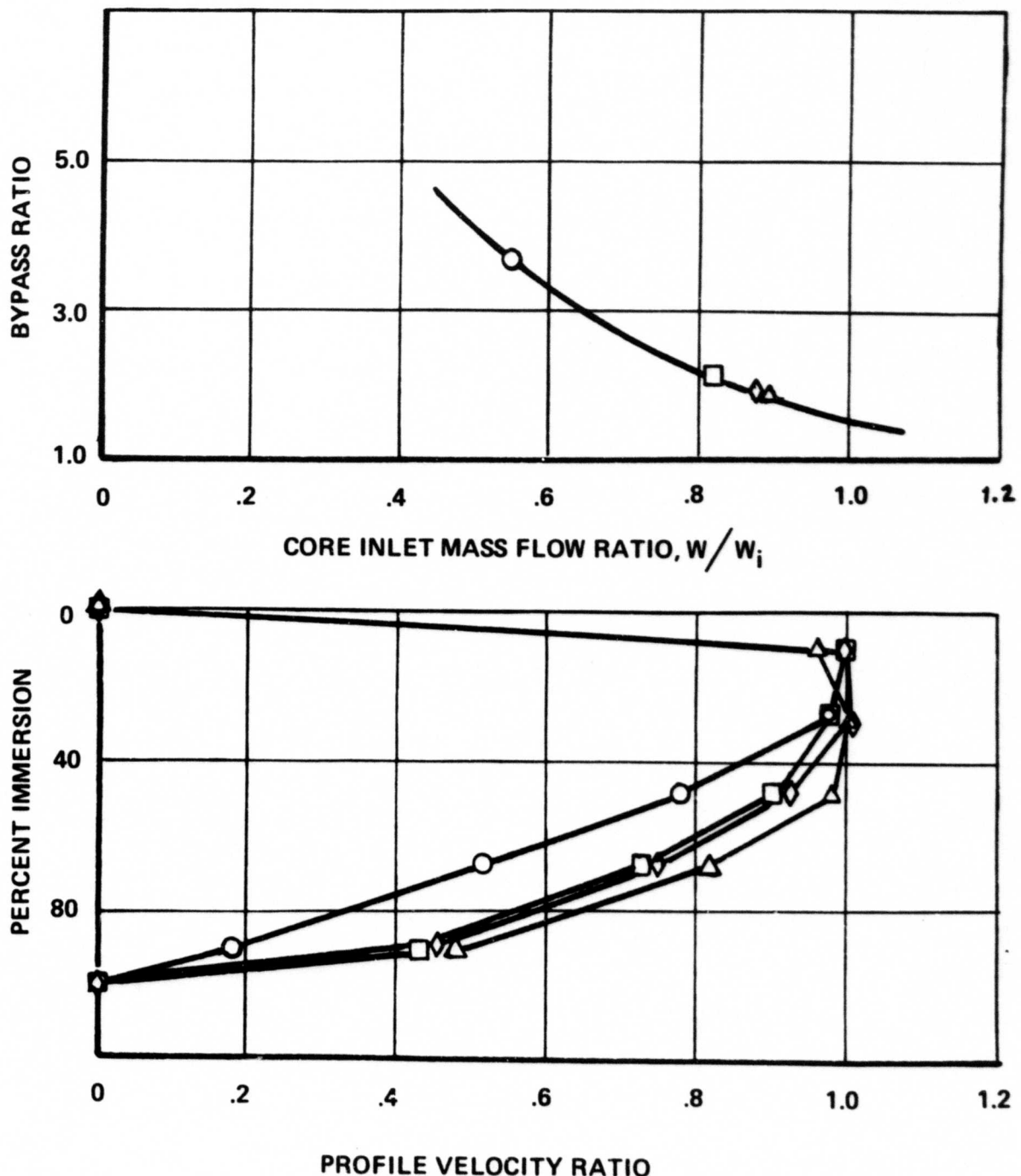


Figure 13. Approximate Bypass Ratio/Core Inlet Mass Flow Ratio Relationship (Engine A) .

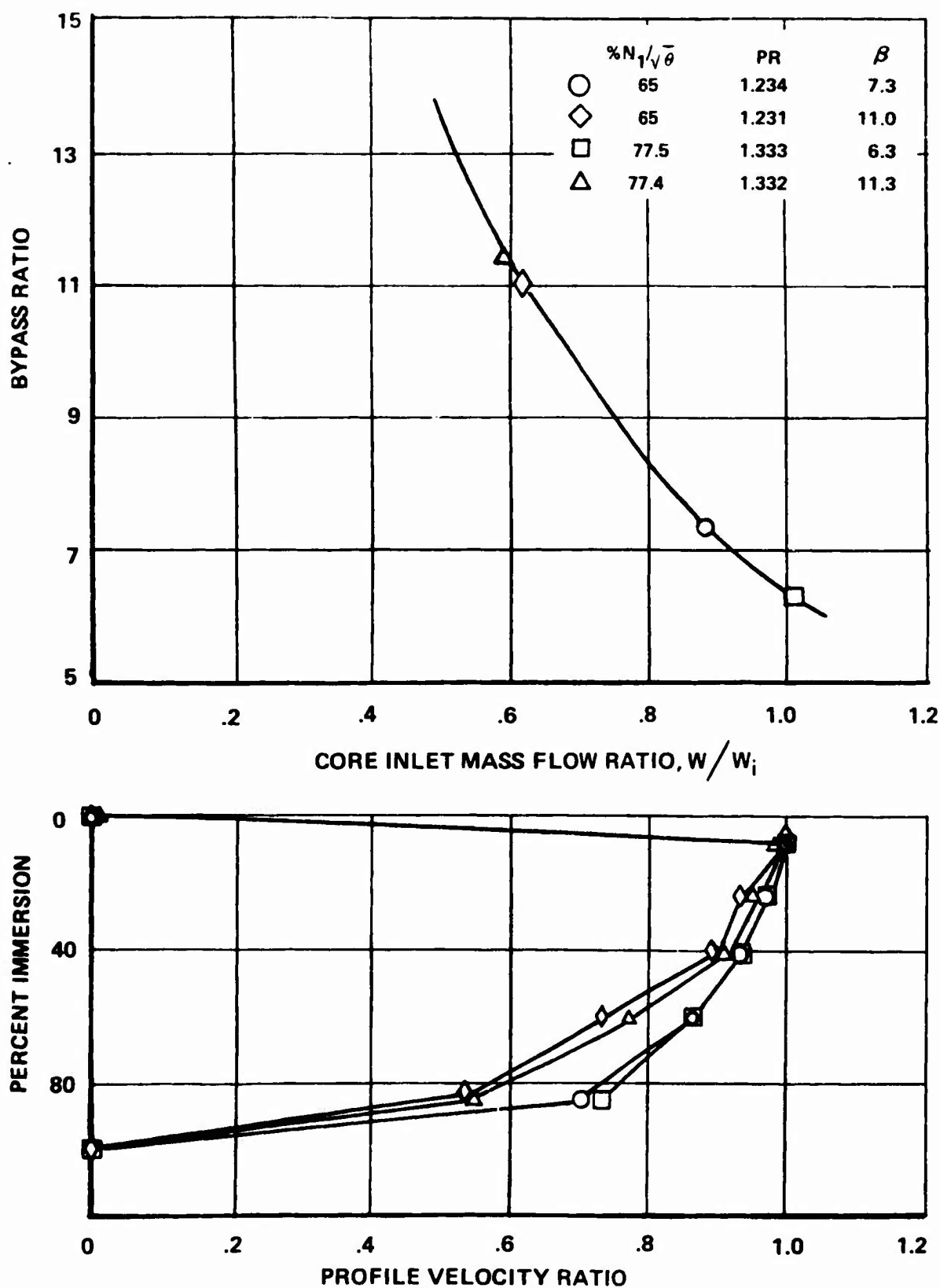


Figure 14. Approximate Bypass Ratio/Core Inlet Mass Flow Ratio Relationship (Engine B).

TABLE IV. BYPASS RATIO VERSUS SPACING PARAMETER

| | β Design | L/H_1 | β Max/ β Design |
|--------------------|----------------|---------|--------------------------------|
| Engine A | 1.5 | .609 | 2.42 |
| Engine B | 6.3 | 1.40 | 1.79 |
| Fan Component Test | 1.85 | 1.00 | 3.12 |
| Fan Component Test | 1.62 | .895 | 1.45 |
| Fan Component Test | 6.7 | .665 | 1.513 |
| Engine C | .88 | 1.037 | ~ 3 |
| Convertible Engine | 5.8 | 3.9 | • geared |
| | | 3.0 | • ungeared |

* Bypass ratio migration in the upward direction, β maximum/ β design, for the convertible engine, will have a value within the range of values listed in this column. However, migration in the downward direction will be much greater. The bypass ratio can approach zero; for the specific case of 25° of fan blade pitch angle closure, the ratio is approximately .06. As discussed above, it is believed that any problem can be satisfactorily handled with the help of one or more known design changes.

FAN AERODYNAMIC DESIGN

GENERAL

The basic aerodynamic design of the fan in normal pitch is conventional. The requirement for a 400-knot thrust did not dictate a high pressure ratio; therefore, a moderate tip speed could be used with consequent minimization of mechanical design difficulty. The main efforts in the aerodynamic design were to devise a method of representing the rotor at reduced blade angles in an existing computer program and to use this to predict the rotor performance at incremental restagger angles. The primary effort was put into the engine configuration, where the air inlet to the fan is used in both fan and shaft modes so that the gas generator is supplied with air via the fan at all times. A promising possible sand separator design, integrated with the engine, which retains this inlet flow configuration, is described under "Engine Preliminary Design".

DESIGN POINT

Tables V through VII show the fan design point performance data at normal pitch.

OFF-DESIGN COMPUTATION

The analytical procedures used for calculating the aerodynamic performance data presented in this study are those developed by the General Electric Company for the design of turbomachinery. The theoretical basis for the method of analysis has been published (Reference 6).

The technique has been programmed for solution on a large scale digital computer and is equally adaptable to the determination of both design and off-design performance. This computer program was employed to calculate the data for the reduced rotor pitch presented herein.

Since the computer program used for this study was devised to handle normal blade stagger angles, some limitations in accuracy at the large deviations in angles is inherent. It was not within the scope of this program to develop a completely new computer procedure; however, this should be considered for future efforts in this area.

RESULTS OF OFF-DESIGN COMPUTATIONS

Figure 15 shows the variation of flow versus rotor restagger from which fan parasitic power can be calculated knowing fan pressure ratio and efficiency. The power absorbed by the fan at 25° restagger angle is calculated at ≈ 400 HP. The following tabulation shows comparisons of fan operating conditions in the fan and shaft modes.

| Flight Condition 400 Knots, S.L | | 95°F 6000 Ft | |
|---------------------------------|--------|------------------------|-------|
| Mode | Fan | Fan (reduced speed) | Shaft |
| Fan Speed | 100% | 80% | 80% |
| Fan Pressure Ratio | 1.44 | 1.29 | 1.29 |
| Fan Efficiency | ≈ 84 | ≈ 84 | ≈ 84 |
| Fan Flow, lb/sec | 253 | 122 | 22.8 |
| Flow/122 | 207% | 100% | 18.5% |
| Fan Blade Angle | Normal | Normal | - 25° |

Figures 16 and 17 indicate the blade settings near the tip in the normal pitch and restaggered positions respectively. It will be noticed that the rotor blades are turned 25° in the "closed" position, while the stator blades are turned only 23°. This is done so that the incidence angles for the stator and the fixed outlet guide vanes become roughly equal. Approximately 28° of blade closure is available before initial blade interference occurs. Cycle calculations show that the flow capacity of the fan at this maximum restagger angle will be the same or even slightly lower than the pumping requirement of the gas generator, at maximum T_4 . For this reason, the angle was limited to 25°. However, if the takeoff condition does not require maximum T_4 , then the 28° angle may be usable with satisfactory flow match between fan and gas generator, i.e., at least a slight excess of fan flow.

The fixed outlet guide vanes are offset somewhat to allow the boundary layers on the suction sides of these blades to be energized by turbulence-free, high-velocity streams from the stator.

Figures 18 through 20 show the variation of incidence angles with blade height for both the design and restaggered conditions. It should be noted that at the angles of incidence encountered in the closed configuration, the loss coefficients and deviations are extremely sensitive. A detailed analysis would be required to determine accurately the level of these parameters. The current design uses values which result in a tolerable level of performance.

Figure 21 shows the estimated loss coefficients for the rotor in the open and closed configurations.

Figure 22 is a streamline plot showing how the flow is redistributed when the rotor is in the maximum restaggered condition. The flow in the bypass duct is slowed down considerably so that the likelihood of having separation is great. Figure 23 is a streamline plot for the design condition.

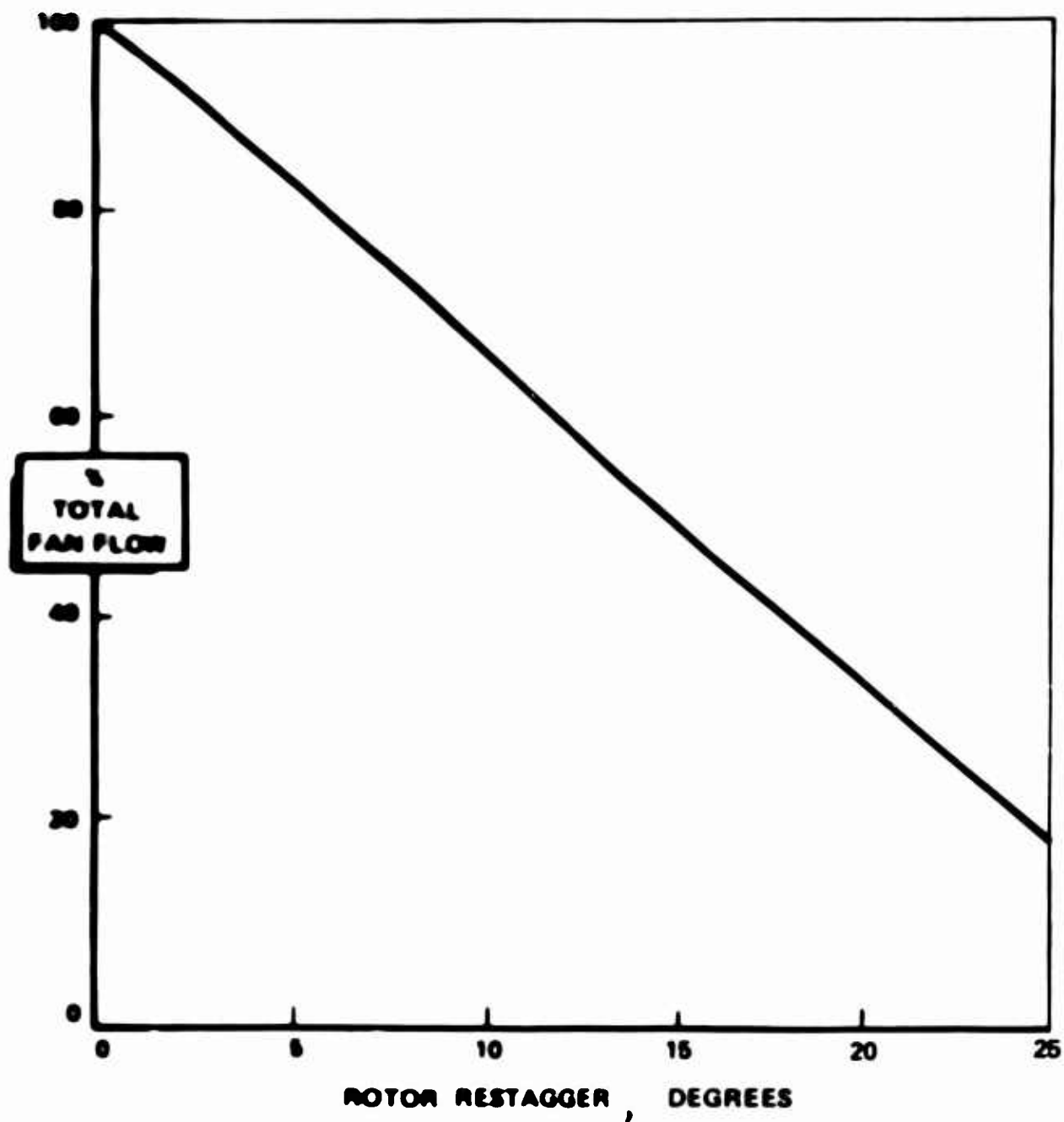


Figure 15. Fan Flow Versus Rotor Restagger.

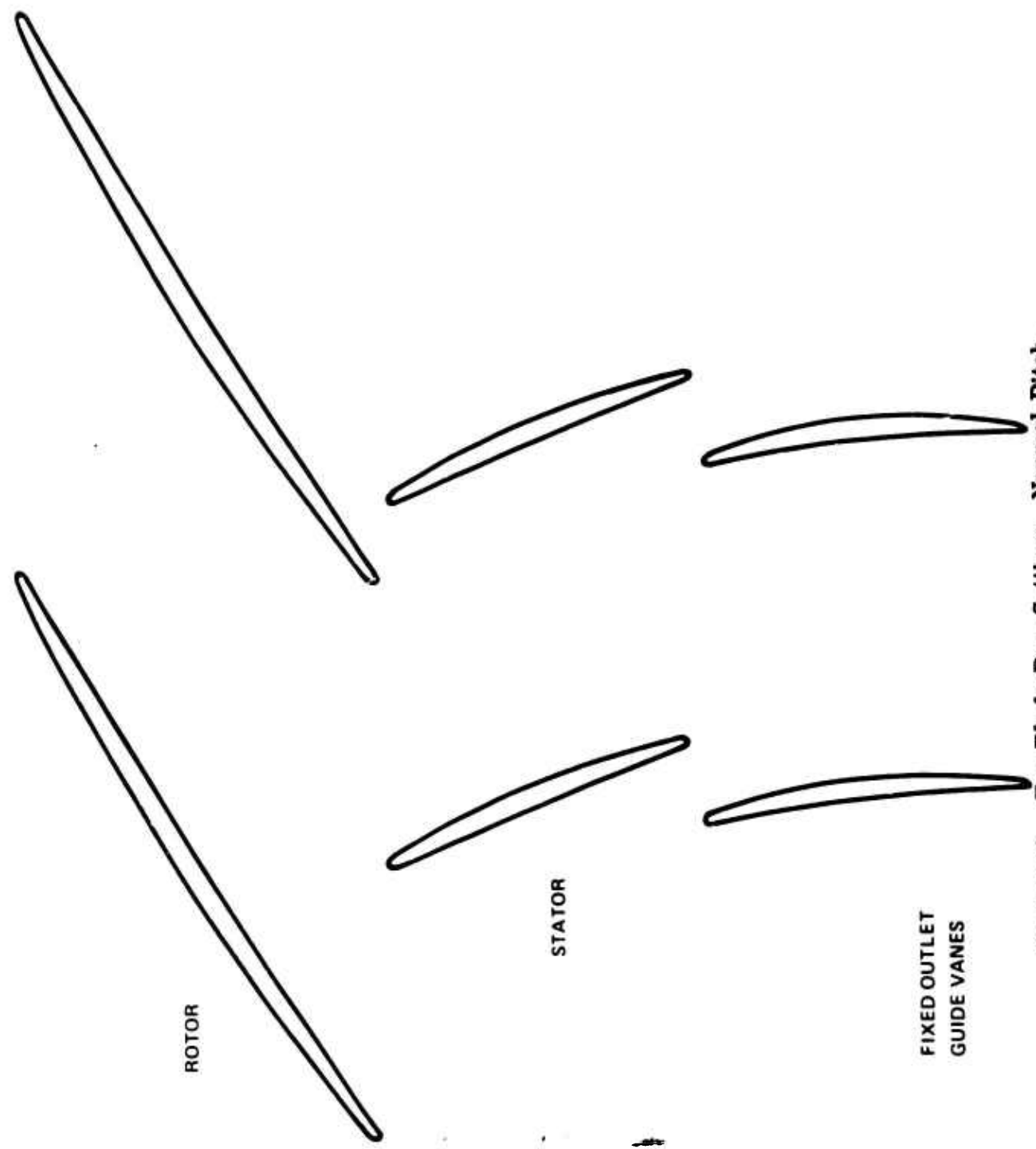


Figure 16. Fan Blade Row Setting, Normal Pitch.

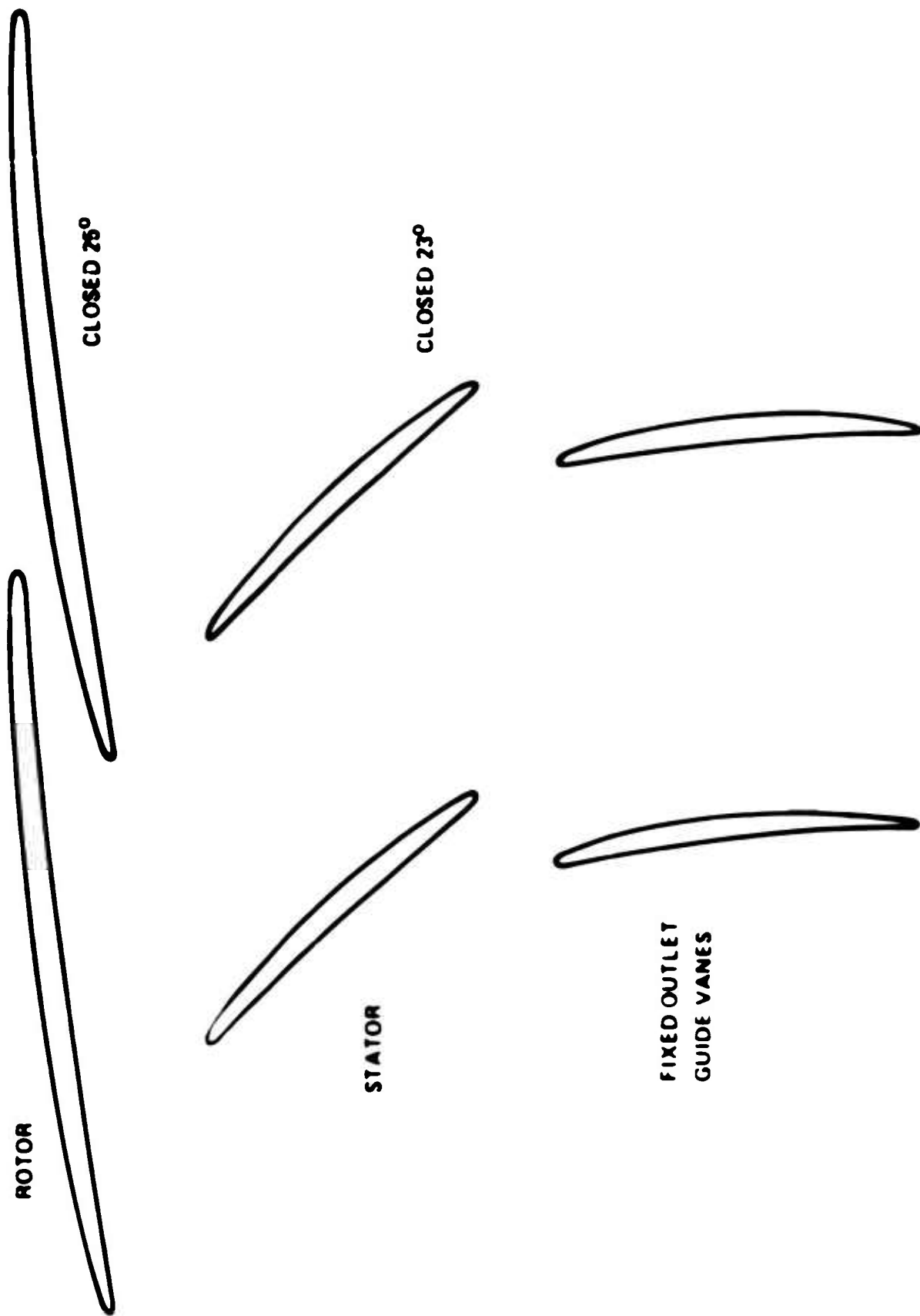


Figure 17. Fan Blade Row Settings. Minimum Pitch.

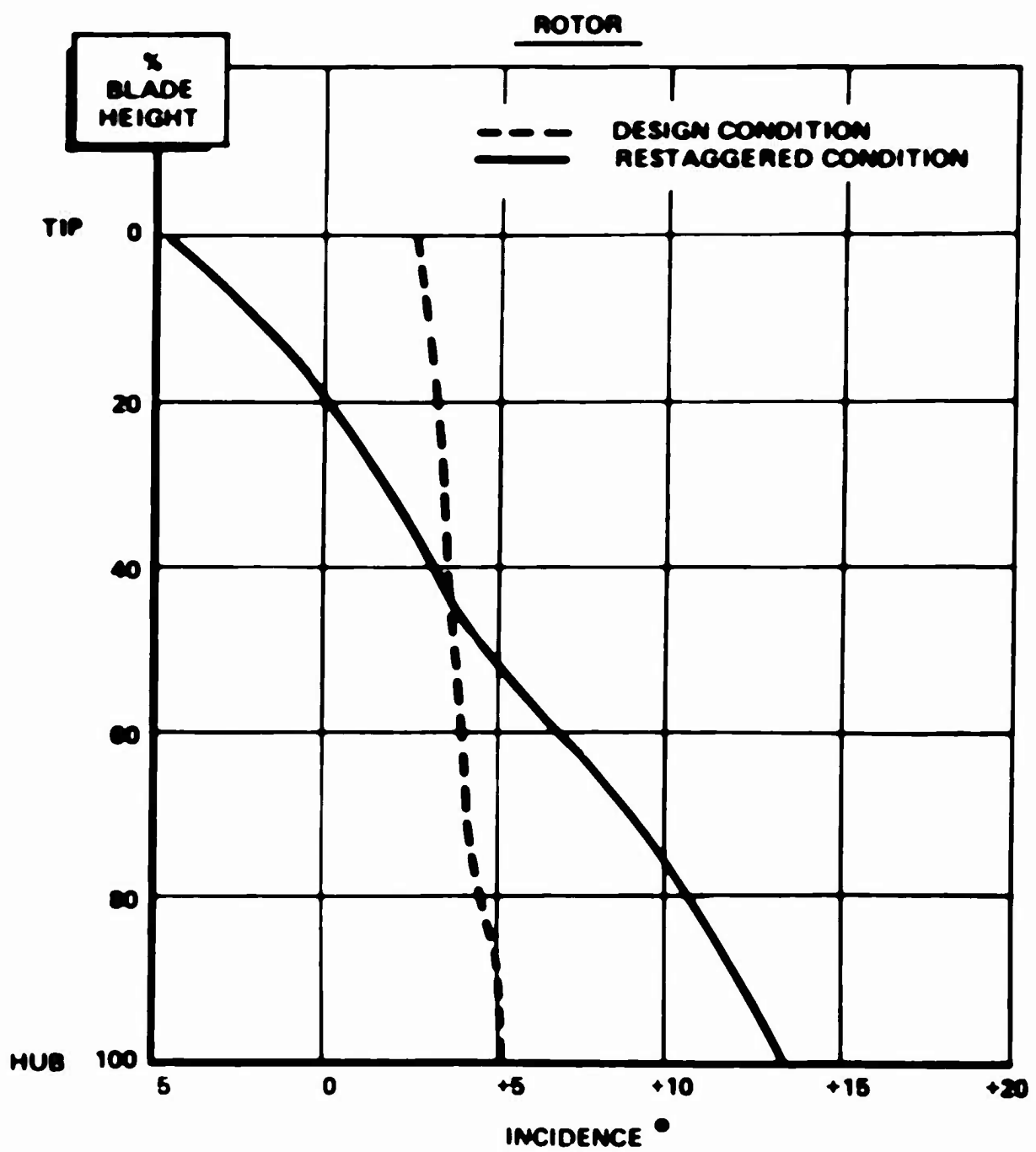


Figure 18. Incidence Versus Percentage Blade Height at Design and Restaggered Conditions.

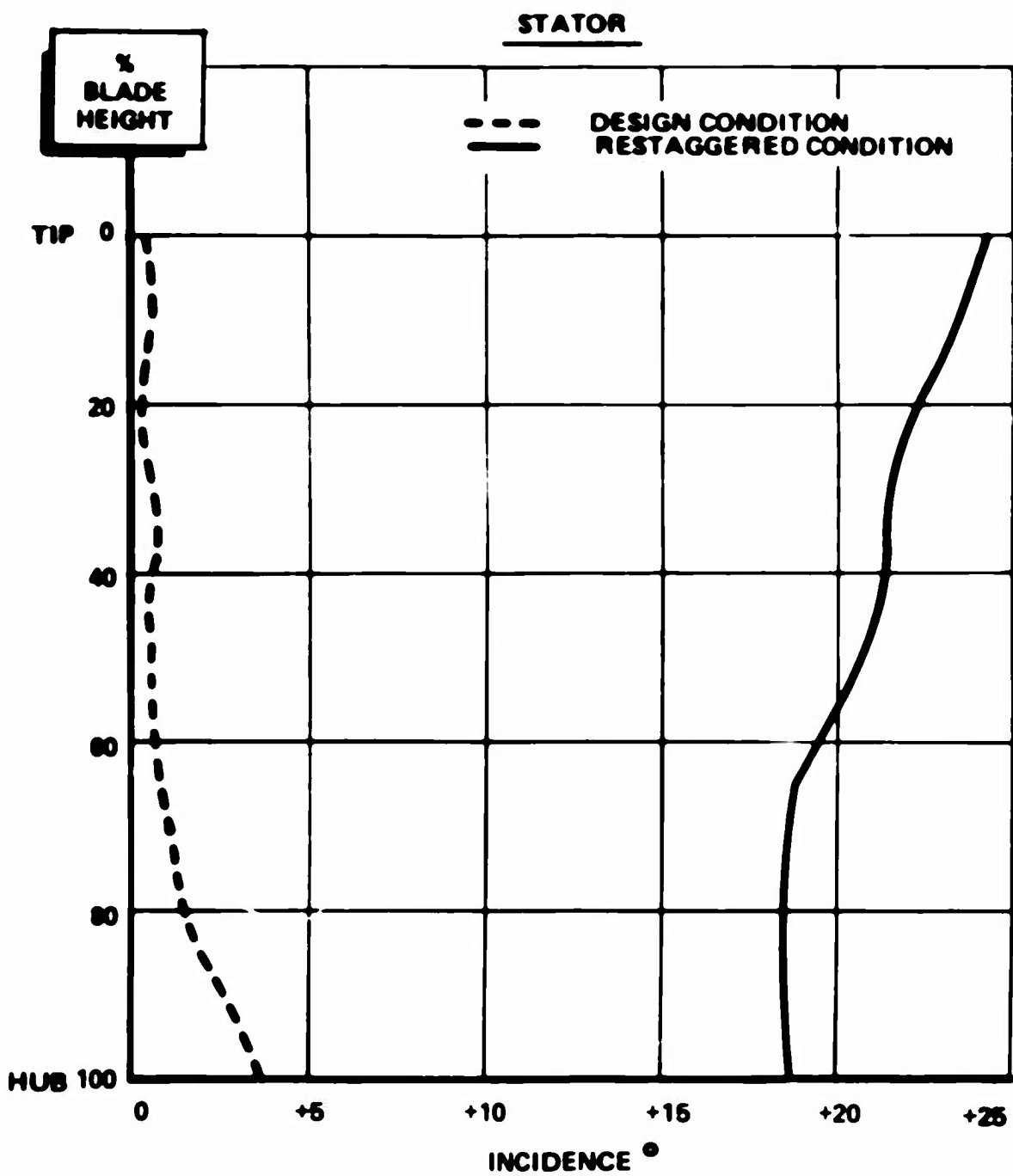


Figure 19. Incidence Versus Percentage Blade Height at Design and Restaggered Conditions.

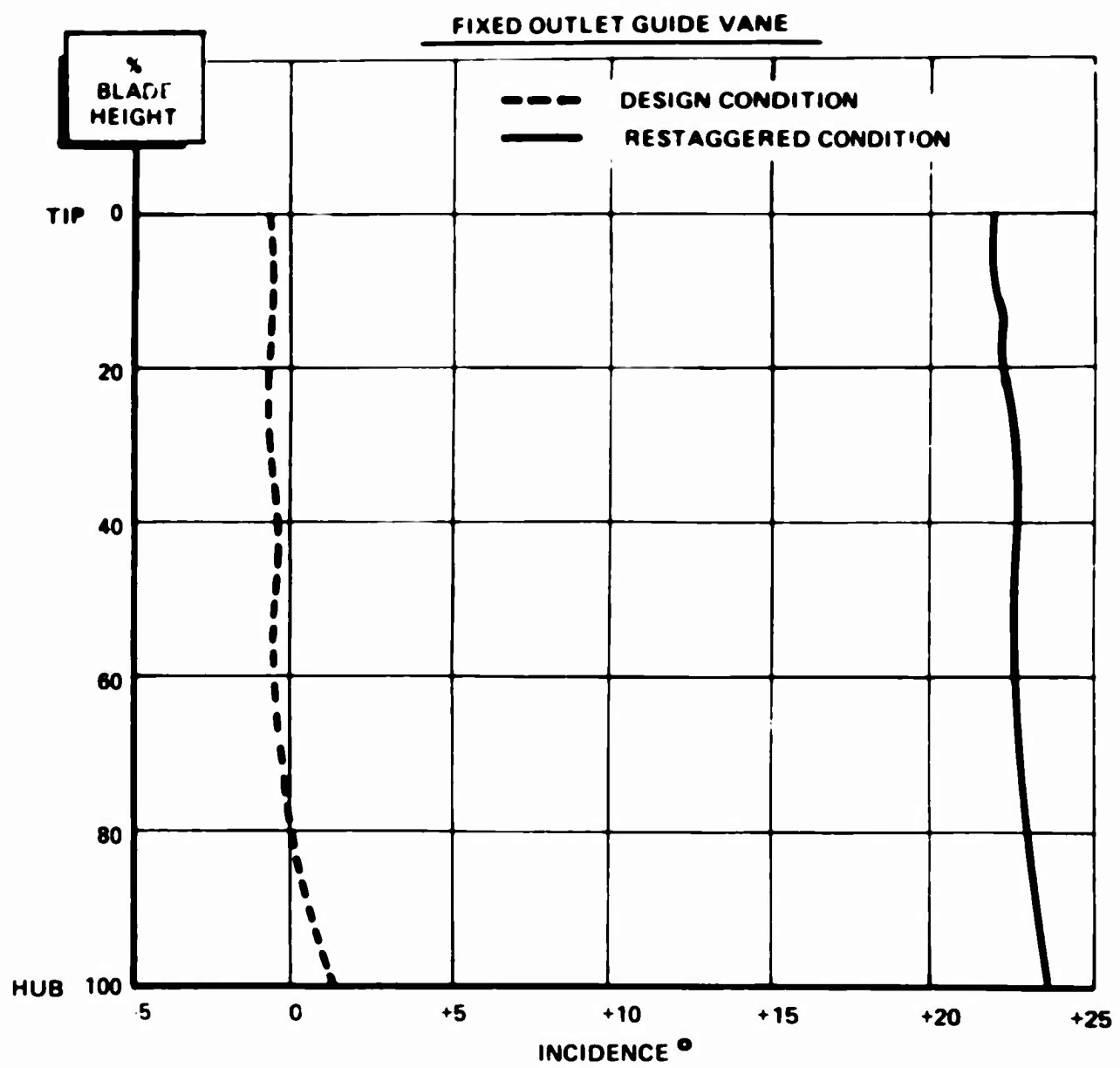


Figure 20. Incidence Versus Percentage Blade Height at Design and Restaggered Conditions.

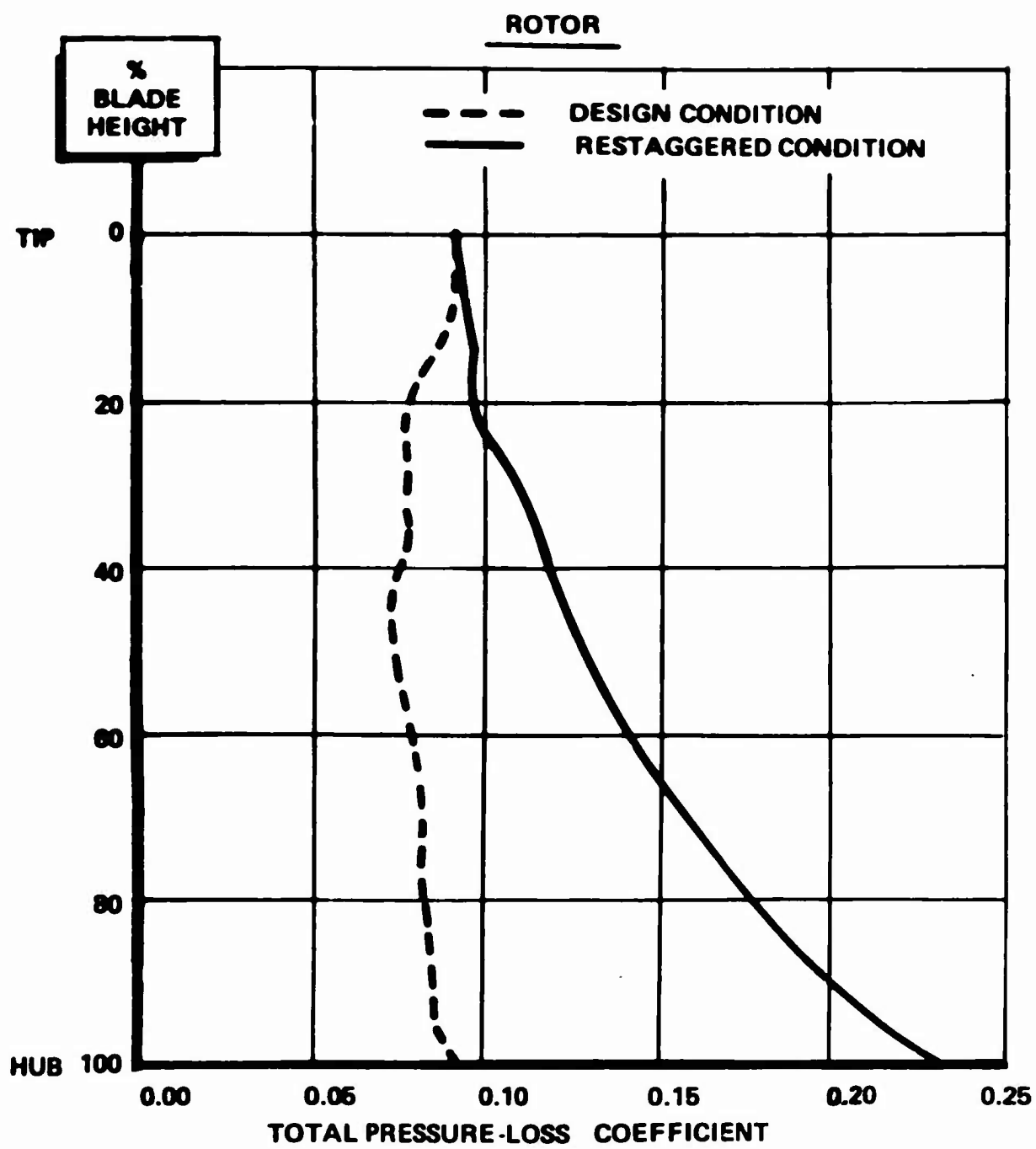


Figure 21. Total Pressure - Loss Coefficient
Versus Percentage Blade Height .

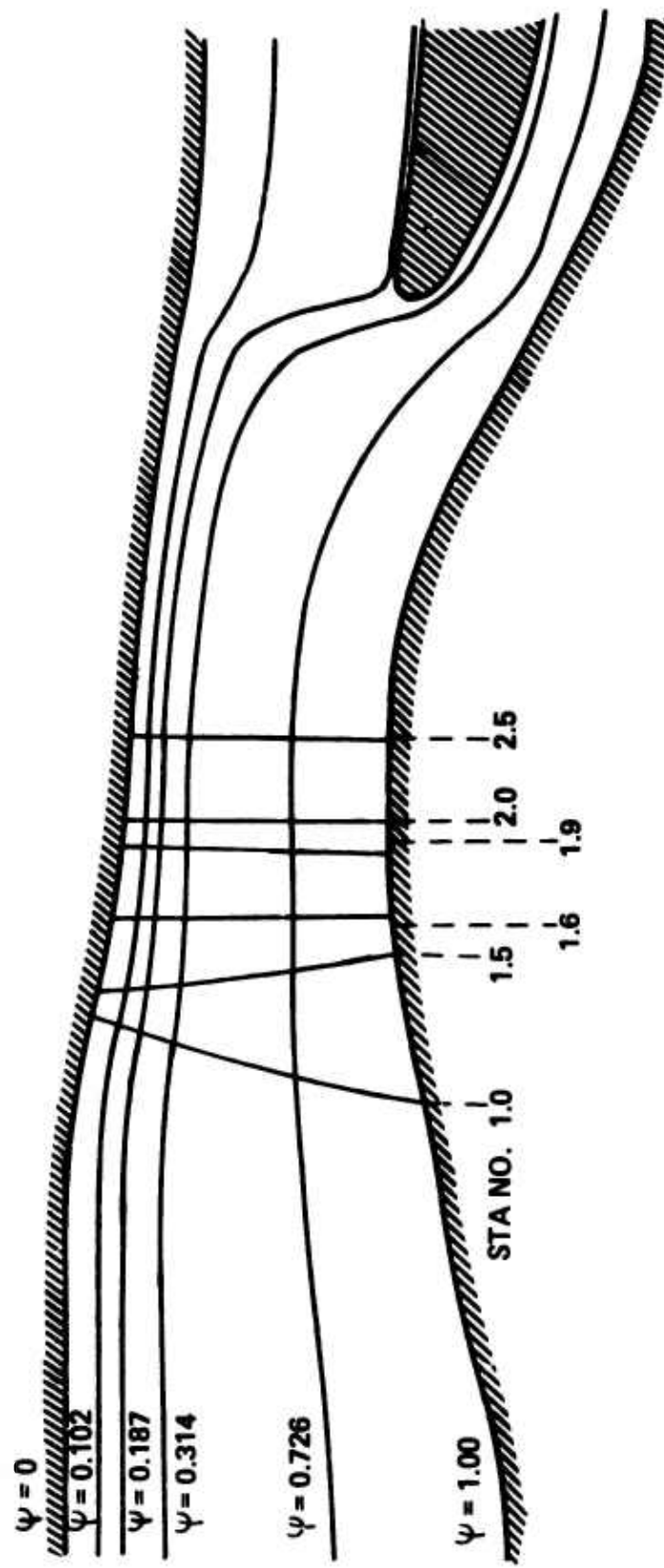


Figure 22. Stream Functions, Maximum Restagger.

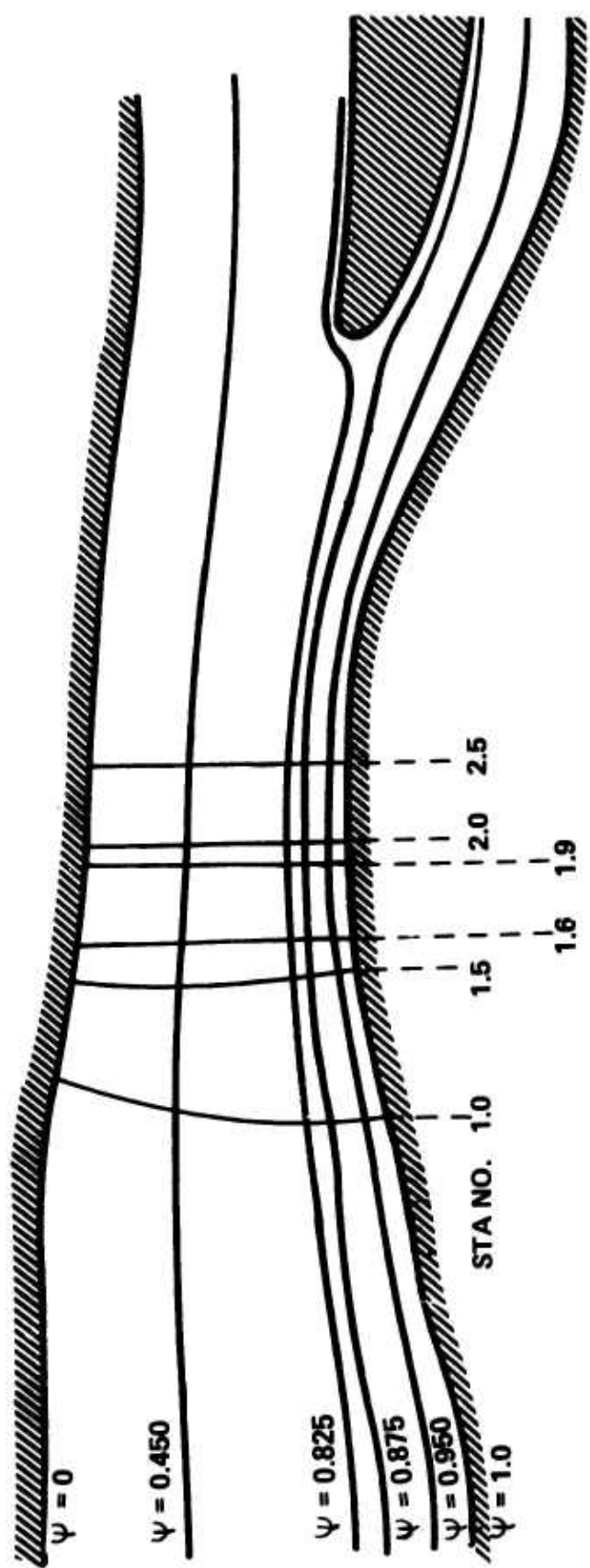


Figure 23. Stream Functions, Normal Pitch.

An identified problem area which will require further investigation is that due to the high diffusion factor of the rotor hub. In the optimization of the final design this may possibly be held to a more tolerable level by redistributing the aerodynamic loading in a radial direction so that the tip region carries more load and the hub carries less.

TABLE V. FAN AERODYNAMIC DESIGN PARAMETERS

$$\text{Corrected Weight Flow} = \frac{W\sqrt{\theta}}{\delta} = 204.9 \text{ lb/sec}$$

$$\text{RPM, Actual} = 8119.3$$

$$\text{Rotor Tip Speed (Inlet)} = U_{\text{tip}} = 1289.5$$

$$\text{Total Pressure Ratio} = \frac{P_2 T}{P_1 T} = 1.45$$

$$\text{Total Temperature Rise} = \Delta T_T = 70.9 ^\circ\text{F}$$

$$\text{Efficiency} = T_{1T} \left[\frac{\left(\frac{P_2 T}{P_1 T} \right)^{\frac{\gamma-1}{\gamma}} - 1}{\Delta T_T} \right] = 0.875$$

$$\text{Temperature Coefficient} = \frac{\Delta T_T}{U_{\text{tip}}^2 / 2g J C_P} = 0.518$$

TABLE VI. FAN DESIGN POINT PERFORMANCE DATA - ROTOR
(26 BLADES - DOUBLE CIRCULAR ARC)

| | INLET | | | | OUTLET | | | |
|--|-------|--------|--------|--------|--------|--------|--------|--------|
| Streamline (ψ) | 1.0 | 0.75 | 0.50 | 0.25 | 0.0 | 1.0 | 0.75 | 0.25 |
| Radius, in. | 9.10 | 12.00 | 14.29 | 16.30 | 18.20 | 9.80 | 12.20 | 14.16 |
| Static Temperature, $^{\circ}\text{R}$ | 526.9 | 524.2 | 524.8 | 527.9 | 533.9 | 563.8 | 577.5 | 583.1 |
| Static Pressure, psia | 15.50 | 15.22 | 15.28 | 15.60 | 16.23 | 19.10 | 20.69 | 21.35 |
| Velocity, abs, fps | 601.0 | 628.1 | 621.7 | 591.0 | 526.1 | 865.1 | 769.9 | 728.6 |
| Velocity, rel, fps | 881.4 | 1056.8 | 1188.1 | 1297.5 | 1392.7 | 629.1 | 702.8 | 828.1 |
| Mach Number, abs | 0.535 | 0.561 | 0.555 | 0.526 | 0.465 | 0.745 | 0.655 | 0.617 |
| Mach Number, rel | 0.785 | 0.943 | 1.060 | 1.154 | 1.232 | 0.541 | 0.598 | 0.701 |
| Air Angle, abs, deg | 0 | 0 | 0 | 0 | 0 | 44.4 | 39.5 | 35.7 |
| Air Angle, rel, deg | 48.0 | 53.6 | 58.4 | 63.0 | 68.1 | 8.6 | 32.2 | 44.4 |
| Metal Angle, deg | 42.9 | 49.5 | 54.8 | 59.8 | 65.5 | -4.8 | 26.3 | 40.1 |
| Incidence, deg | 5.1 | 4.1 | 3.6 | 3.2 | 2.6 | - | - | - |
| Deviation, deg | - | - | - | - | - | 13.4 | 5.9 | 4.3 |
| Total Pressure Loss Coefficient | - | - | - | - | - | 0.0923 | 0.0806 | 0.0732 |
| Solidity * | - | - | - | - | - | 1.80 | 1.61 | 1.46 |
| Diffusion Factor | - | - | - | - | - | 0.483 | 0.490 | 0.425 |

* Based on Cylindrical Sections

TABLE VII. FAN DESIGN POINT PERFORMANCE DATA - STATOR
(38 BLADES - 65 SERIES)

| Streamline (ψ) | INLET | | | | | OUTLET | | | | |
|--|------------|-------------|-------------|-------------|------------|------------|-------------|-------------|-------------|------------|
| | 1.0 Hub | 0.75 Hub | 0.50 Hub | 0.25 Hub | 0.0 Tip | 1.0 Hub | 0.75 Hub | 0.50 Hub | 0.25 Tip | 0.0 Tip |
| Radius, in. | 9.53 | 12.20 | 14.11 | 15.77 | 17.25 | 10.08 | 12.20 | 14.03 | 15.64 | 17.04 |
| Static Temperature, $^{\circ}\text{R}$ | 563.4 | 574.8 | 580.5 | 583.8 | 586.9 | 577.1 | 586.4 | 589.1 | 589.4 | 589.6 |
| Static Pressure, psia | 19.05 | 20.34 | 21.01 | 21.28 | 21.33 | 20.60 | 21.73 | 22.04 | 21.94 | 21.63 |
| Velocity, abs, fps | 867.9 | 791.4 | 750.0 | 733.8 | 731.8 | 766.6 | 696.9 | 677.4 | 686.2 | 708.9 |
| Mach Number, abs | 0.747 | 0.675 | 0.636 | 0.621 | 0.617 | 0.652 | 0.588 | 0.570 | 0.578 | 0.597 |
| Air Angle, abs, deg | 43.6 | 38.2 | 34.7 | 32.1 | 30.4 | 27.8 | 25.0 | 22.6 | 20.2 | 18.4 |
| Metal Angle, deg | 39.9 | 37.1 | 34.1 | 31.8 | 29.9 | 25.2 | 21.5 | 19.0 | 16.6 | 14.8 |
| Incidence, deg | 3.7 | 1.1 | 0.6 | 0.3 | 0.5 | - | - | - | - | - |
| Deviation, deg | - | - | - | - | - | 2.6 | 3.5 | 3.6 | 3.6 | 3.6 |
| Total Pressure Loss Coefficient | - | - | - | - | - | 0.0211 | 0.0173 | 0.0154 | 0.0132 | 0.0123 |
| Solidity * | - | - | - | - | - | 1.60 | 1.33 | 1.16 | 1.04 | 0.95 |
| Diffusion Factor | - | - | - | - | - | 0.199 | 0.212 | 0.193 | 0.166 | 0.139 |

* Based on Cylindrical Sections

TABLE VIII. FAN DESIGN POINT PERFORMANCE DATA - FIXED STATOR
(38 BLADES - 65 SERIES)

| Streamline (↓) | INLET | | | | | OUTLET | | | | |
|------------------------|------------|-------|-------|-------|-------|------------|--------|--------|--------|--------|
| | 1.0 Hub | 0.75 | 0.50 | 0.25 | 0.0 | 1.0 Tip | 0.75 | 0.50 | 0.25 | 0.0 |
| Radius, in | 10.08 | 12.17 | 13.96 | 15.55 | 17.00 | 10.06 | 12.09 | 13.85 | 15.42 | 16.06 |
| Static Temperature, °R | 577.8 | 583.7 | 586.9 | 589.6 | 593.4 | 585.3 | 589.6 | 591.6 | 593.4 | 596.1 |
| Static Pressure, psia | 20.69 | 21.38 | 21.76 | 21.96 | 22.13 | 21.53 | 22.06 | 22.09 | 22.40 | 22.42 |
| Velocity, abs, fps | 760.6 | 719.6 | 696.4 | 684.7 | 675.0 | 698.6 | 668.3 | 654.8 | 649.6 | 650.2 |
| Mach Number, abs | 0.647 | 0.609 | 0.588 | 0.576 | 0.566 | 0.590 | 0.563 | 0.550 | 0.545 | 0.544 |
| Air Angle, abs, deg | 28.0 | 24.3 | 22.1 | 20.4 | 19.4 | 0 | 0 | 0 | 0 | 0 |
| Metal Angle, deg | 26.8 | 24.5 | 22.5 | 21.0 | 20.0 | -5.9 | -6.0 | -5.9 | -5.9 | -6.0 |
| Incidence, deg | 1.2 | -0.2 | -0.4 | -0.6 | -0.6 | - | - | - | - | - |
| Deviation, deg | - | - | - | - | - | 5.9 | 6.0 | 5.9 | 5.9 | 6.0 |
| Total Pressure | - | - | - | - | - | 0.0227 | 0.0188 | 0.0175 | 0.0159 | 0.0148 |
| Loss Coefficient | - | - | - | - | - | 1.60 | 1.33 | 1.16 | 1.04 | 0.95 |
| Solidity * | - | - | - | - | - | 0.229 | 0.226 | 0.222 | 0.219 | 0.212 |

* Based on Cylindrical Sections

FAN MECHANICAL DESIGN

The method devised to support the fan rotor blades affords essentially a simple tangential dovetail attachment to a double disk - an ideal structural arrangement - despite incorporating the variable pitch feature. Figure 24 shows a complete preliminary layout of the fan rotor.

The essence of the attachment is the unique geometry of the surfaces of contact between the blades and disks which absorb the motion of blade pitch change by rolling. A simple model demonstrating the kinematics of rolling has been constructed (Figure 25). Although relatively crudely constructed, the model demonstrates the principles involved and works satisfactorily without any apparent dependence on constructional accuracy. Figure 26 illustrates the model's pertinent geometric surfaces. Only small segments of these surfaces physically exist on the blades and disks, as will be described below. A spherical internal surface on each of the disks contacts an external spherical surface of somewhat smaller radius on the blade. The two disk semispheres overlap the blade axis so that for each disk a radial line through the point of contact is colinear with the corresponding radial line for the blade. Since the surfaces are all axisymmetric, any arbitrary rotation of the three surfaces about their own axes, or rotation of the blade axis about the engine axis, does not affect the geometry, as illustrated in the plane of intersection of the engine axis and the blade axis. In this application, the mating surfaces are coupled by the condition that sliding at the points of contact is not allowed. Hence, any given angular rotation between the disks yields a corresponding specific angular rotation of the blade about its axis. The relative motion between the blade and disk at any instant may be described by two components: rotation about the colinear radial line and rolling about the point of contact. This motion is similar to that of the ball relative to the race of an antifriction bearing. The two important differences that permit the high loading are the large effective diameter of the ball and the spherical surface of the race. The race of an antifriction bearing is a cylinder curved into a torus.

A section through the blades and disk is shown in Figure 27. A ring segment of the basic internal spherical surface is incorporated into each disk. Appropriate segments of the corresponding outer surface on the blade are on the two separate bearing plates mounted on the blade root. The front disk is retained at the hub by a thrust ring and may be actuated to rotate in relation to the shaft while the rear disk is fixed to the shaft. Under ideal conditions, the centrifugal load of the blade is distributed over a small circular area centered on the geometric point of contact. Axial displacements are prevented by the opposed catenary shapes of the webs, which absorb the axial component of the blade loading without bending stresses. Rolling of the rims is prevented by the rims' axial extensions, which are counterbalanced against the asymmetric blade loading.

The maximum contact (Hertz) stress may be held down to a conservative value; this stress is estimated at 66,000 psi for the design as shown at full speed, while

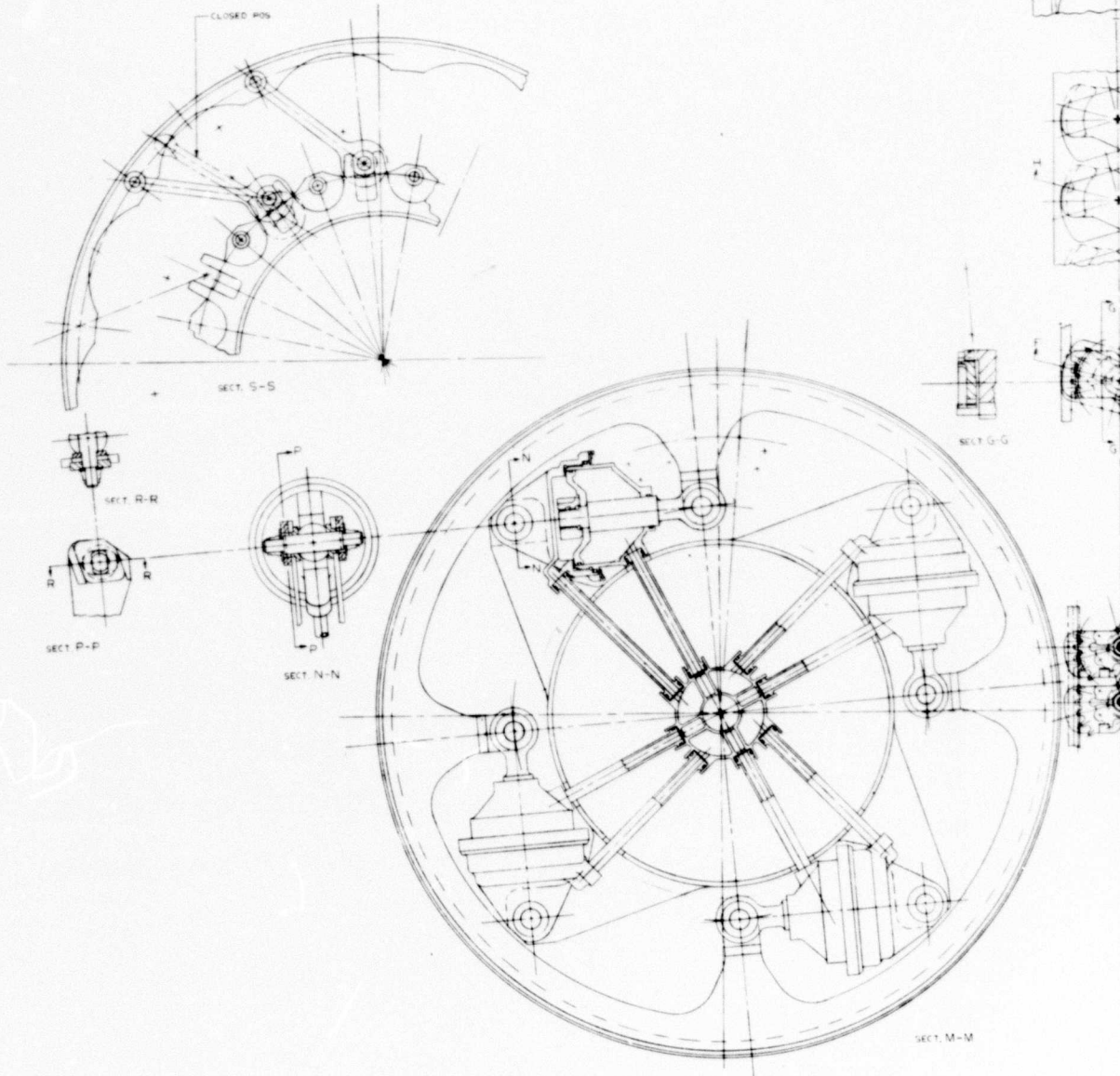
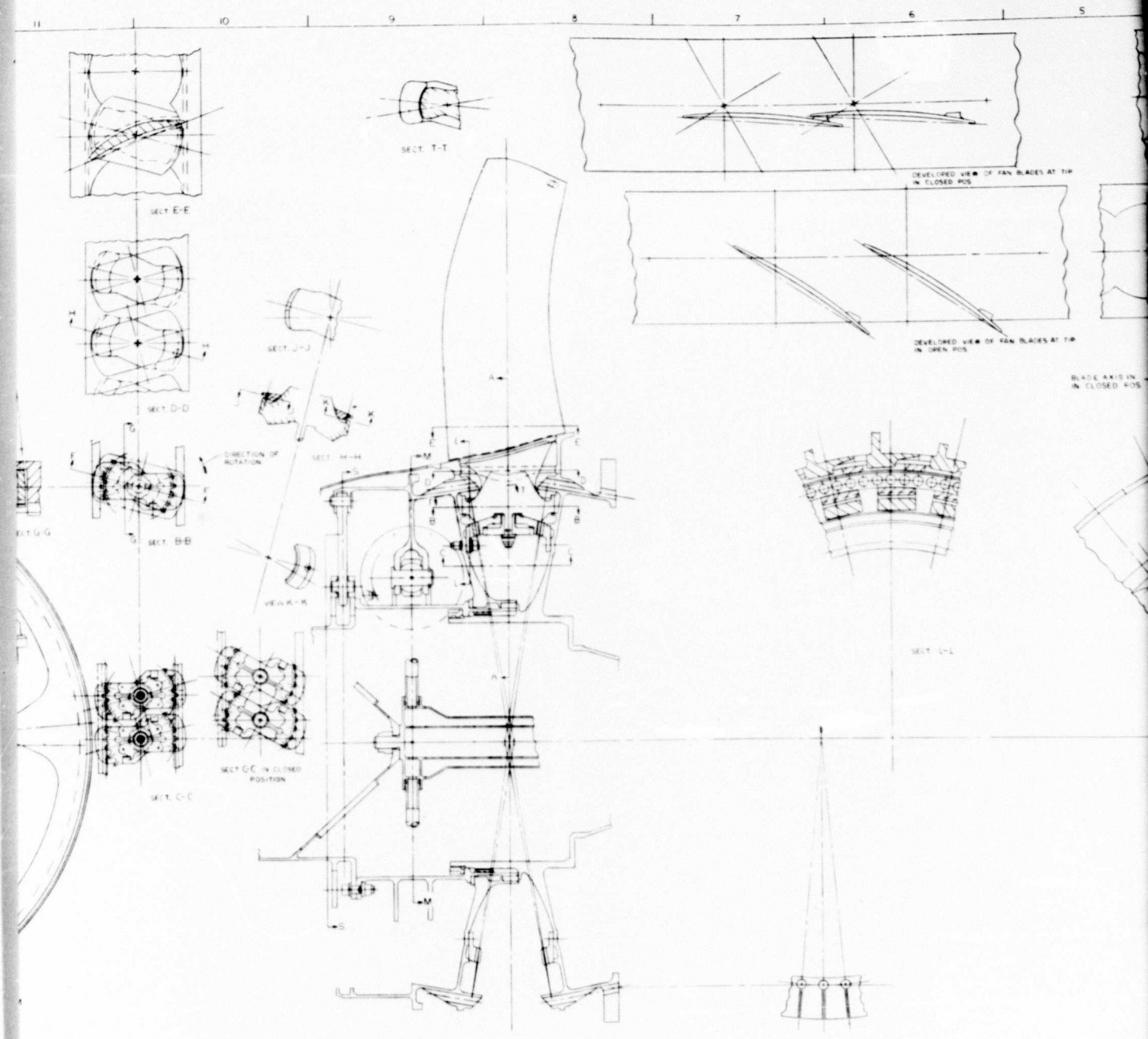
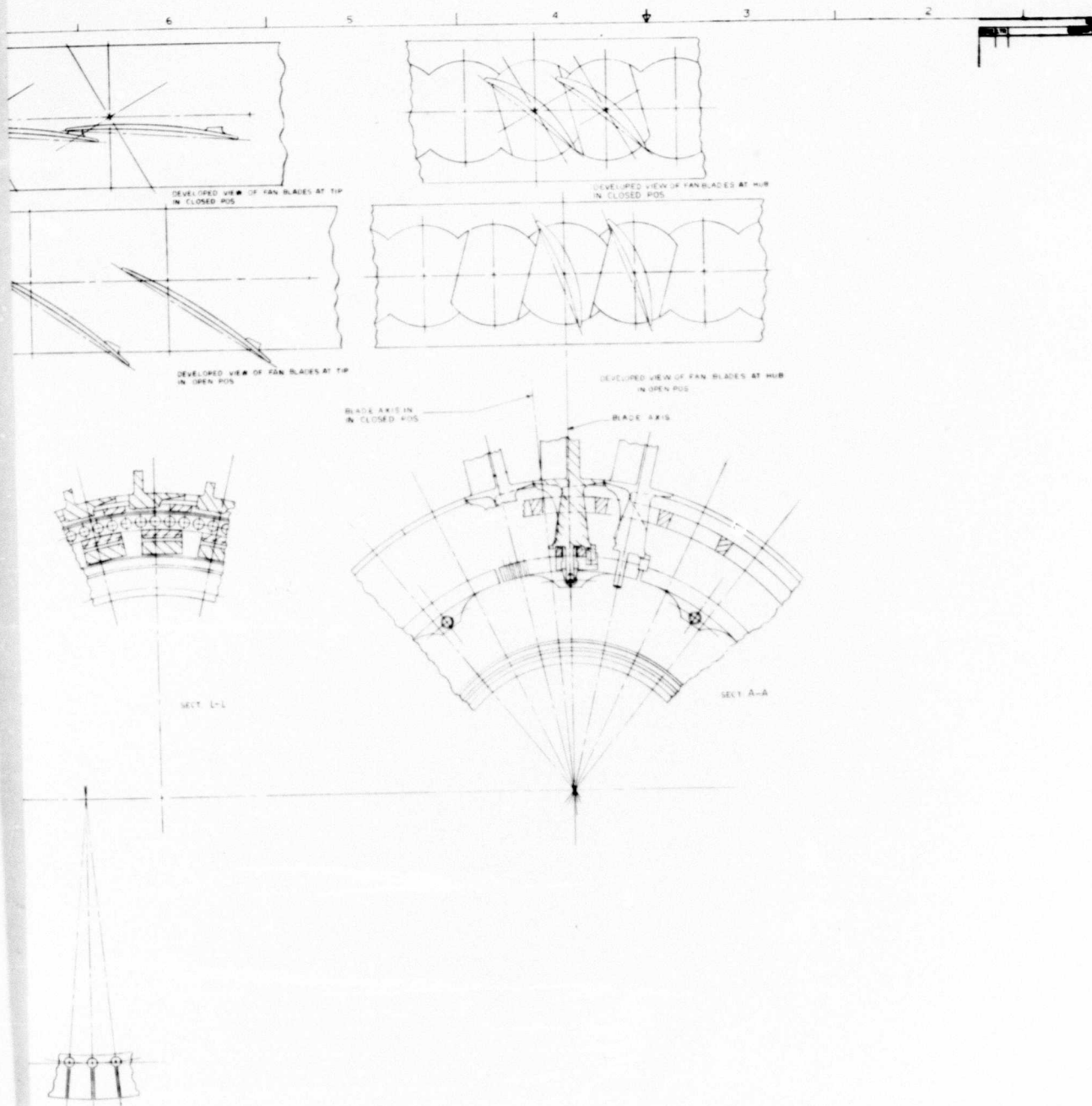


Figure 24. Preliminary Design of Fan Rotor.



B



C

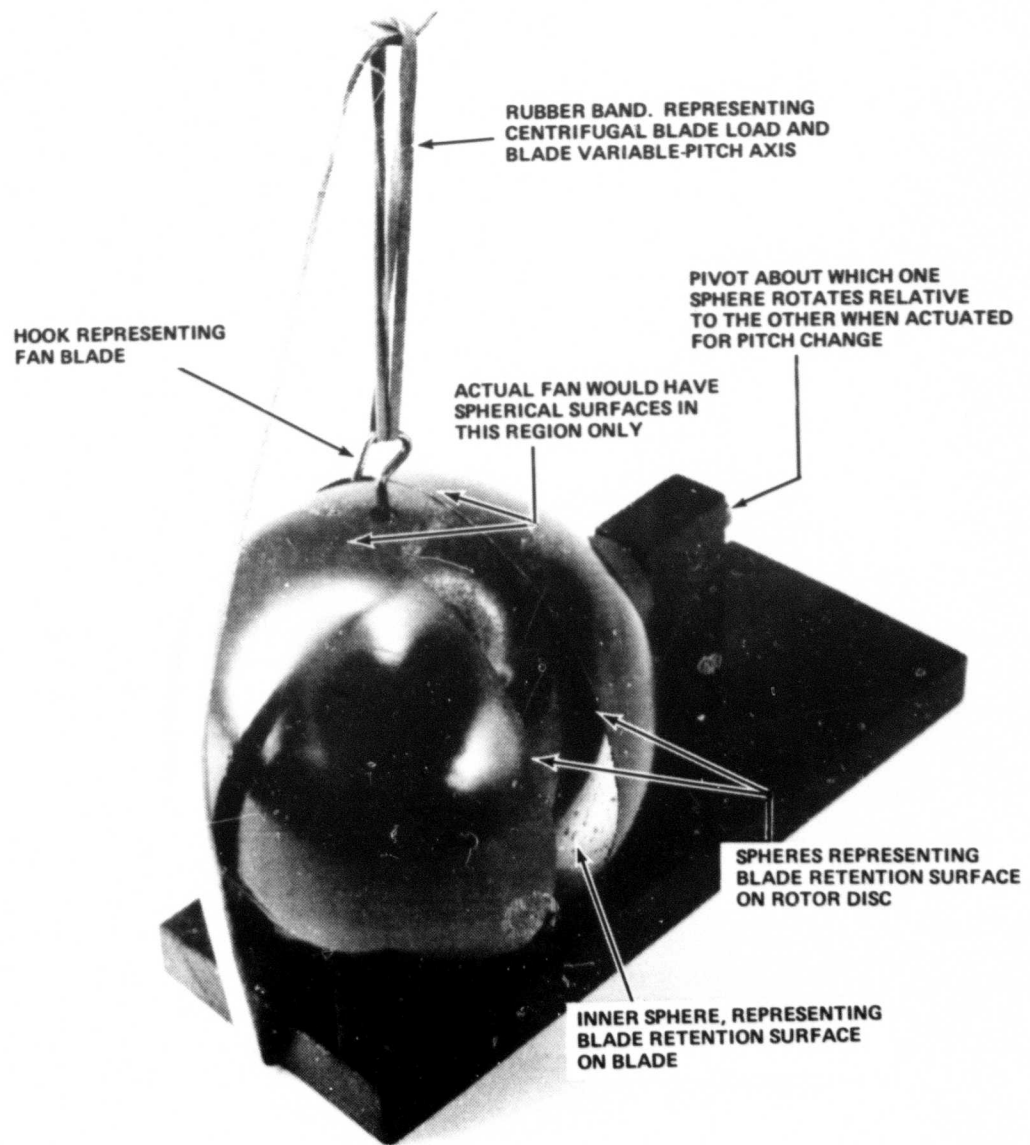


Figure 25. Model of Variable-Pitch Principle.

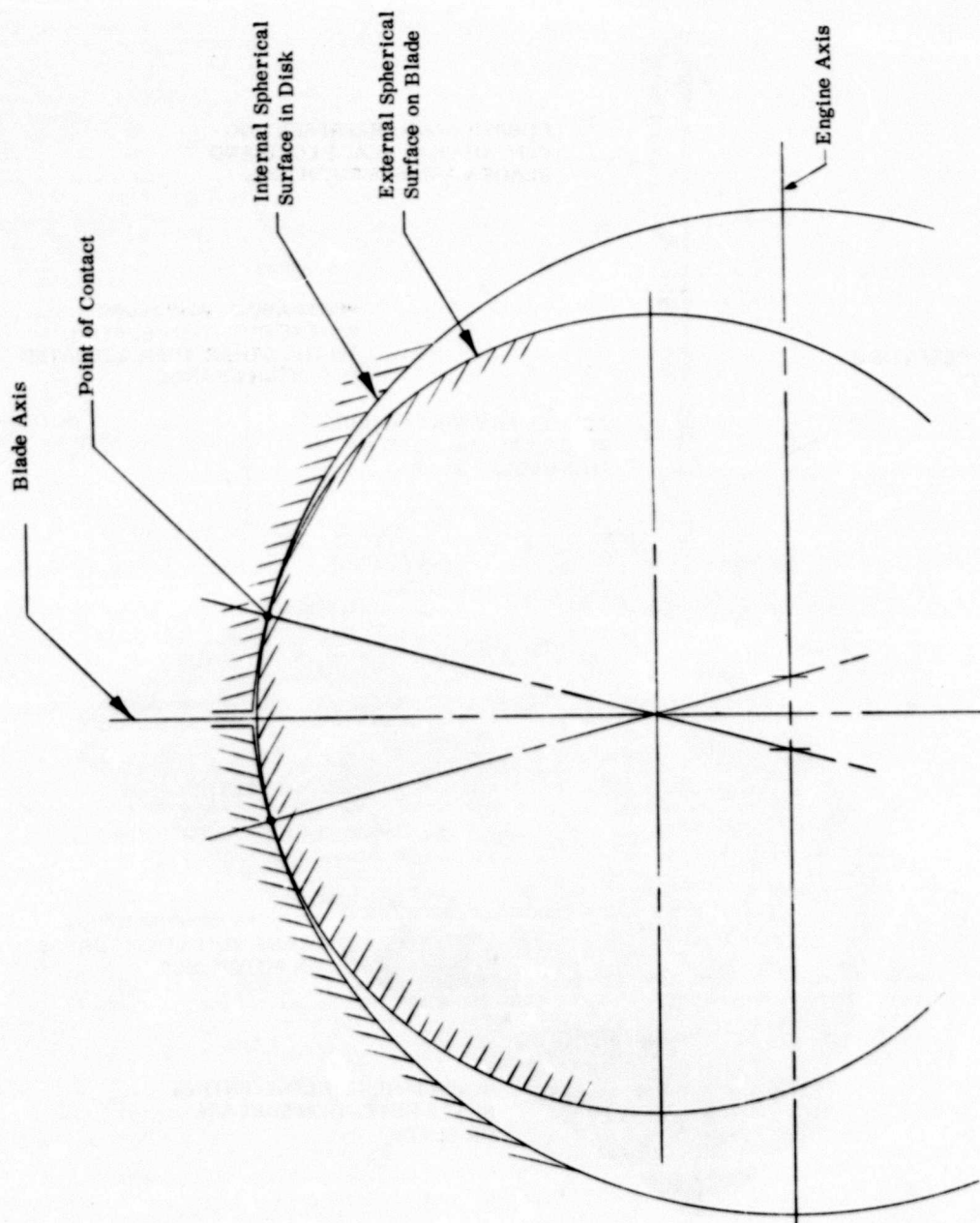


Figure 26. Geometric Surfaces of Blade Mechanism.

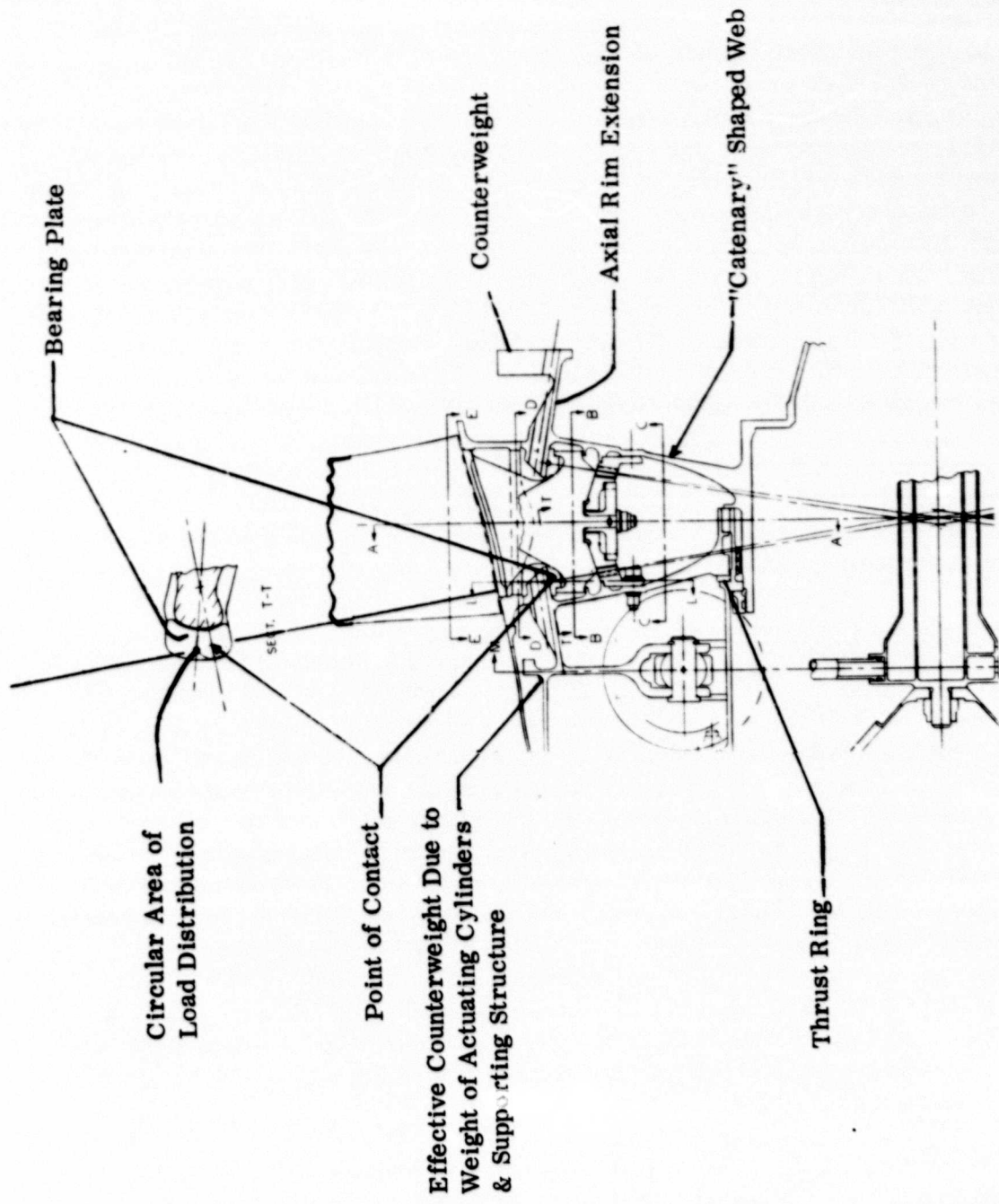


Figure 27. Primary Structural Features of Blades and Disks.

pitch change movement will occur at a reduced speed of approximately 80%. Since there occurs only a small amount of skidding - that due to rotation about the point of contact - it is expected that excessive friction and wear will be avoided. The disks are of a nickel alloy and may be coated on their loaded surfaces. The titanium blades are protected by the bearing plates. Some simulated testing of promising material and surface finish combinations prior to testing of a rotor would be desirable (see "Recommendations").

To synchronize the motion and to absorb torque and tangential loading on the blade, a partial bevel gear at the inner end of each blade engages a mating gear fixed to each disk, as shown in Figure 28. The greatest portion of the load on the gear teeth is due to blade centrifugal torque. The two lugs on each blade engage the slots in the gear to transmit the torque as shown in Sections B-B and G-G. The tangential gas force, which is low, is transmitted through the adapter shown in Section C-C. Because of its low loading, this adapter is sufficiently flexible to effectively isolate the gear teeth from possible loading due to blade vibration or misalignment. Although the gear theoretically does not absorb any loads due to the motion of pitch change, it may be subject to additional load due to the actual effective center of the loaded contact surface not coinciding exactly with the line about which the gear rolls. This additional transient load would be small and, again, would occur only at a reduced rotor speed. The gear is isolated from torsional vibratory loading by friction on the loaded surfaces and from bending, both vibratory and steady, by its flexible mounting.

The four actuating cylinders within the front spinner rotate the front disk to vary fan pitch. The relatively high centrifugal torque on the blades is balanced by centrifugal loads on the asymmetrically hinged counterweights, shown in Figure 29 and on the pistons of the actuating cylinders. Since both of these balancing loads reduce when the blades move from the open, or turbofan, to the closed, or turbo-shaft, position, the net loading on the complete system is such that the actuating cylinders are loaded against their end stops in either position without the assistance of internal fluid pressure. Thus, actuator pressure must be supplied only when actuation is required; normal steady operation in either mode does not require this pressure, with consequent fail-safe features. Pneumatic pressure is preferred if the control mode adopted permits a two-position fan pitch. However, if modulated pitch is required, hydraulic pressure may be used. The estimated pressure is 200 psi to balance steady centrifugal loading and an additional transient pressure of 1500 psi to overcome friction at full design speed. Either modulated or two-position fan pitch actuation may be required, as discussed under "Cycle Analysis and Selection".

The features that are designed to prevent excessive leakage at the tip and root of the blade are shown in Figure 30. A sphere symmetric with respect to the blade axis defines the limit that may not be exceeded by the blade tip in the open position if interference in the closed position is to be avoided. For a conventional blade, the clearance over the forward portion of the blade would be excessive because of

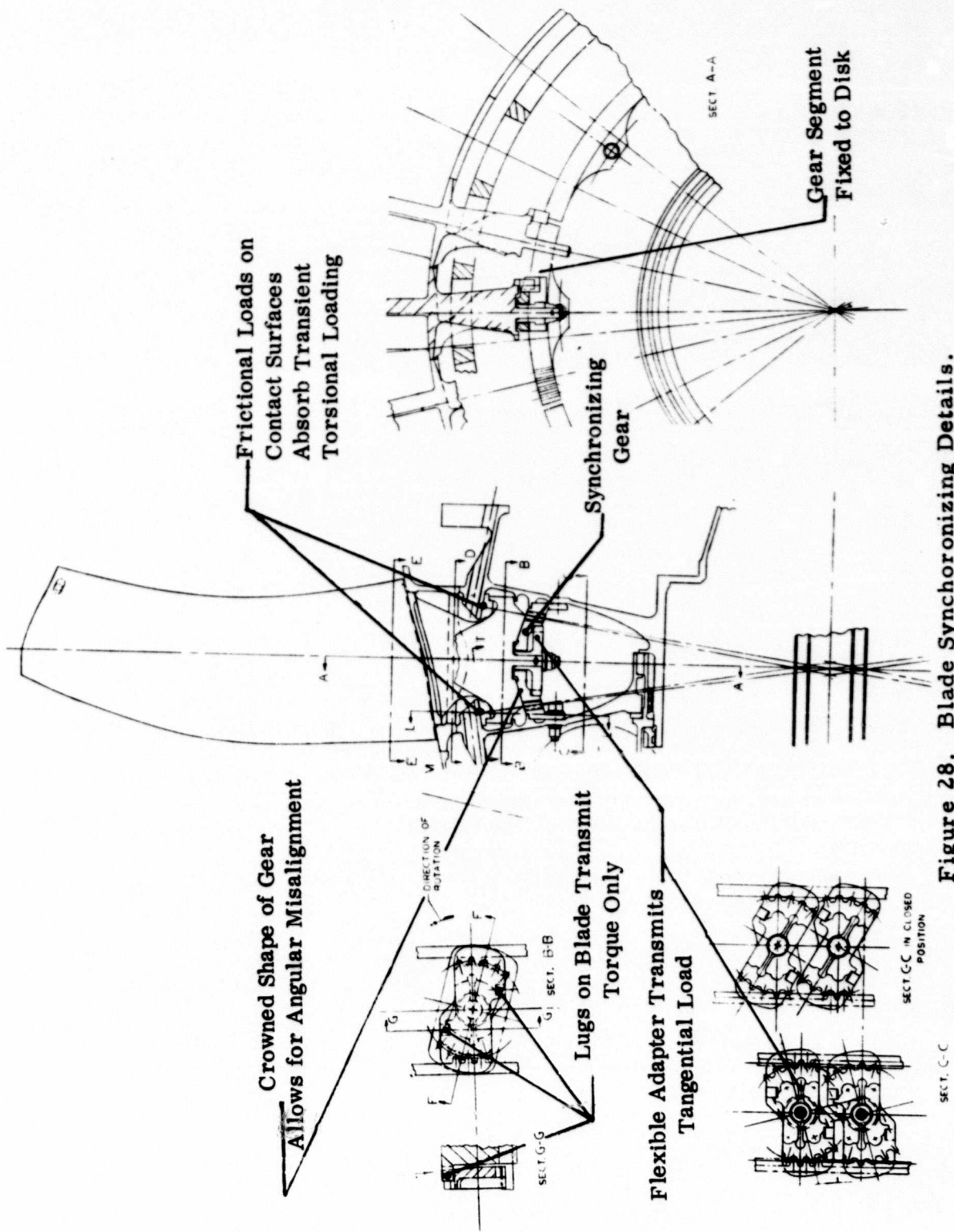


Figure 28. Blade Syncronizing Details.

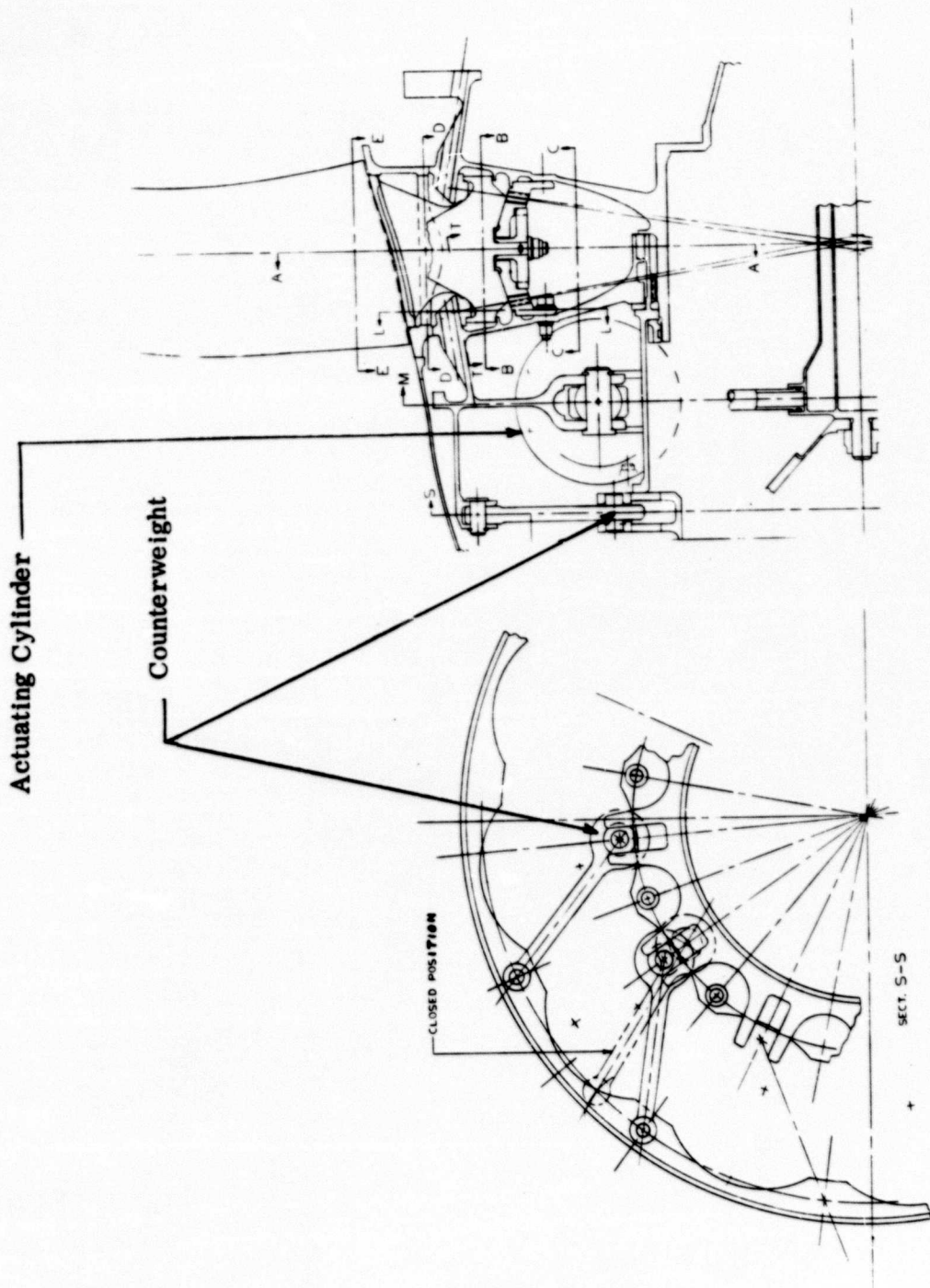


Figure 29. Blade Counterweight Details.

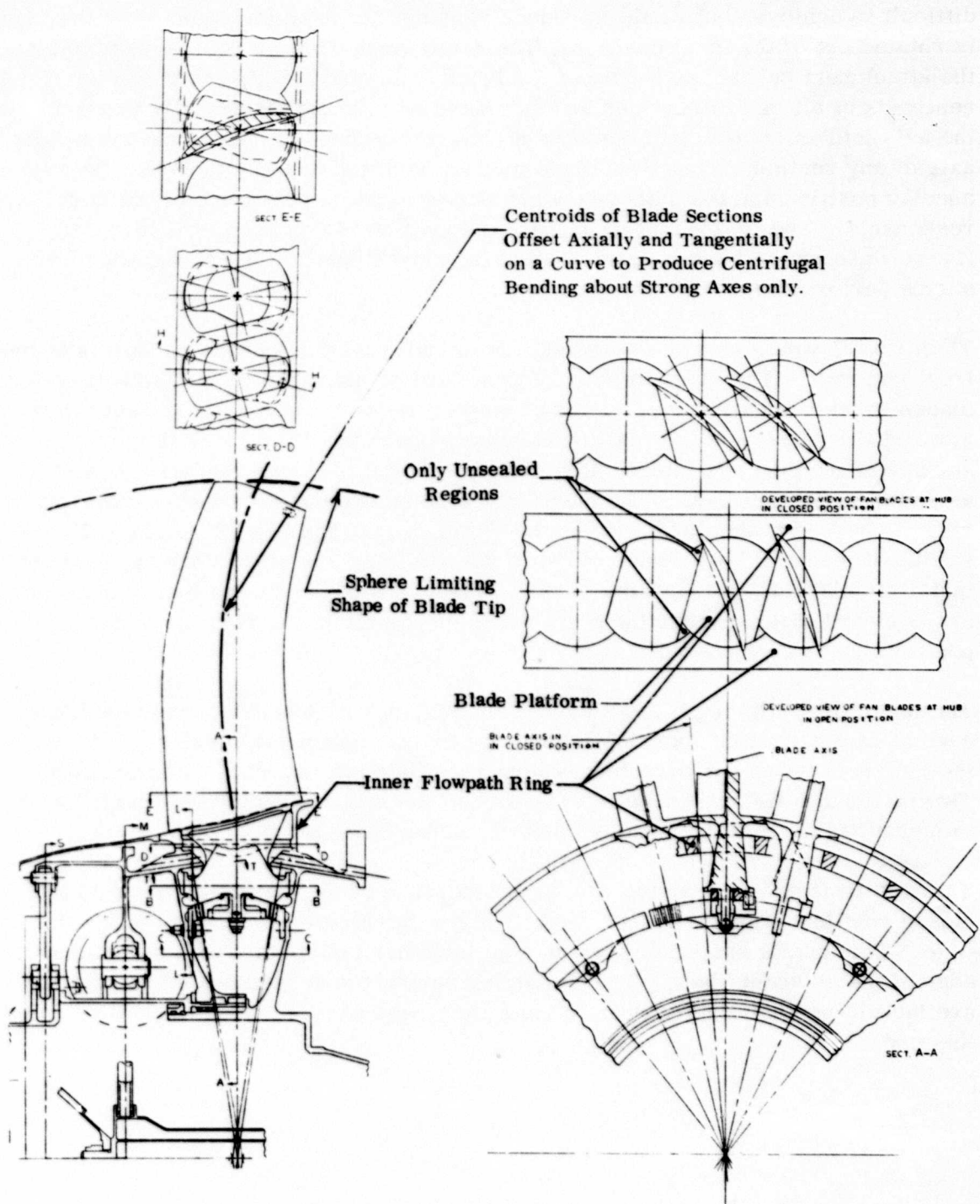


Figure 30. Tip and Root Leakage Prevention Details.

the slope in the flowpath. Therefore, it is desirable that the axis of rotation intersect the tip near the front of the blade to reduce this clearance. An axis of rotation that is not normal to the engine axis (as is indicated in Reference 2) is not only difficult to achieve but would introduce bending into the attachment when the blade is rotated out of the ideal position. The configuration shown retains symmetry of the attachment but moves the tip of the blade backward relative to the axis. The centroids of all airfoil sections are displaced axially and tangentially relative to the axis into an appropriate curve so as to produce bending only about the strong axis of any section. Thus, the blade may be balanced at the attachment for any angular position, and the steady bending stresses due to curvature of the airfoil are reasonable. The tip clearance in the open position is compromised very little. Its increase as the blade rotates toward the closed position is not significant to engine performance.

The inner flowpath ring seals against the circular portions of the platforms at the front and rear. The sides of the platforms are straight and seal effectively between blades in the two extreme positions of blade rotation. Only small triangular regions at the corners of the platforms remain unsealed. The holes through the outer surface of the ring are intersecting circles that cut the ring into two end portions as shown in Section E-E. The shape of the holes through the inner surface of the ring is changed to an elongated slot, as shown in Section D-D. This shape leaves sufficient material between the holes to join the two ends while allowing clearance for installation and actuation of the blades. The shape of the flowpath allows the edges of the airfoil that overhang the platform to fit closely to the ring in the open position.

The inner flowpath ring follows the blades as they roll relative to the disks, as the cage of an antifriction bearing follows the balls. Hence, the angular position of the ring relative to the rear disk is directly related to the blade pitch position. Two additional EMF transducers, mounted on the stator structure behind the ring to measure this relative angular position, sense blade pitch.

To avoid fretting of the airfoil due to interference of the blades at the tip in the closed position, a pad is raised slightly above the airfoil surface at the trailing edge. This pad is shaped to provide a suitable area of contact with the leading edge of the adjacent blade. The contacting surfaces are hard coated, and blades are locked together tightly when in the fully closed position. Figure 31 illustrates this pad.

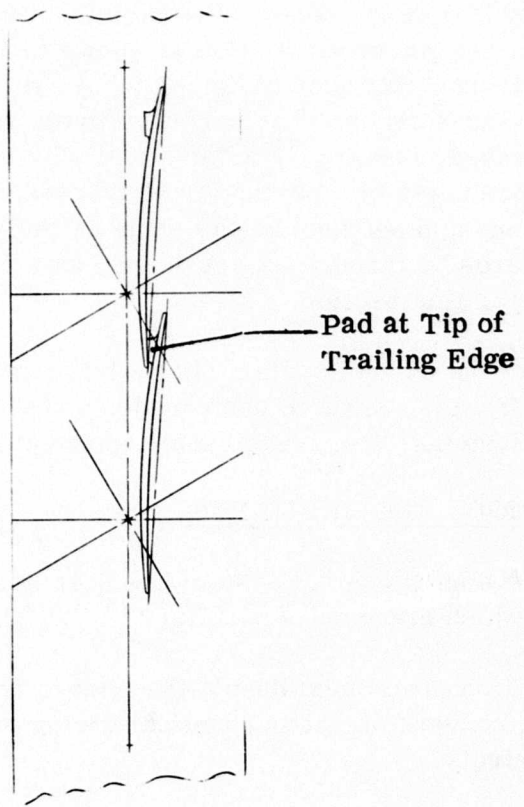


Figure 31. Blade Tip Antifretting Pad.

CONTROL MODE ANALYSIS

SUMMARY

The transition control system is shown in Figure 32. The system was developed from an existing turboshaft control system with the addition of functions required for transition control. The control system, the engine cycle, and the shaft load characteristics have been simulated on a computer by the Dynasar program. The computer was used for transient computations, which have led to the detailed system design shown by Figure 33. Information from rotary-wing airframe manufacturers showed that rotor systems having either horizontal or vertical axes of rotation might be used in convertible vehicles. Thus, four basic cases are needed to cover transition mode simulation as shown in Figures 34 through 37. These depict typical transient time histories for fan-to-shaft and shaft-to-fan conversion, each for both vertically and horizontally stowed rotor simulations. The controls may be sequenced manually or automatically by a sequencing mechanism designed to meet requirements of a particular airframe installation. This sequencing has few restrictions and need not be the same as that employed in the simulations shown in Figures 34 through 37. A discussion of a typical transient time history is given later in this section.

The results of the control system study show that satisfactory engine/control/rotor conversions from fan mode to shaft mode, and vice versa, can be made with either of the rotor systems, i.e., rotor shaft horizontal or vertical.

CONTROL MODE REQUIREMENTS

The fan/shaft engine control system has been designed to meet the following requirements, which are mostly peculiar to a fan/shaft engine:

1. Cockpit controls must enable the pilot to control engine and rotor thrust during conversion without critical timing or excessive manipulation of cockpit controls.
2. Existing helicopter and fan engine control concepts and hardware should be utilized to perform their normal function.
3. Additional controls required for conversion should be the minimum required for engine conversion.

CONTROL SYSTEM DESCRIPTION

Figure 31 is a functional block diagram of the control system. Cockpit levers include a conversion lever in addition to levers conventional to fan engine and shaft engine controls. The function of each lever is outlined on the diagram. The conversion lever selects the required engine geometry and converts the control

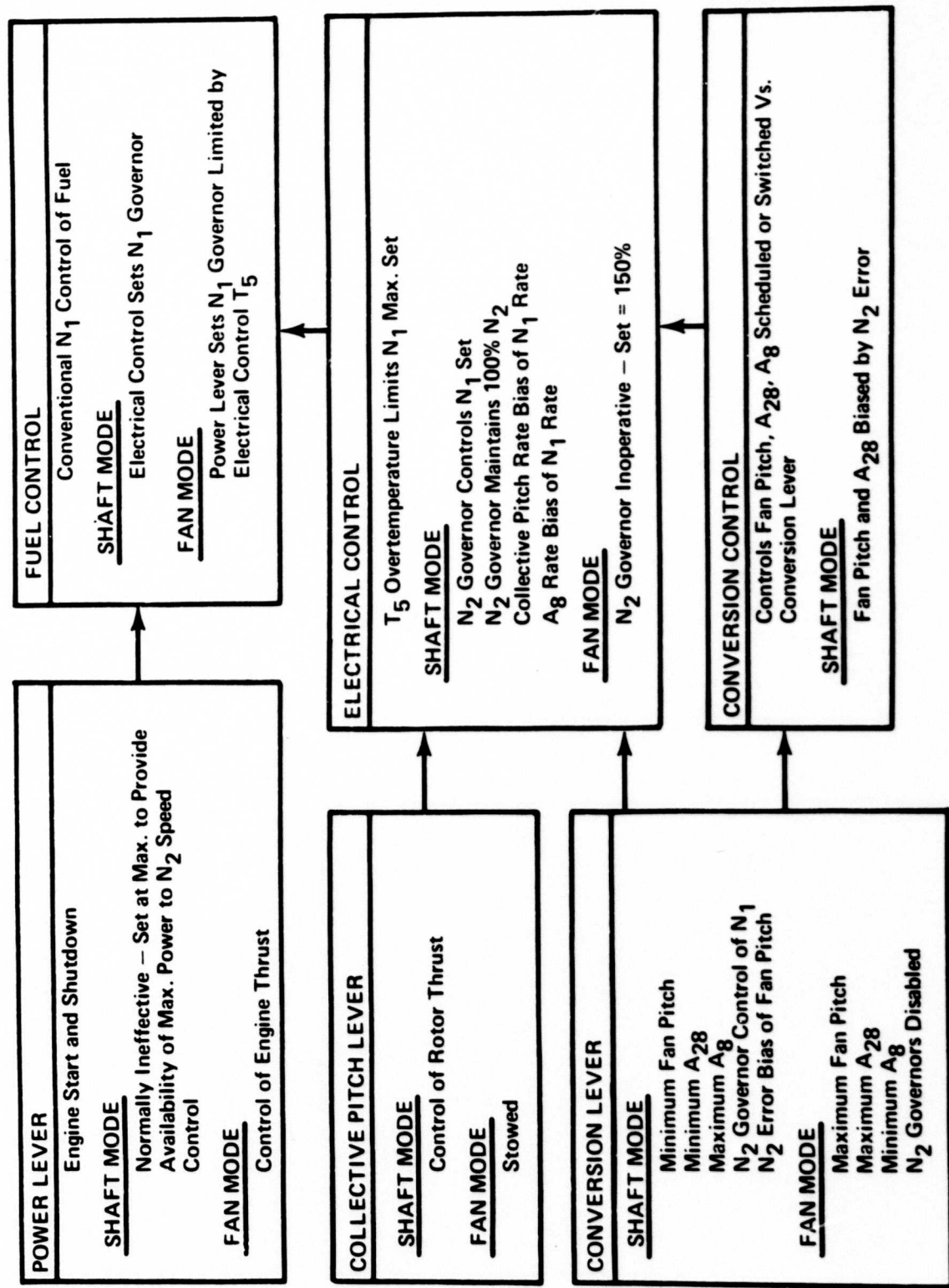


Figure 32. Fan/Shuttle Engine Control Functional Block Diagram.

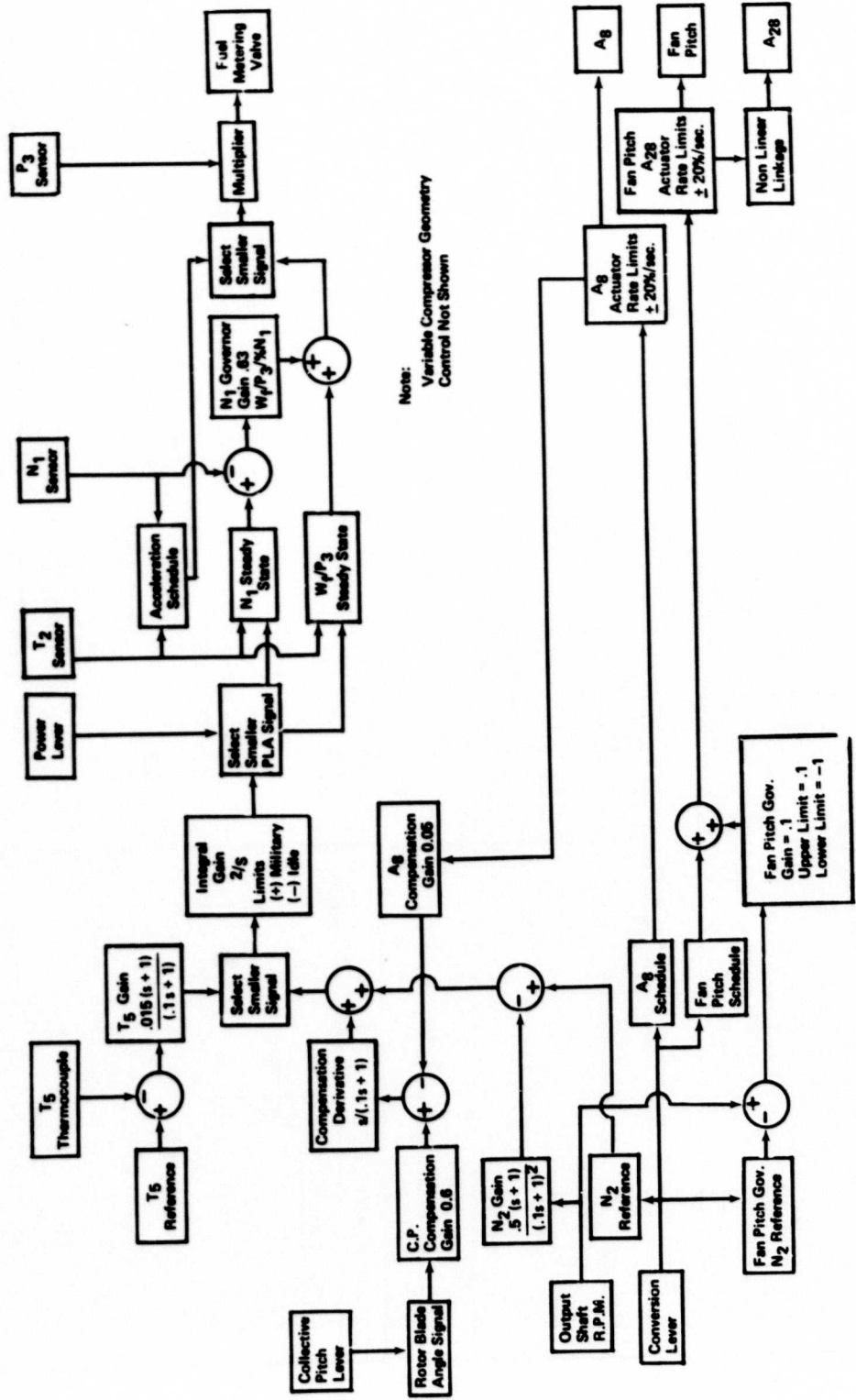


Figure 33. Fan/Shaft Engine Control System.

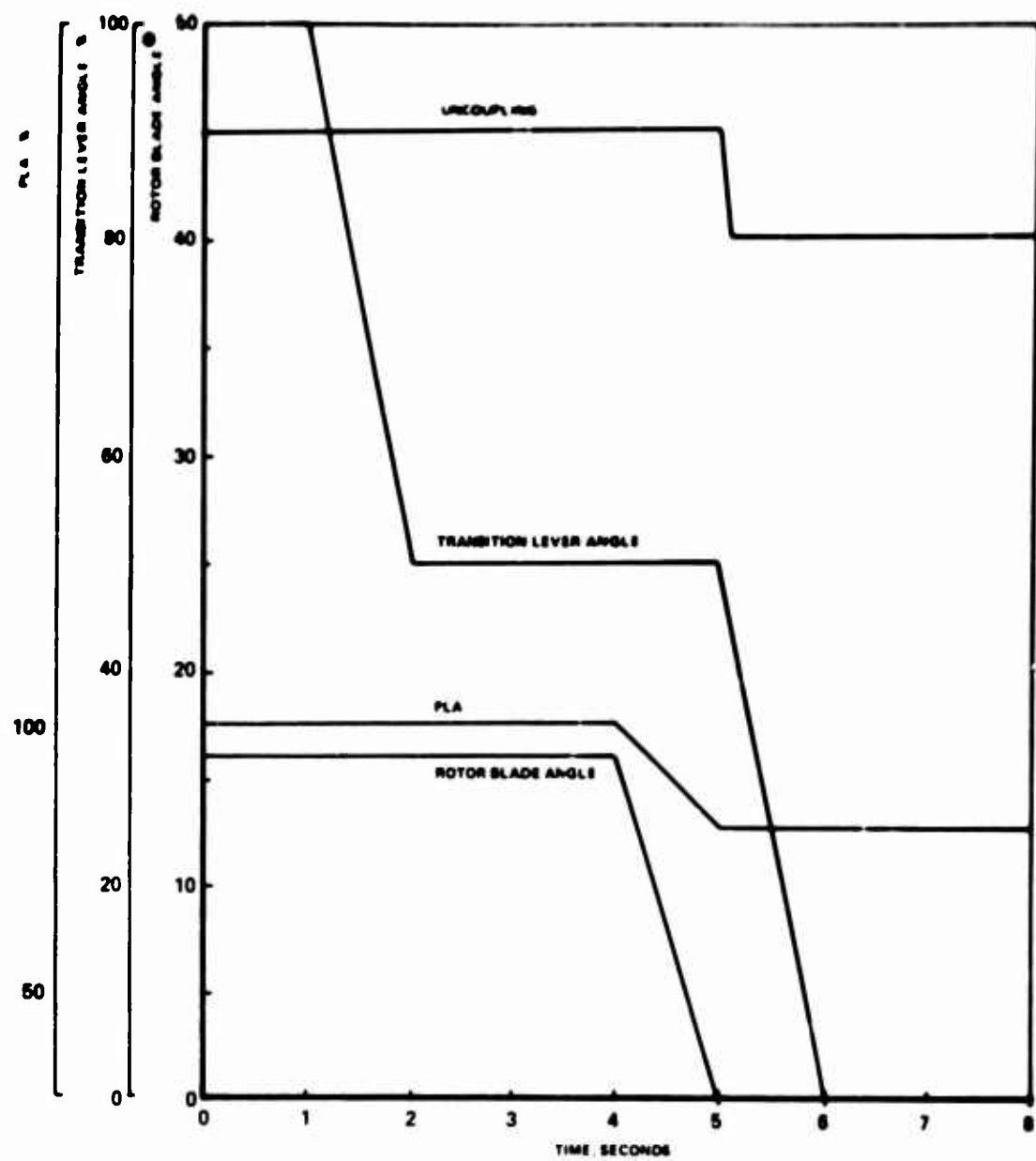


Figure 34a. Time History Shaft to Fan Conversion, Rotor Vertical.

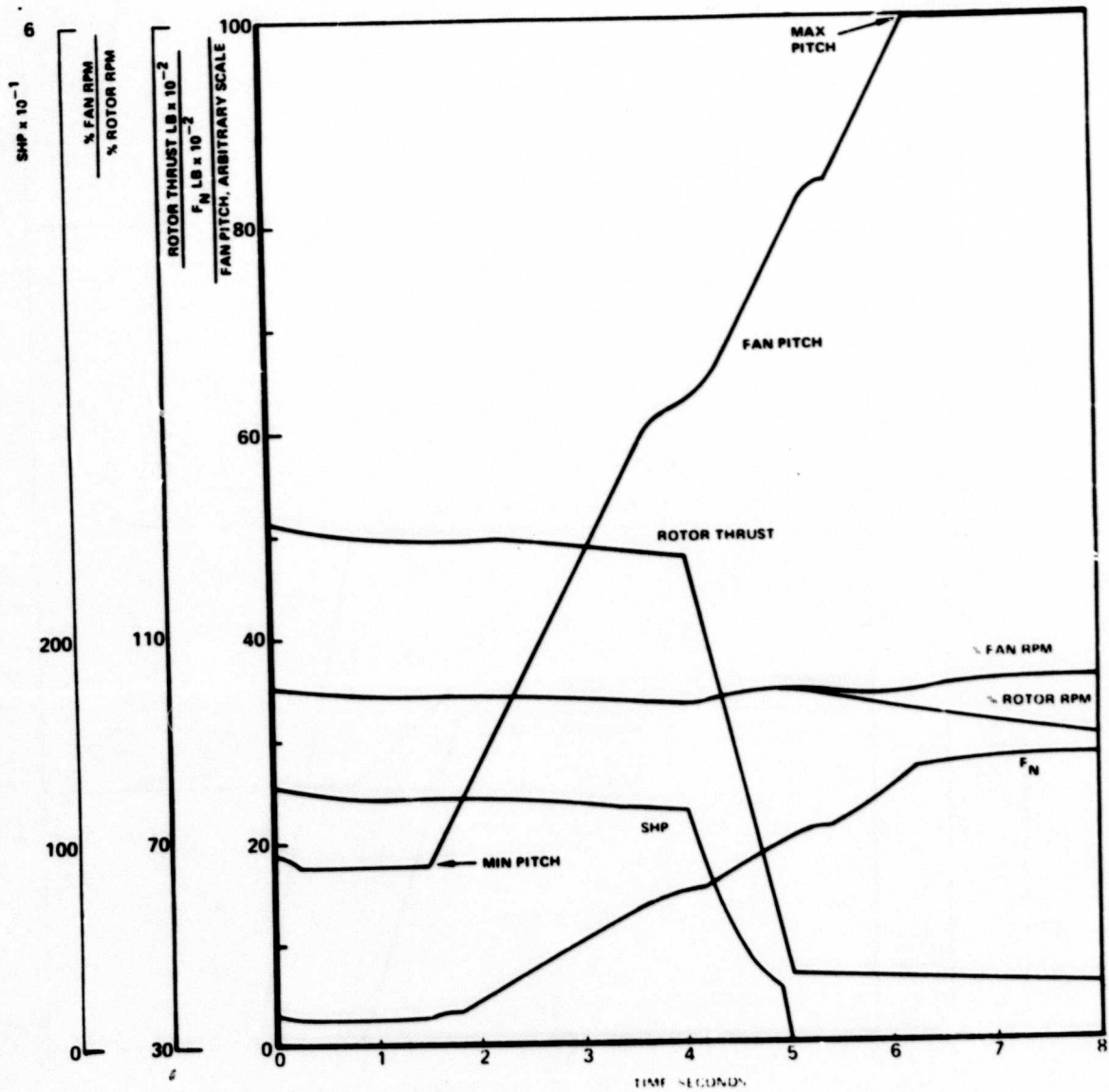


Figure 34b. Time History Fan to Shaft Conversion, Rotor Vertical.

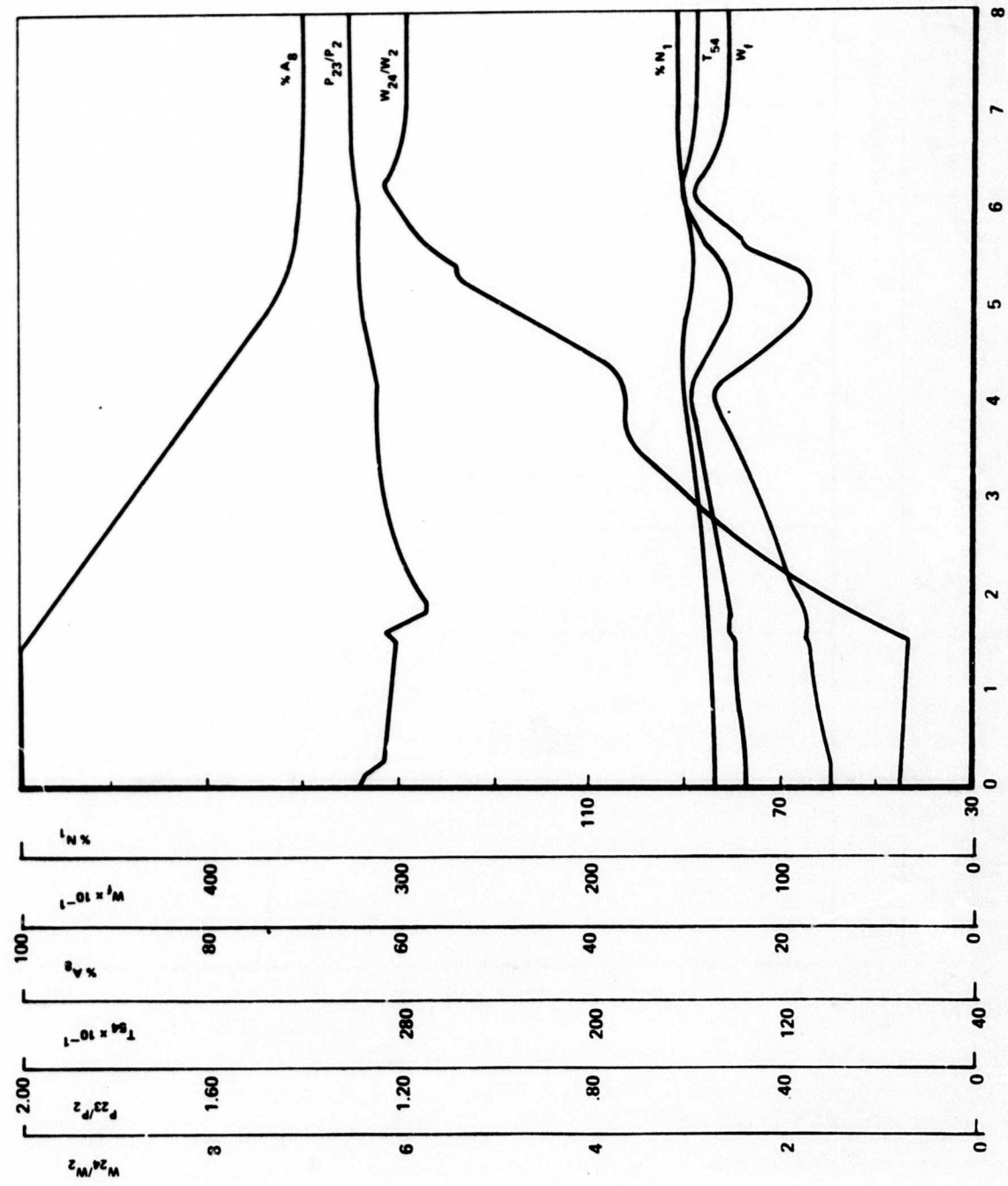


Figure 34c. Time History Fan to Shaft Conversion, Rotor Vertical.

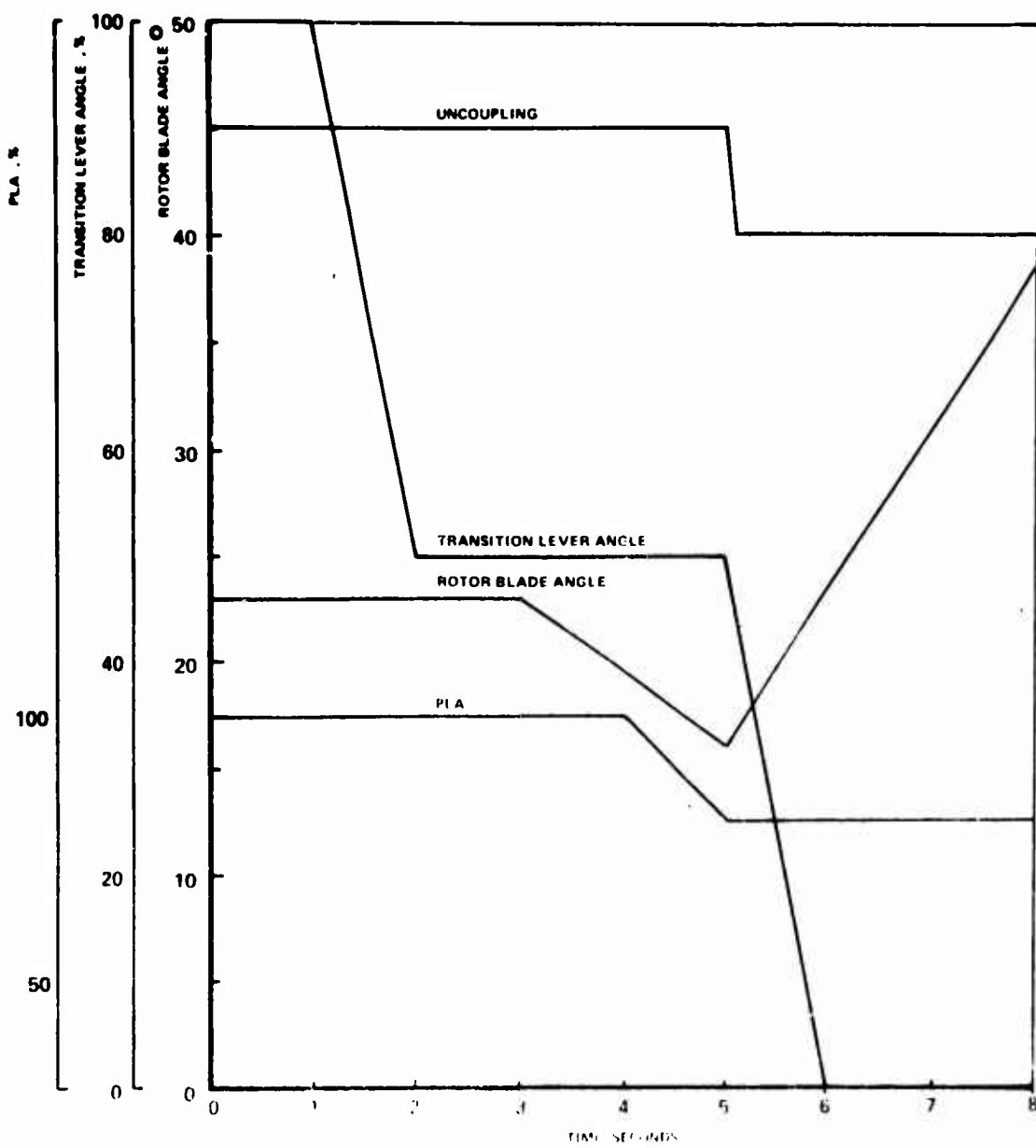


Figure 35a. Time History Shaft to Fan Conversion, Rotor Horizontal.

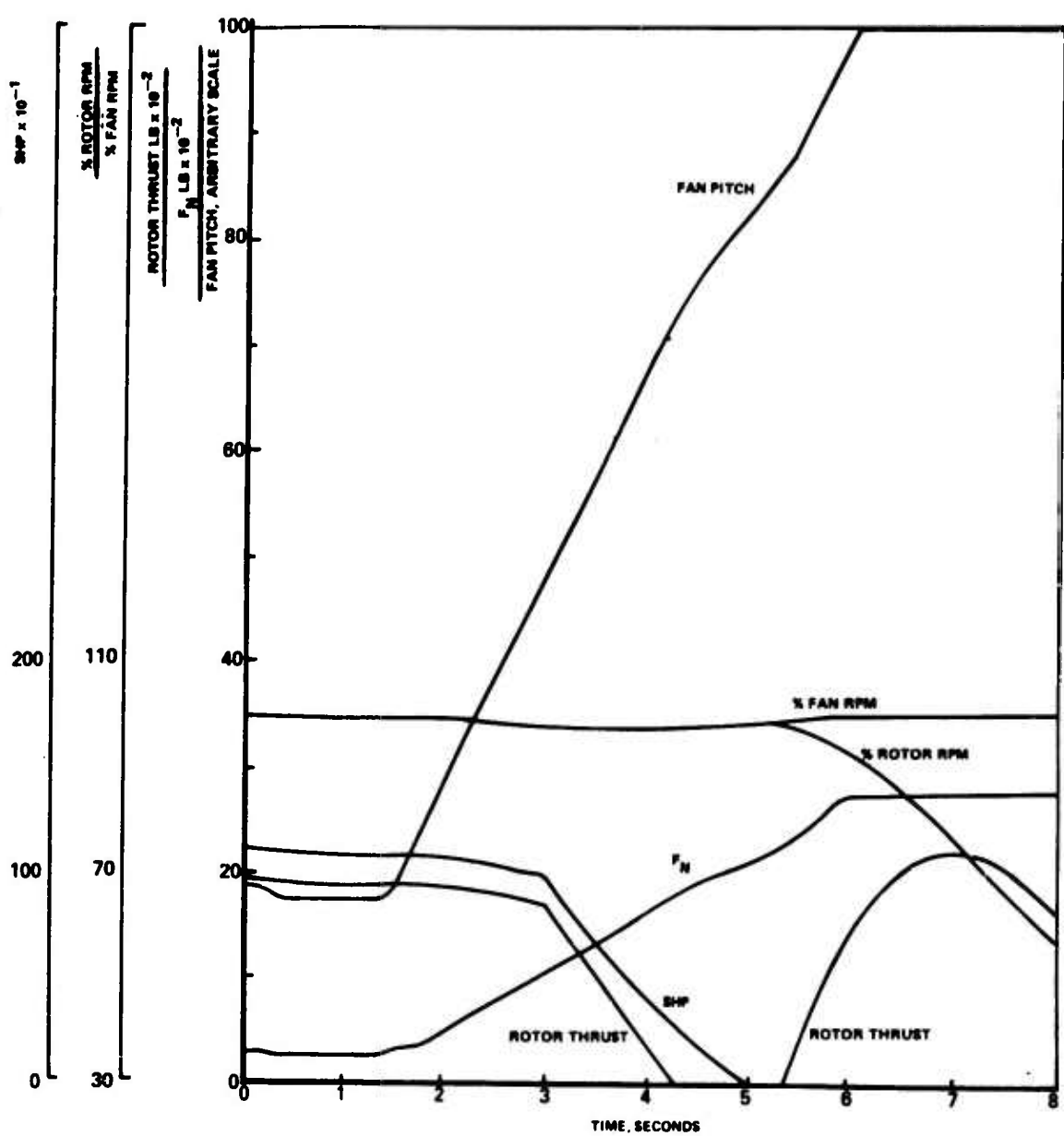


Figure 35b. Time History Shaft to Fan Conversion, Rotor Horizontal.

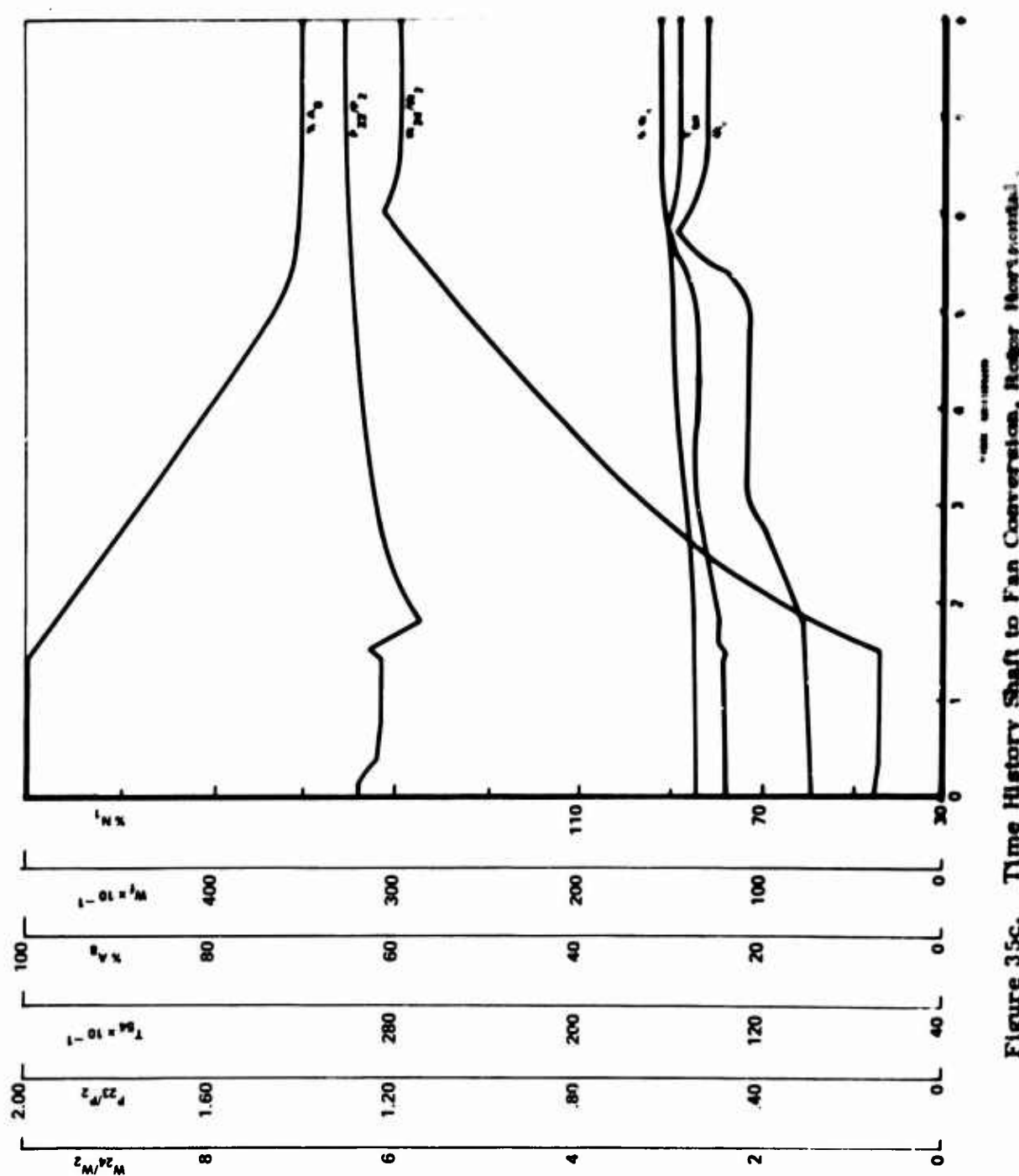


Figure 35c. Time History Shaft to Fan Connection, Rotor Horizontal.

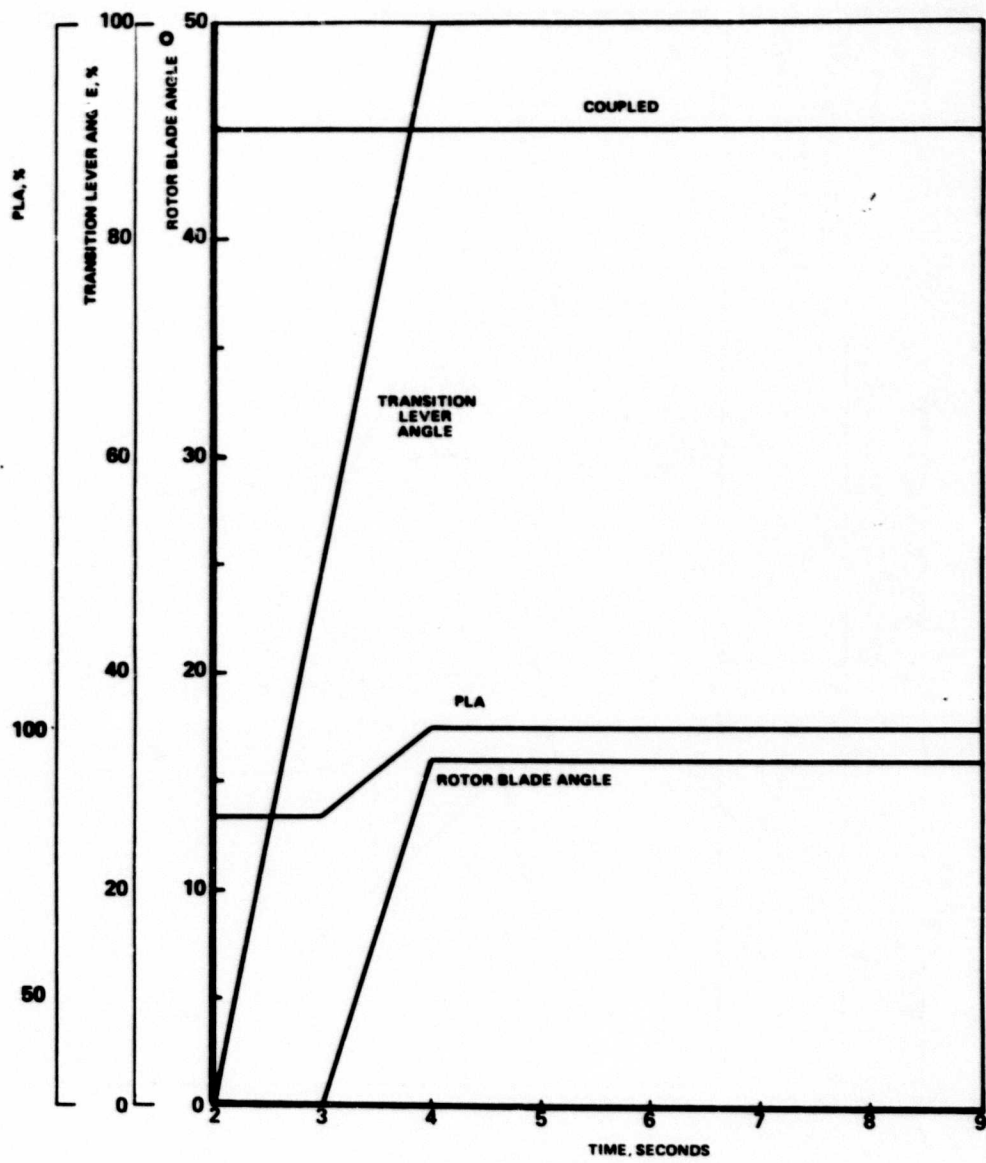


Figure 36a. Time History Shaft to Fan Conversion, Rotor Vertical.

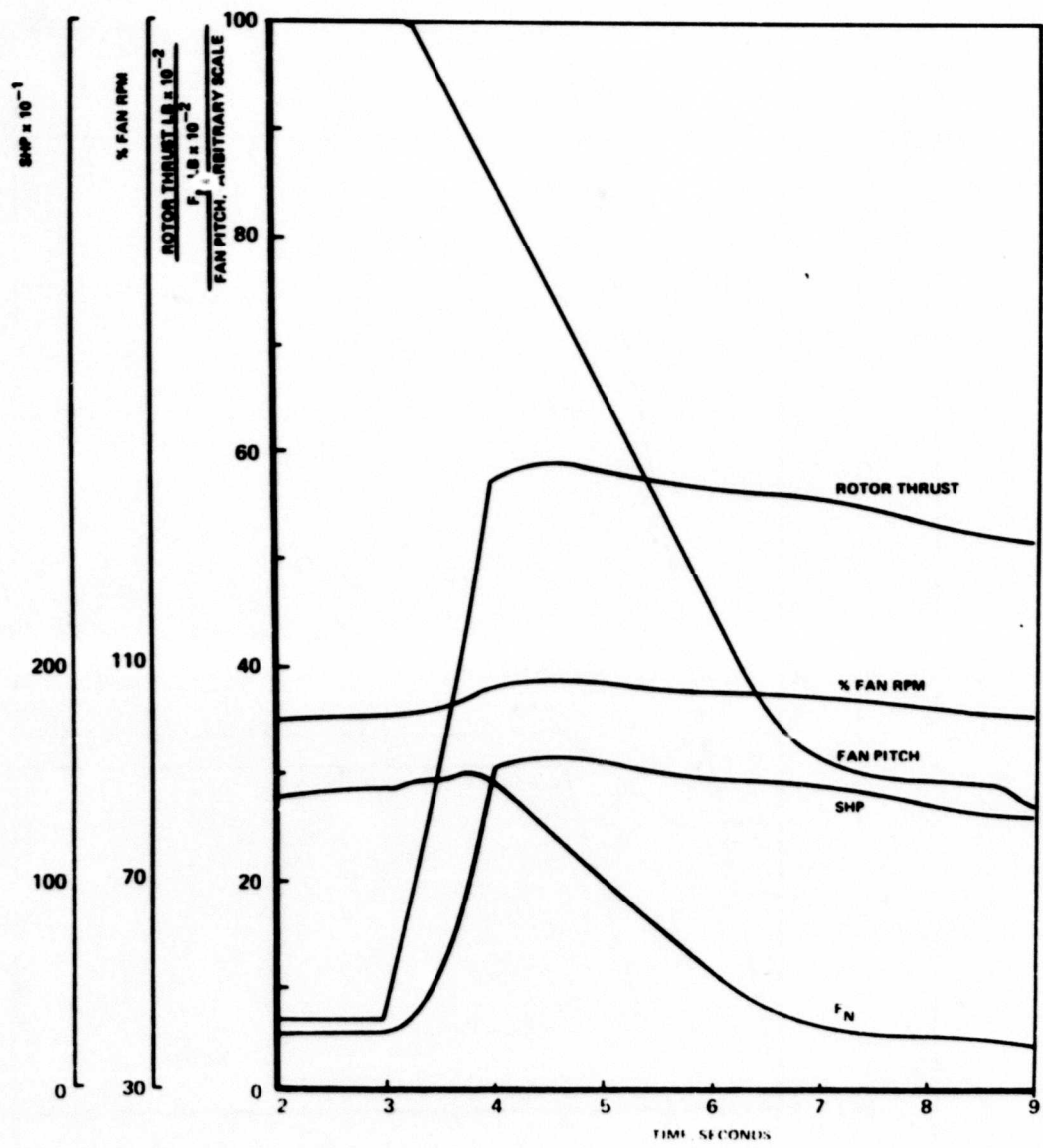


Figure 36b. Time History Fan to Shaft Conversion, Rotor Vertical.

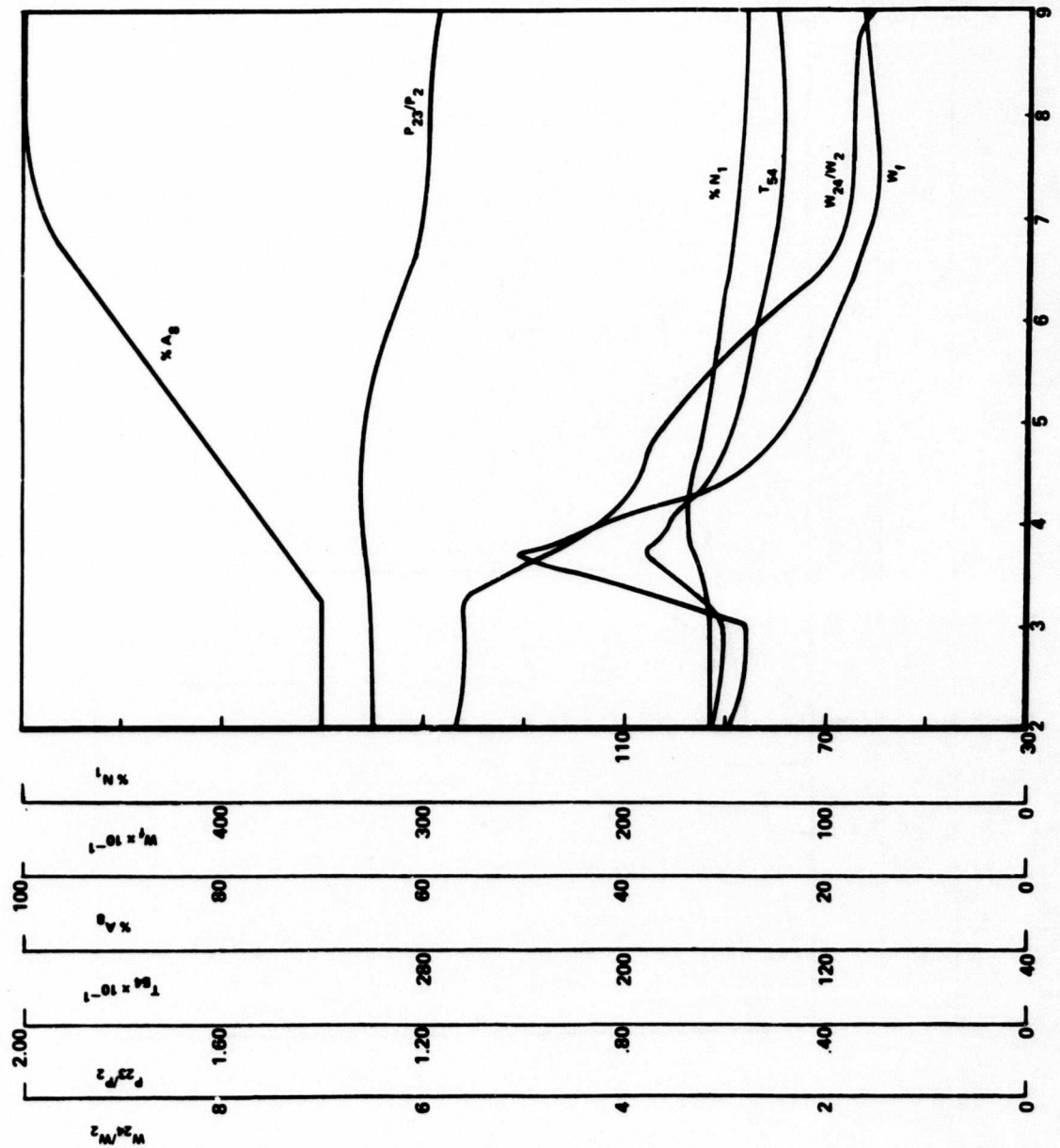


Figure 36c. Time History Shaft to Fan Conversion, Rotor Vertical.

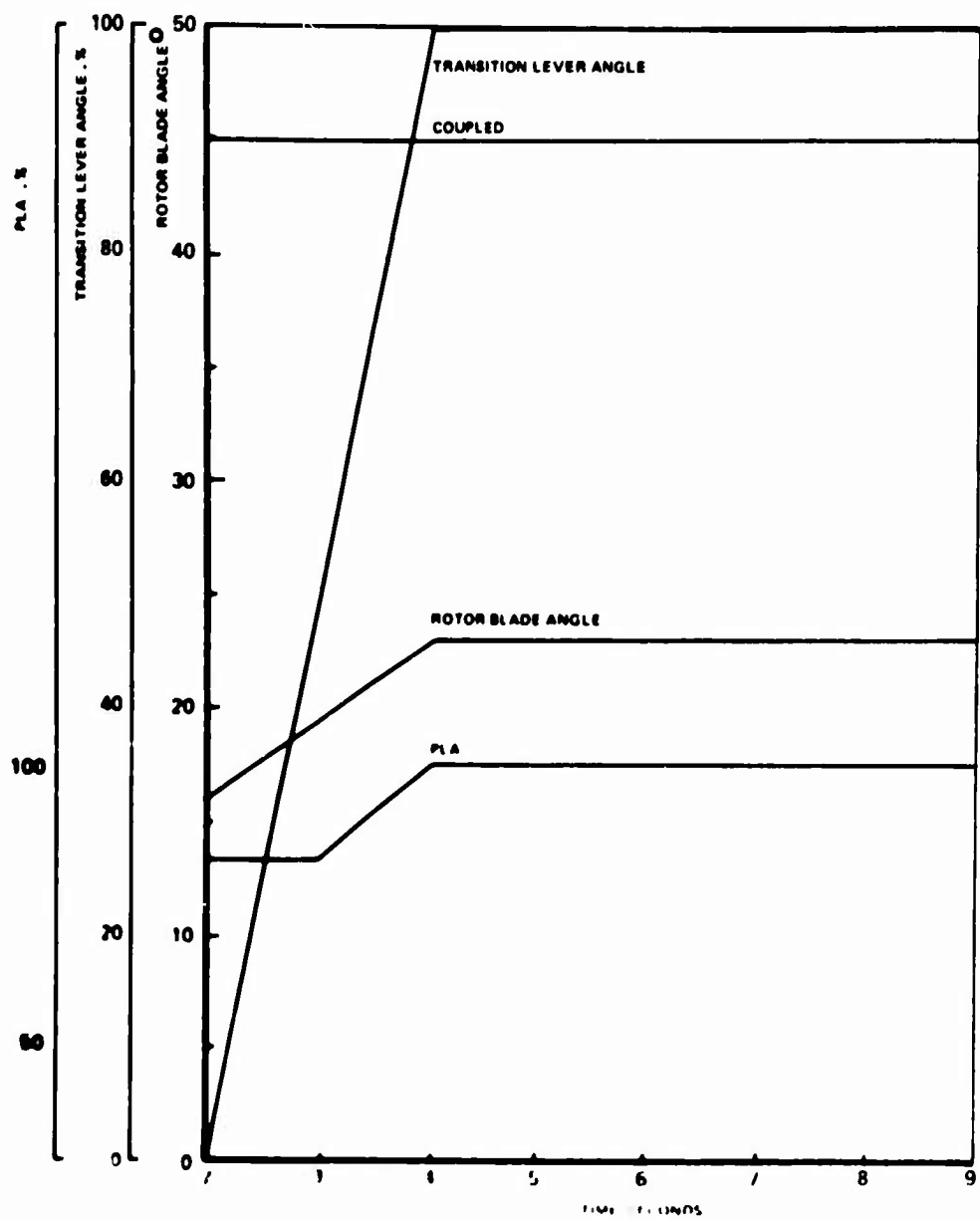


Figure 37a. Time History Fan to Shaft Conversion, Rotor Horizontal

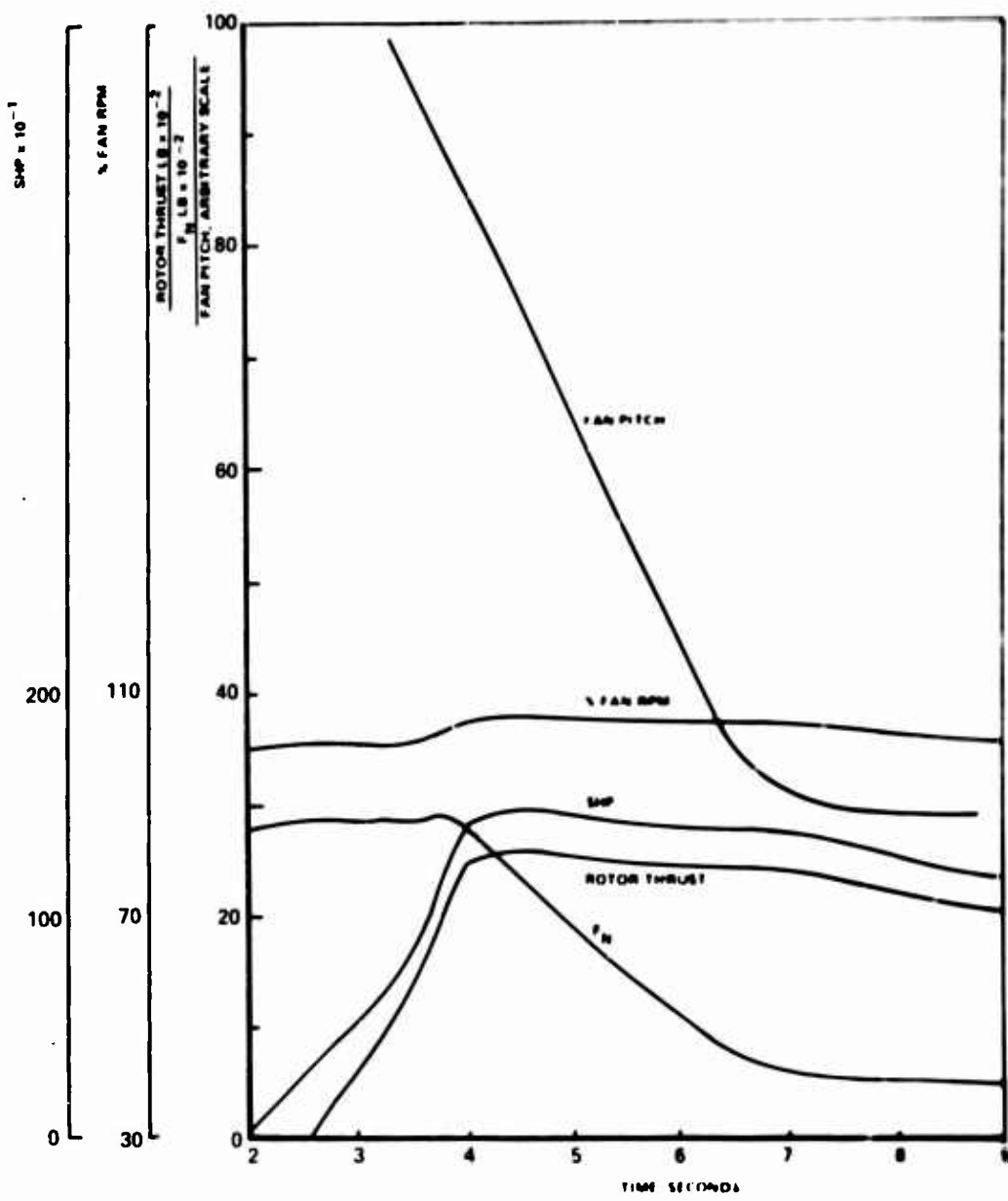


Figure 37b. Time History Fan to Shaft Conversion, Rotor Horizontal.

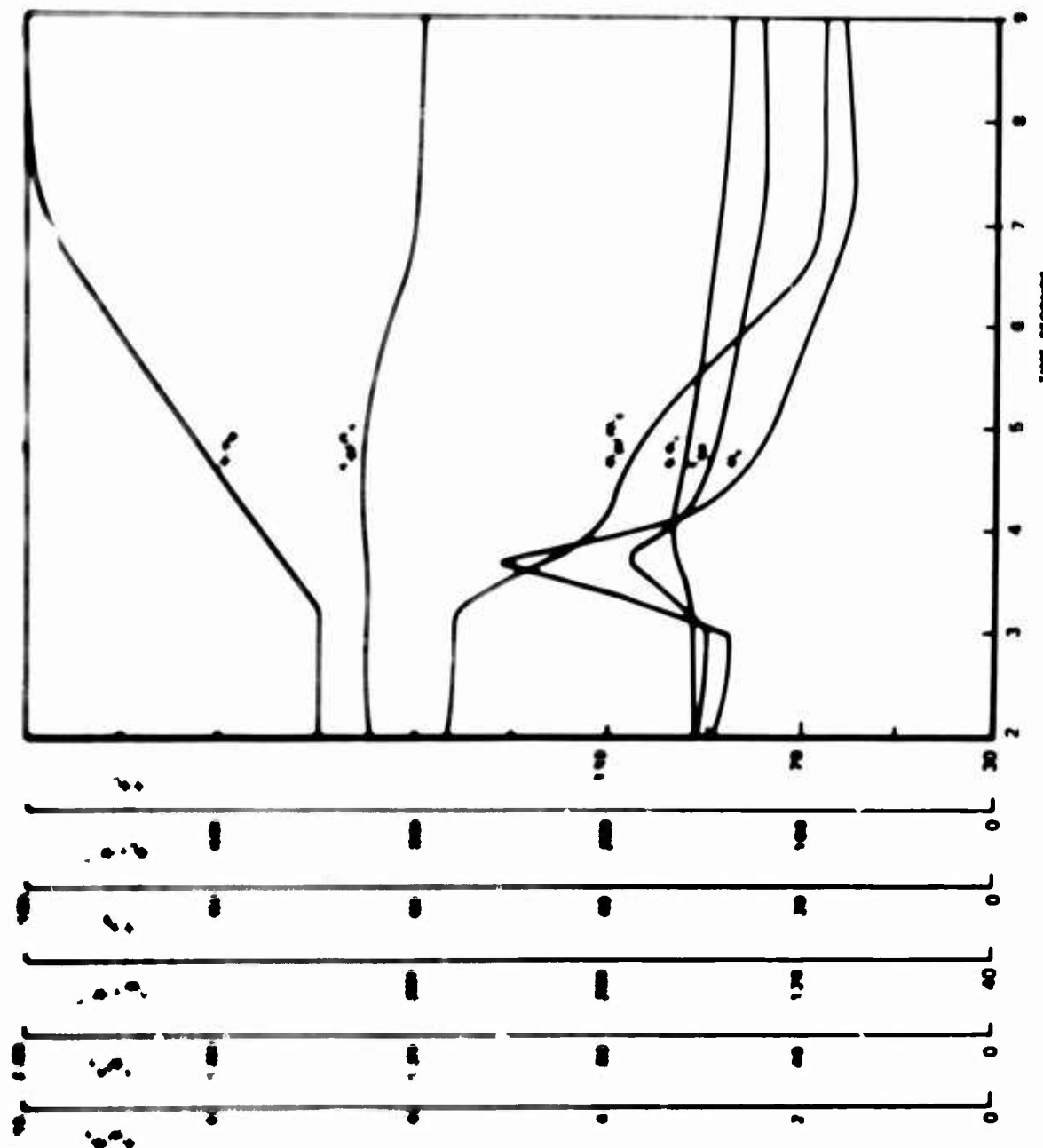


Figure 37c. Time History Fan to Shaft Conversion, Rotor Horizontal.

mode between (1) output shaft speed governing for shaft mode operation and (2) power lever control of gas generator power for fan mode operation.

The fuel control and electrical control are essentially similar to an existing shaft engine control system with minor adaptation to allow conversion to and from a shaft engine system. The conversion control provides those additional major functions required for conversion of engine geometry. The functions of each control in each mode of operation are outlined in Figure 32. The conversion control provides (1) control of engine exhaust area (A_e) and (2) control of fan pitch angle and bypass exit area (A_{2e}), both as required by the position of the cockpit conversion lever.

Figure 33 is a detailed control system block diagram interrelating the fuel control electrical control and conversion control functional details.

Figure 38 shows some of the scheduled parameters most significant to engine conversion.

DISCUSSION OF CONVERSION TRANSIENTS

Figure 34 shows a conversion from shaft mode to fan mode for an airframe whose rotor axis is stowed in a vertical orientation. Figure 34(a) shows the sequence of control lever motions assumed for this simulation. The conversion lever was first moved halfway to call for the change of fan pitch and A_e required in the fan mode. Figure 34(b) shows the resulting increase in engine thrust. Figure 34(a) shows that airframe rotor blade angle was next reduced to achieve near-zero torque and that the power lever was retarded to a position to suitably limit fan mode power. Figure 34(c) shows a reduction of fuel flow resulting from the action of the collective pitch rate signal which counteracts the tendency toward overspeeding following a shaft load reduction. Upon reaching flat pitch, the rotor is uncoupled. Figure 34(b) shows the resulting tachometer split.

After power has been limited by retarding the power lever, the conversion lever motion is completed to disable the N_2 governors and to allow N_1 to be established solely by power lever position. N_2 to be established by gas generator power, and fan pitch to be established by the conversion lever schedule. Figures 34(b) and 34(c) show fan pitch and A_e changing over approximately a 5-second interval in accordance with the slew rate of their actuators. Interruptions of the steady increase in fan pitch are caused by an N_2 governor action to reduce loading during an incipient underspeed condition. Fuel flow increases through most of the transient as a result of both (1) the N_2 governor underspeed condition calling for an increasing N_1 setting and (2) the action of the A_e rate signal which counteracts the tendency toward underspeeding as a result of the reduction of turbine torque and increasing fan torque. It is shown that the conversion has been accomplished without any large excursions of either N_1 or N_2 .

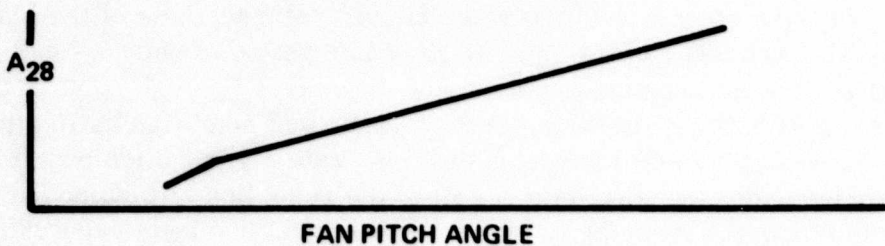
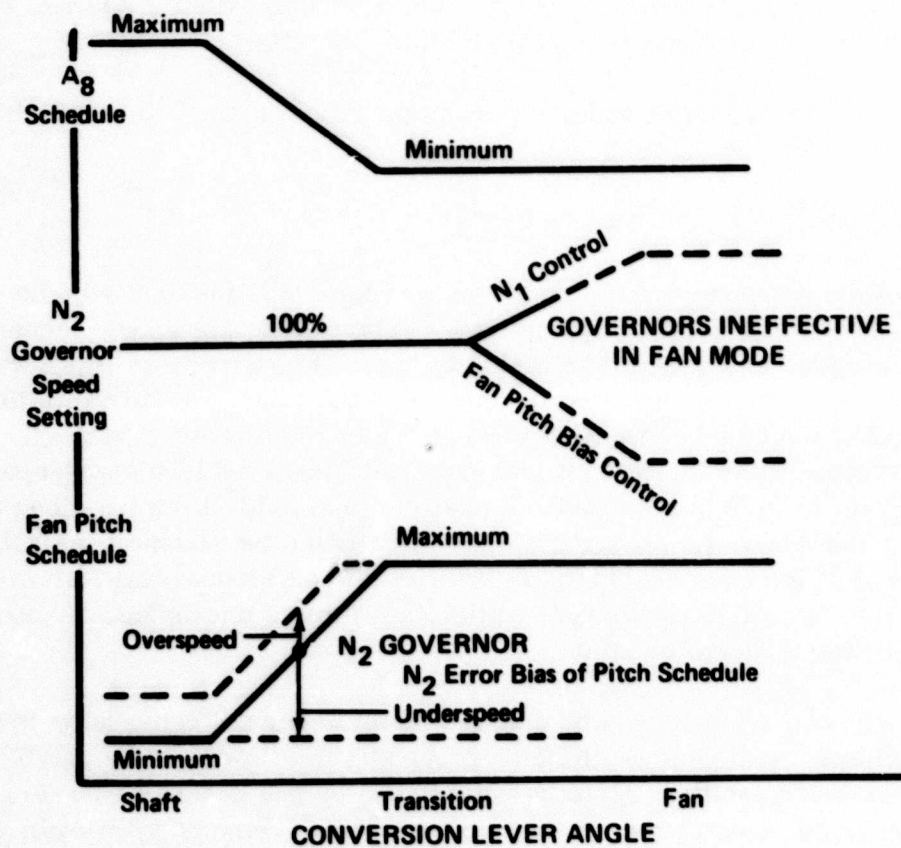
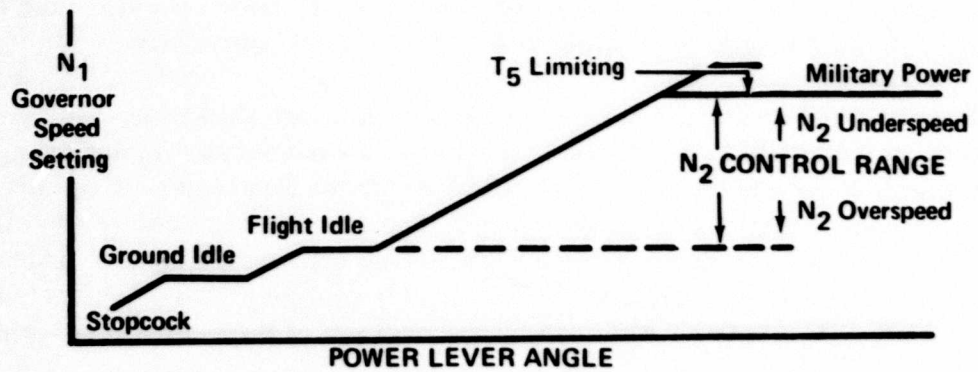


Figure 38. Engine Control Scheduled Parameters.

Figure 35 shows a fan-to-shaft mode conversion for an airframe whose rotor axis is horizontal during conversion. The transient calculations assume that the rotor has been turned horizontal prior to zero time. This computation is quite similar to that of the vertically stowed rotor, with the assumption that the airframe rotor is uncoupled and feathered after the blade pitch has been reduced to obtain near-zero shaft loading.

Figures 36 and 37 show fan-to-shaft conversions for vertically and horizontally stowed rotors respectively. It is shown that the control levers may be moved simultaneously, without large excursions of N_1 or N_2 . The increment in fuel flow is caused by the increase of the power lever calling for higher N_1 ; this is then reversed by action of the T_1 and N_2 controls.

The control system has not been optimized but has been developed to show that good conversion performance can be obtained. Sequencing of controls is not important, although more desirable sequencing may be employed, depending on specific airframe requirements.

ENGINE AND CONTROL SIMULATION

Figure 39 is a diagram of the computer simulation of the control system. Figure 40 represents the simulation of the dynamics of the engine rotors and shaft loading. Figure 41 is an example of the simulation of engine components, showing only the aerothermodynamics of the variable-pitch fan. All other engine components, for instance the compressor, are represented in a similar manner but are not shown here, since Figure 41 is typical.

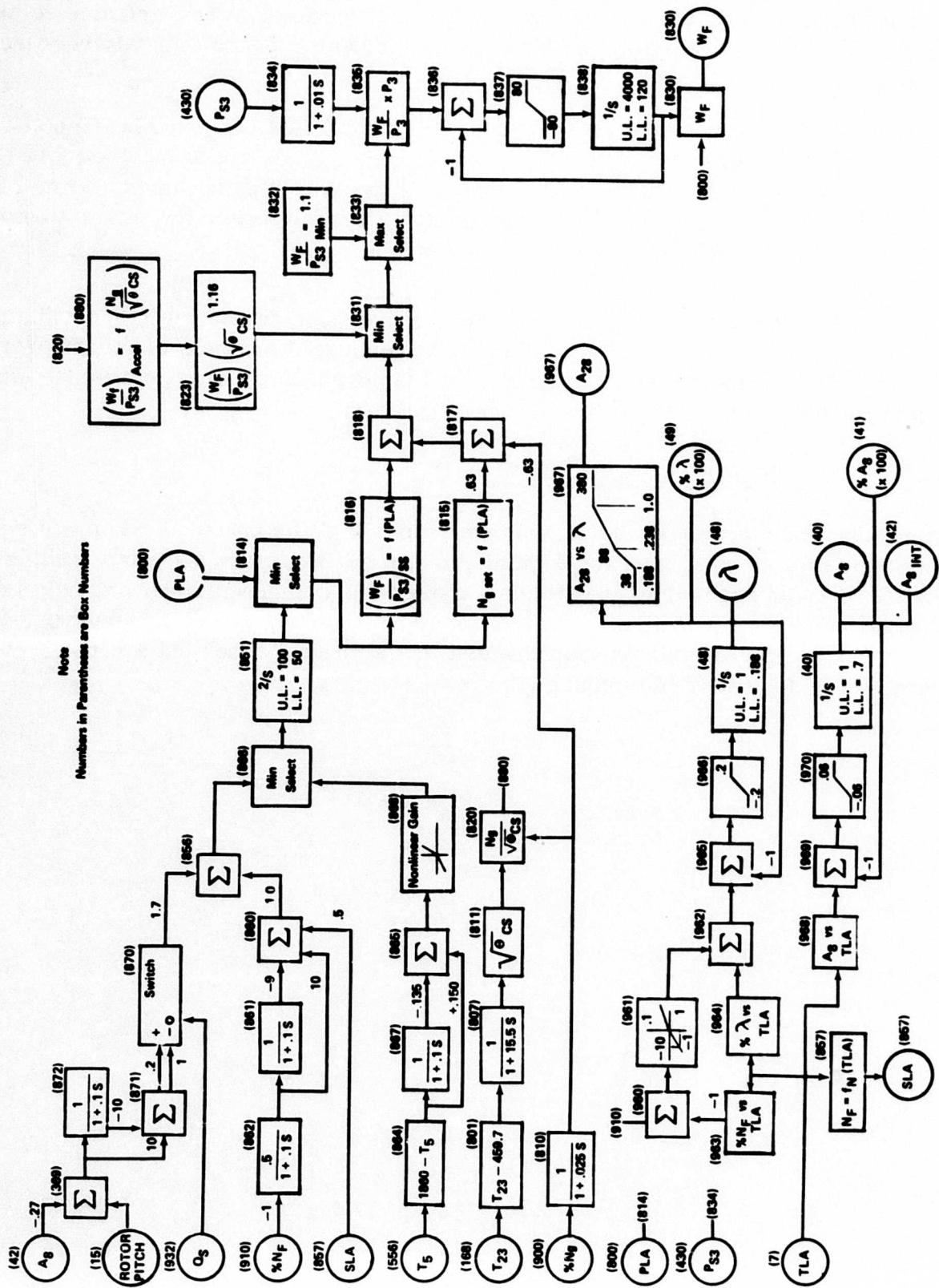


Figure 39. Computer Simulation, Control System.

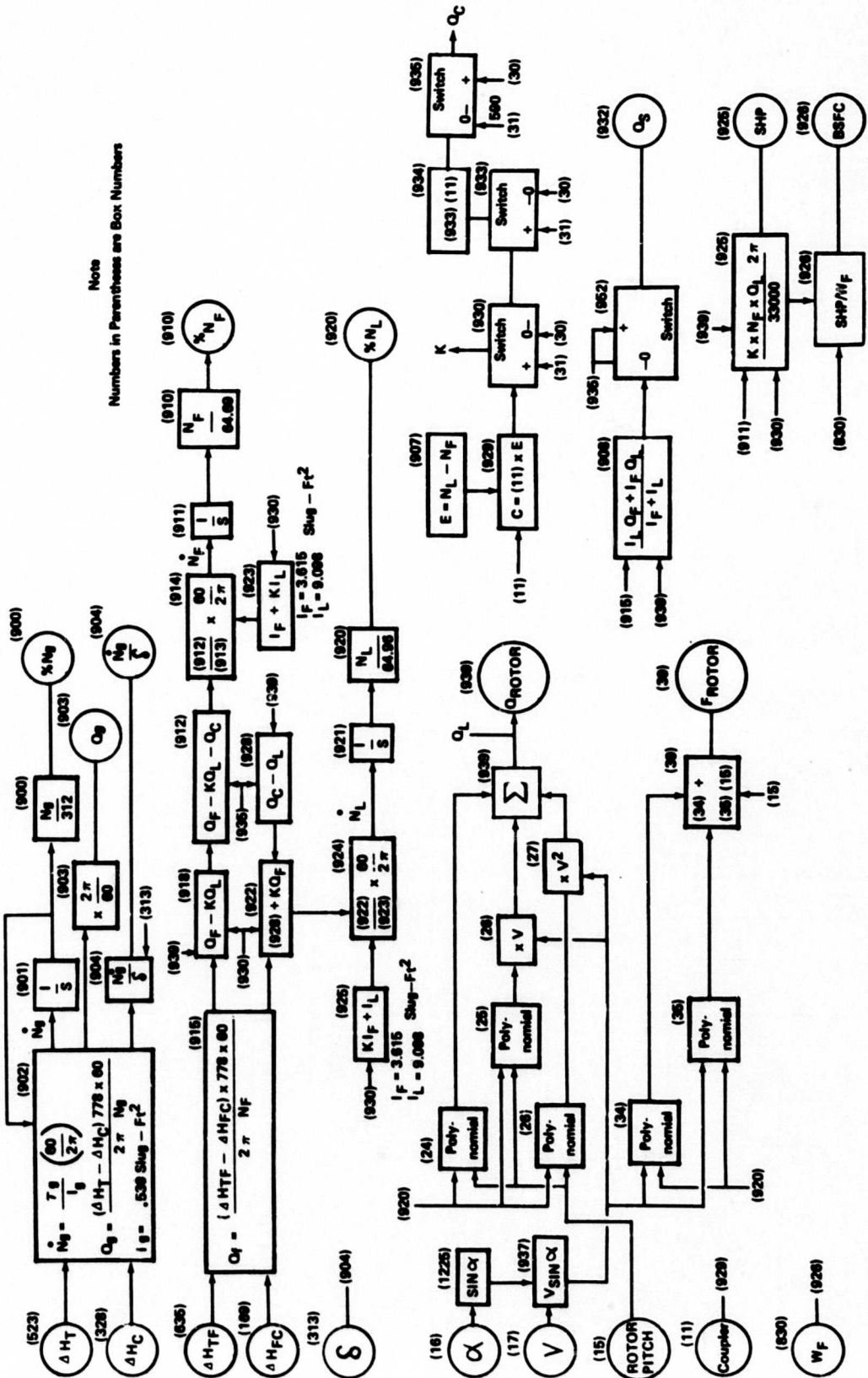


Figure 40. Computer Simulation, Engine Dynamics.

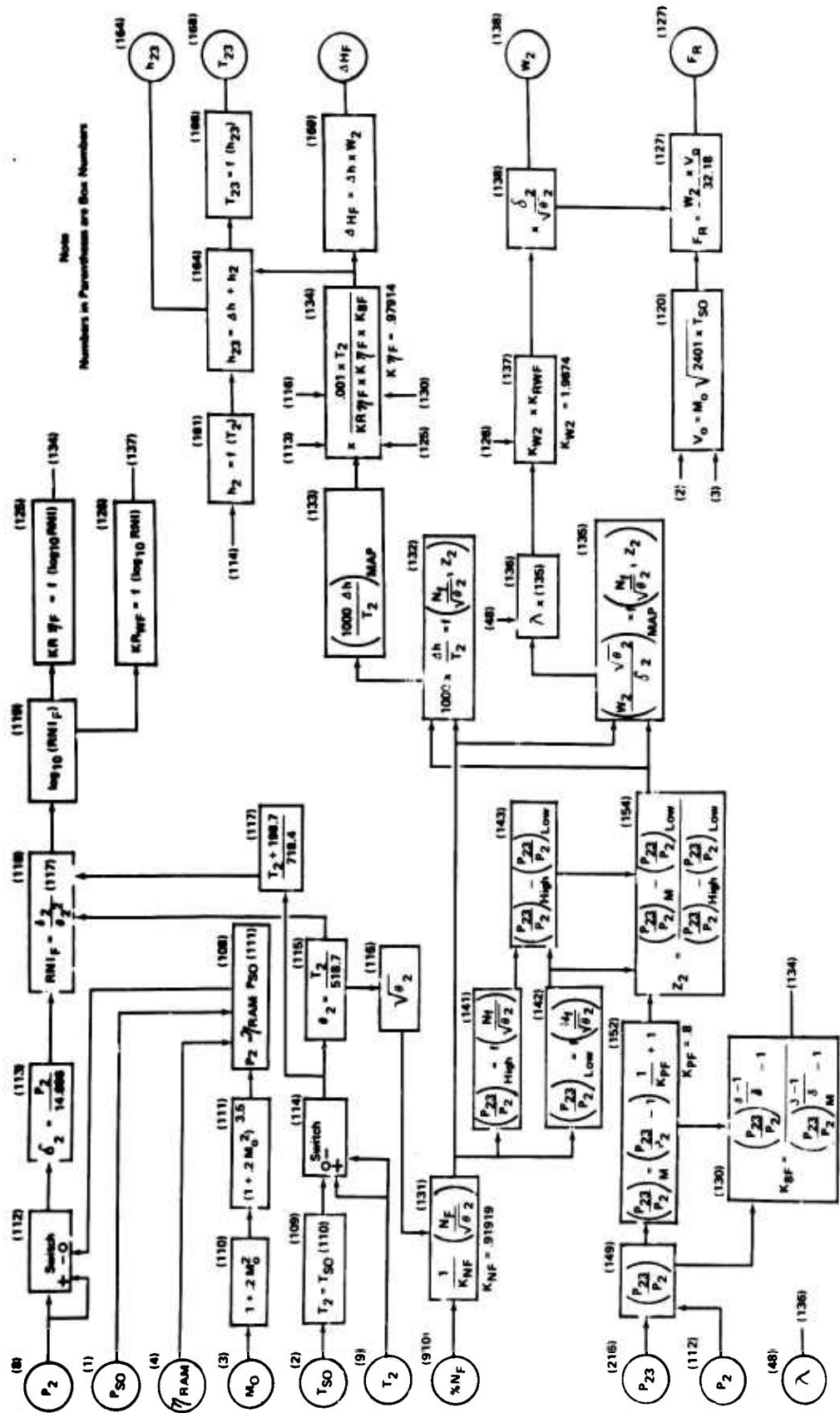


Figure 41. Computer Simulation, Fan.

ENGINE PRELIMINARY DESIGN

Cross-sectional layouts of two versions of the convertible engine are shown in Figures 42 and 43. Figure 42 shows the geared version with shaft power extracted at either side of the engine. Shaft power is extracted directly at the front for the ungeared engine shown in Figure 43.

The bevel gear arrangement designed to extract engine power at either side serves also to reduce fan speed. The pinion drives the larger fan drive gear through two inclined idler gears. Shaft power is extracted from either one of the idler gears. The gears shown have not been analyzed for tooth stresses; they have been drawn to represent loadings similar to those used in Reference 2. A relatively low spiral angle (approximately 12°) is assumed so as to minimize, but never reverse, the axial load on the high-speed pinion. The maximum axial load on the power takeoff gear, or idler, occurs when the full power is transmitted to the fan. Under this condition, the spiral angle does not contribute to this axial load. The fan shaft is flexibly attached to the fan drive gear for transmission of torque and axial load only; it is supported radially in separate roller bearings. The front bearing is softly mounted and damped by an oil film to compensate for possible fan rotor unbalance. The seals for pressurizing the fan rotor pitch actuators fit at the end of the fan shaft, where the diameter, and hence peripheral speed, is low.

The lower speed of the power turbine in the ungeared engine increases the number of stages from two to five. The pressurizing seals are moved to the outside of the shaft, where the peripheral speed is much higher and may cause leakage or heating problems. Figure 44 shows an alternate method of pressurizing the actuators. The transfer tubes extend the full length of the shaft to the rear end, where seals of small diameter are used. Although the small diameter may be necessary to avoid seal problems, the length of the tubes and the consequently large axial displacement to be absorbed by the seals are undesirable features. The front seal location is believed to be preferable.

The gas generator shown for both versions incorporates a compressor of five axial stages with one centrifugal stage at the rear and a turbine of two axial stages. The centrifugal stage avoids the very low blade height that would be required at the rear of a fully axial compressor and reduces the engine length. Its increased diameter fits within the bypass flowpath without any particular compromise. Selection of an axicentrifugal compressor is directly related to the specific sizing requirement of the study; if a larger engine were required, the alternative of an all-axial compressor would be available.

A set of double-hinged flaps on the exhaust bullet varies the gas generator exhaust nozzle area (A_s). Since the shape of the bullet is critical only in the cruise condition, the construction of the flaps is simple - they do not overlap. They fit in slots in the bullet to form a smooth surface in the cruise condition. They reduce the area by moving outward to form a series of obstructions at the nozzle throat

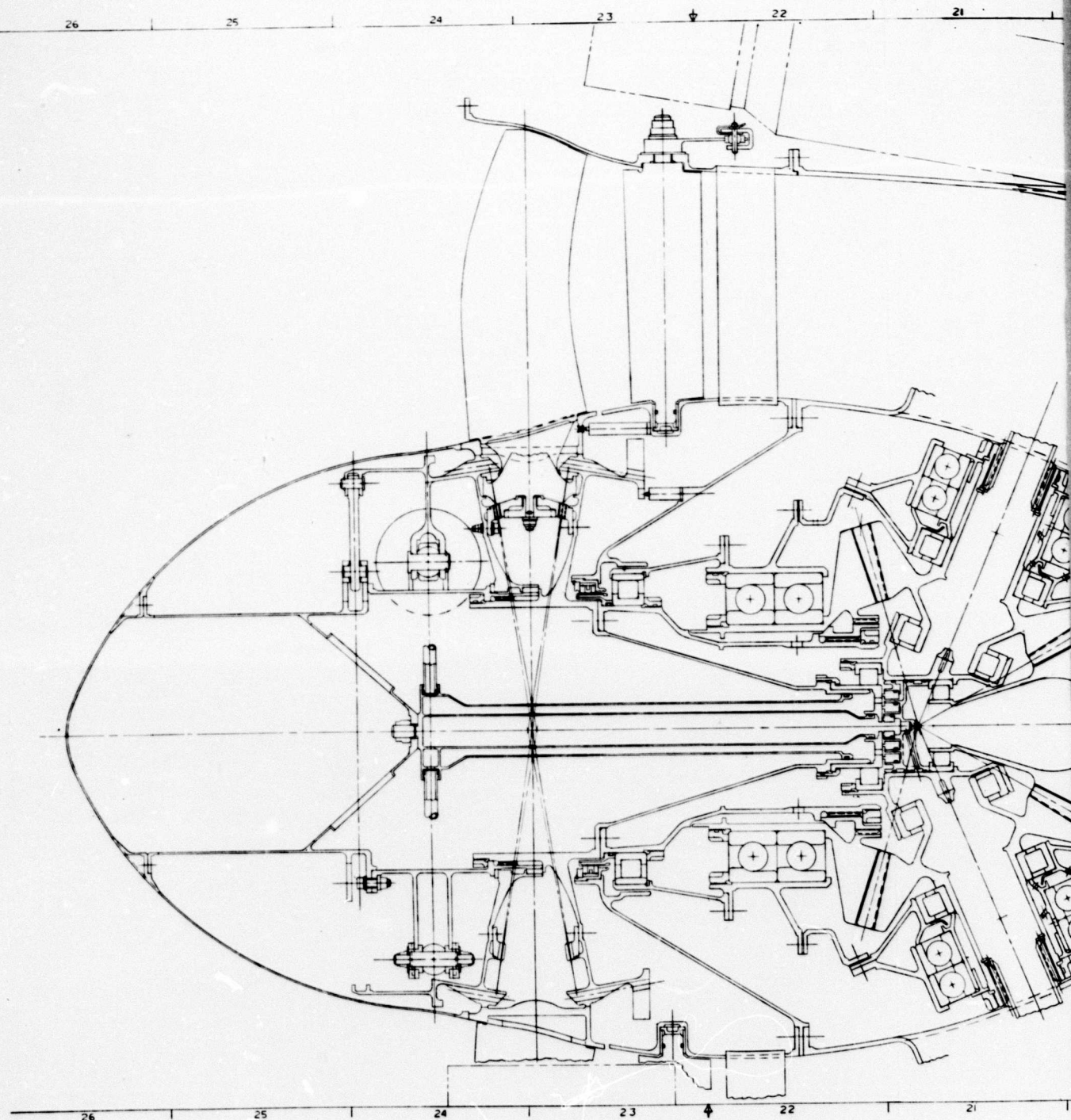
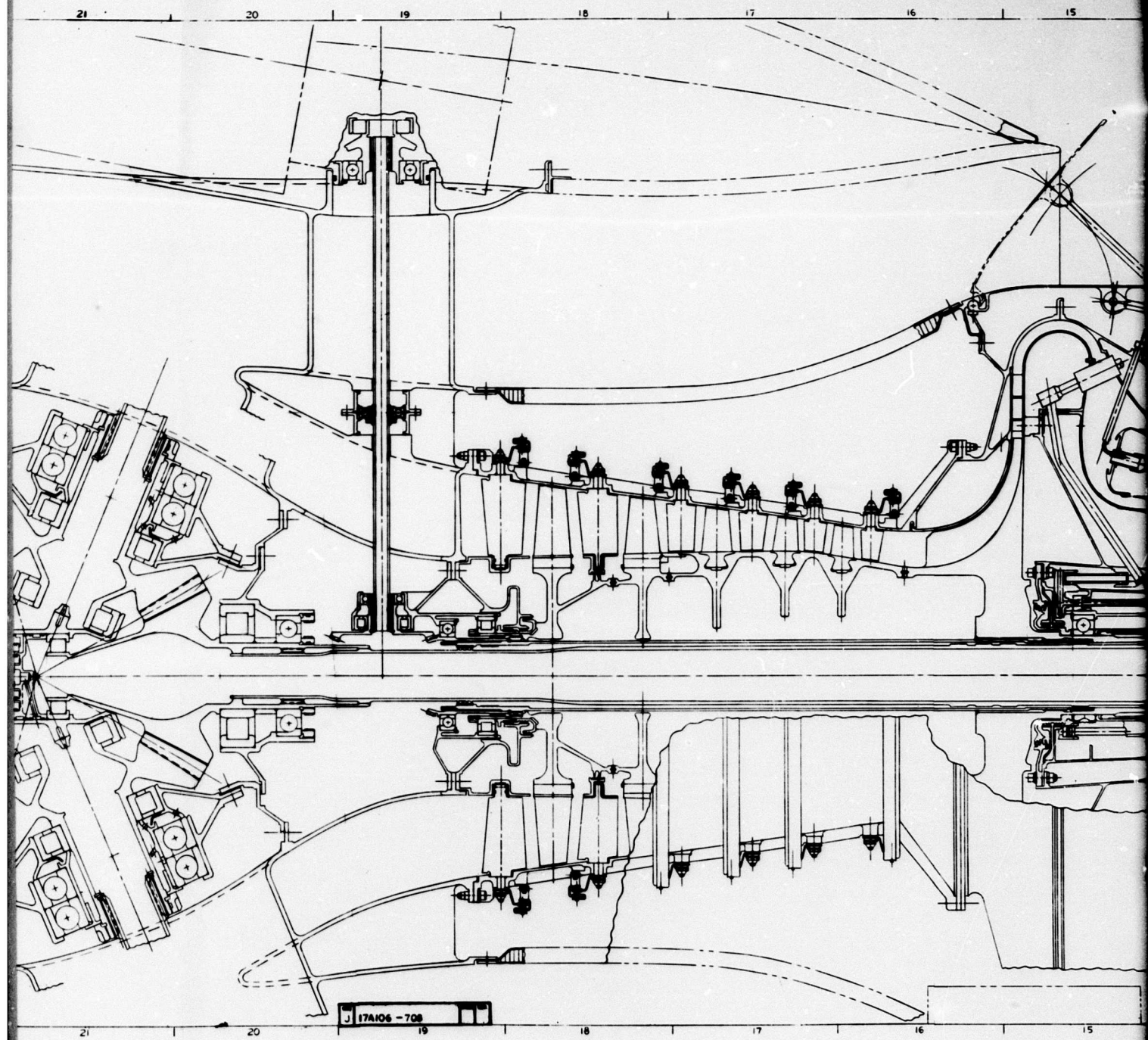
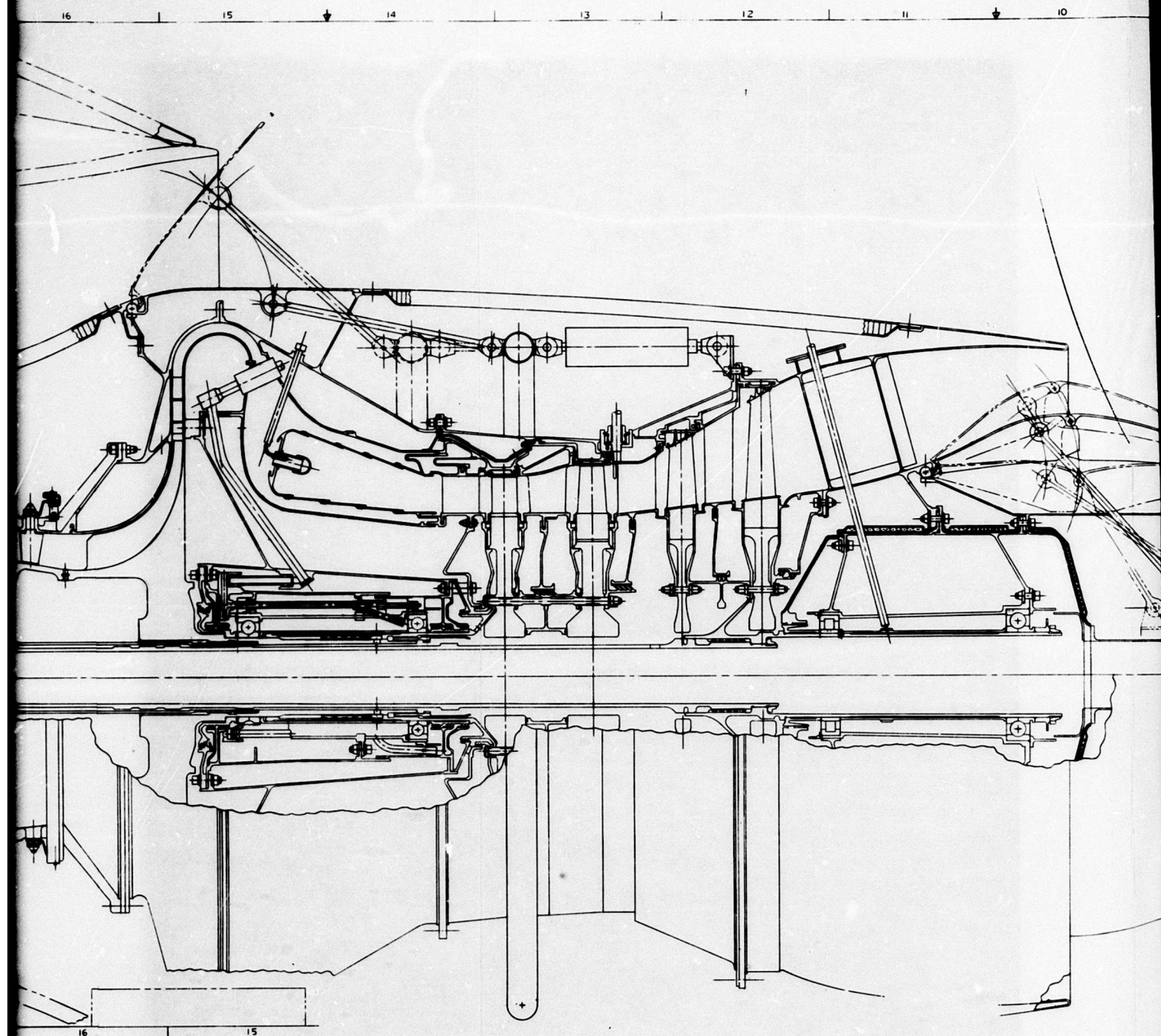


Figure 42. Cross Section, Geared Engine.





13

12

11

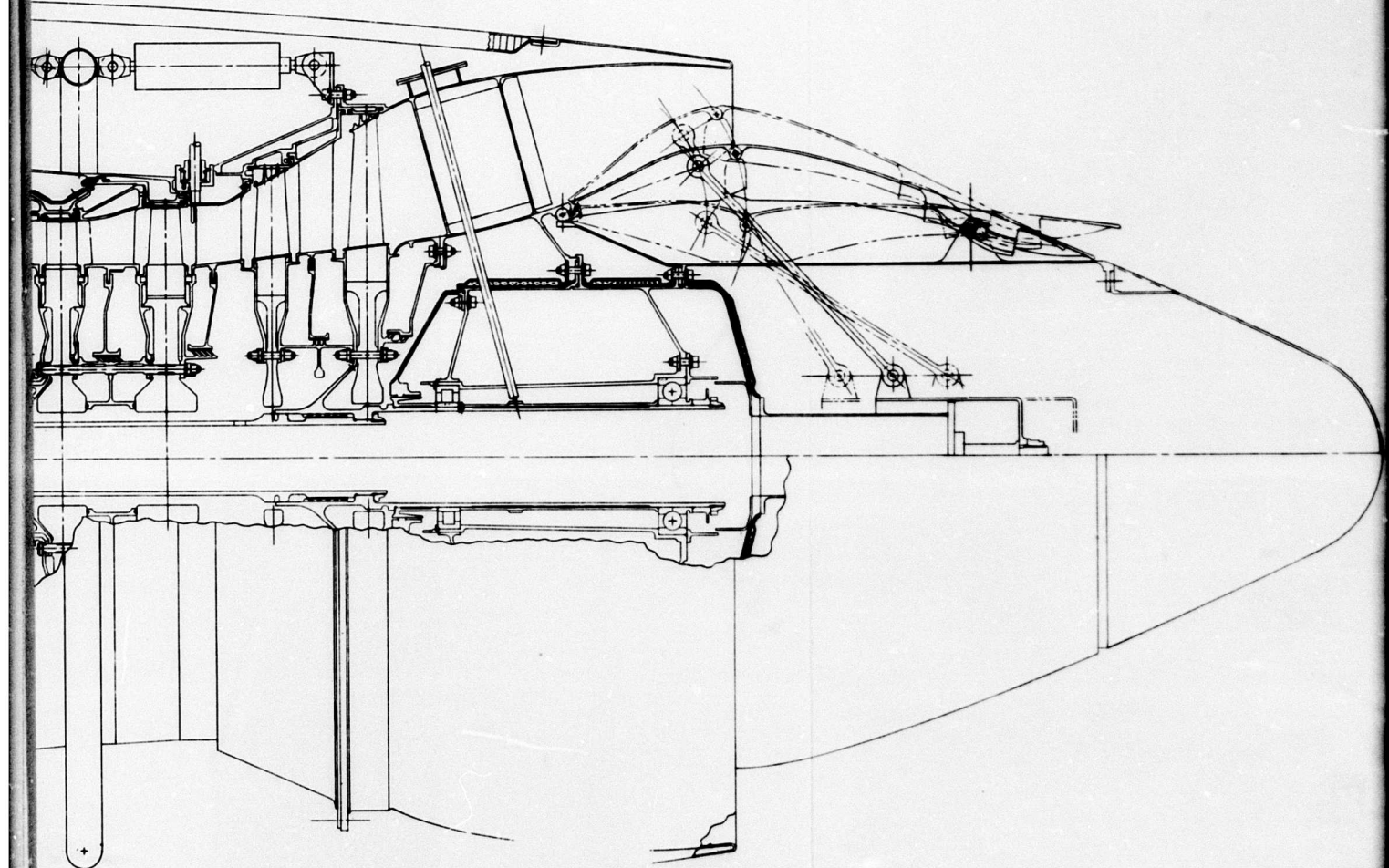
↓

10

9

8

7



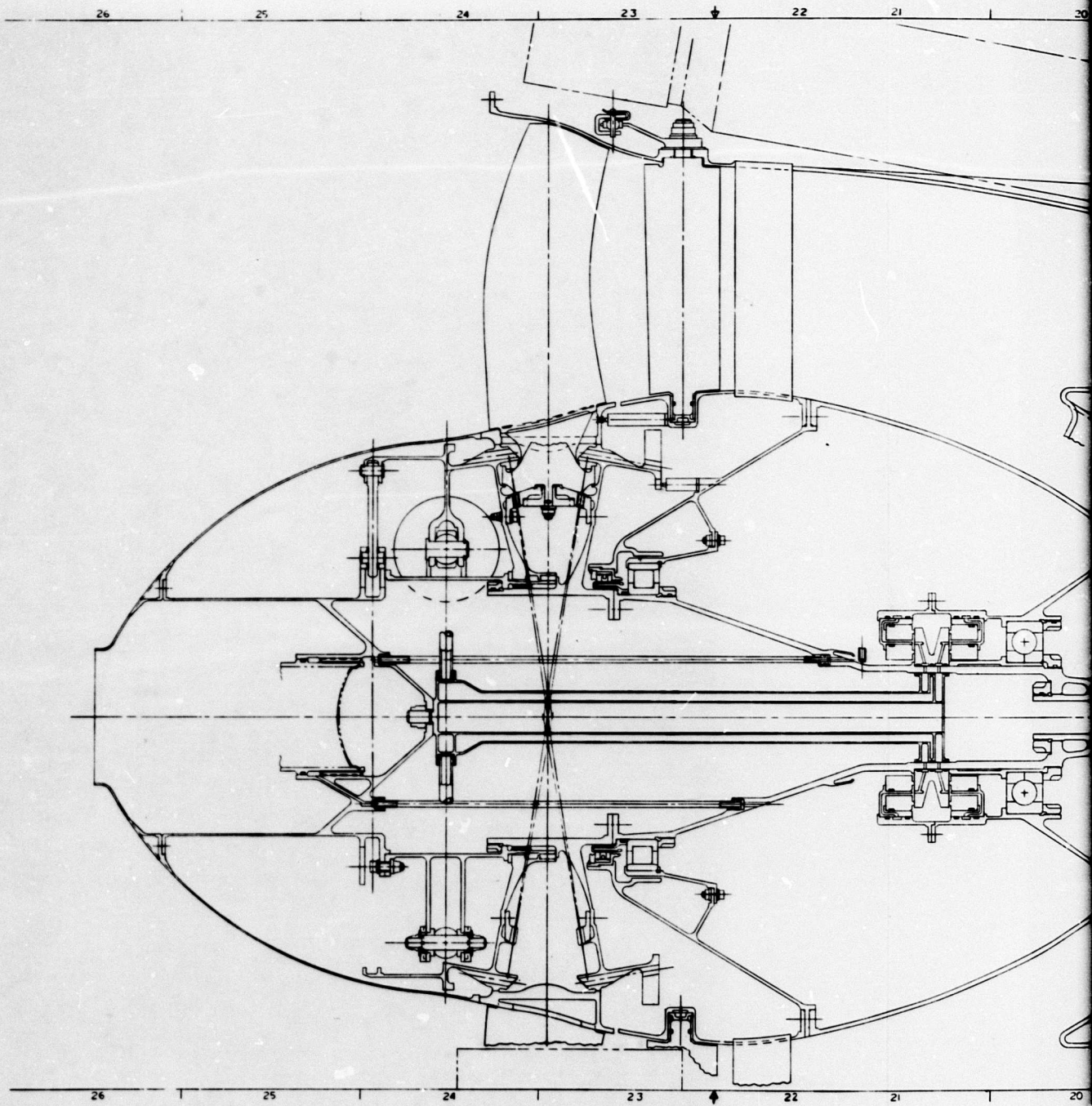
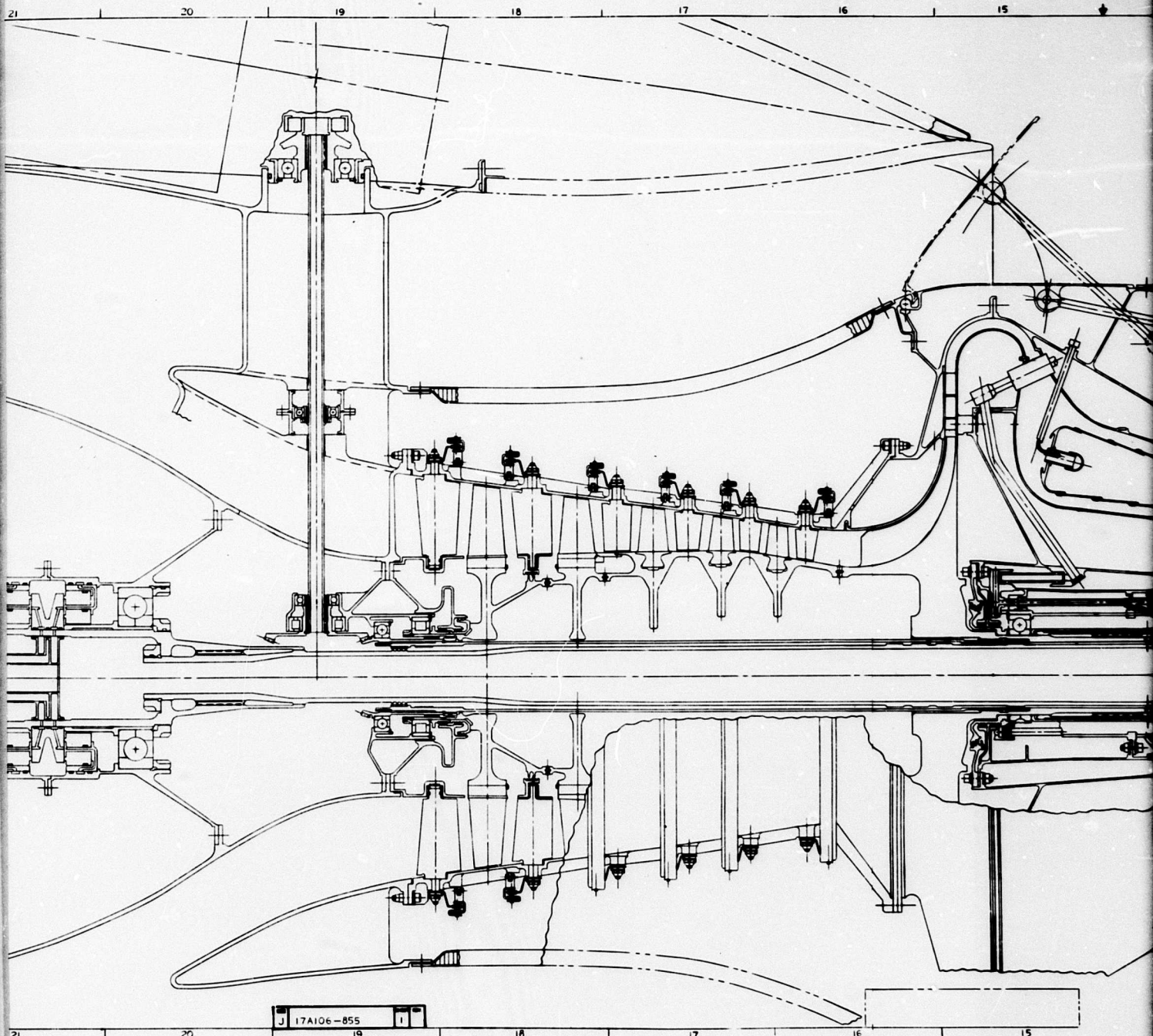
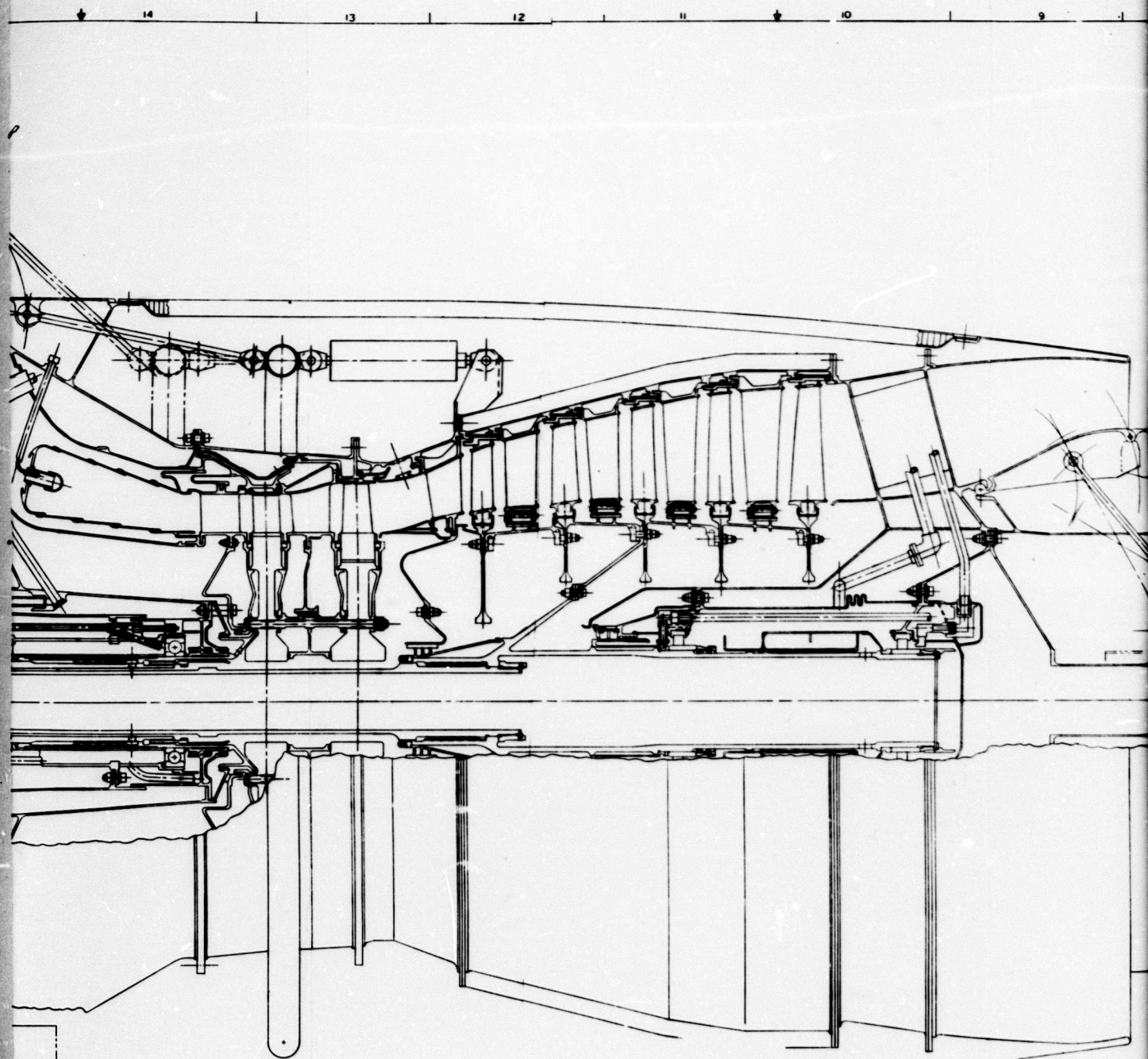


Figure 43. Cross Section, Ungeared Engine.

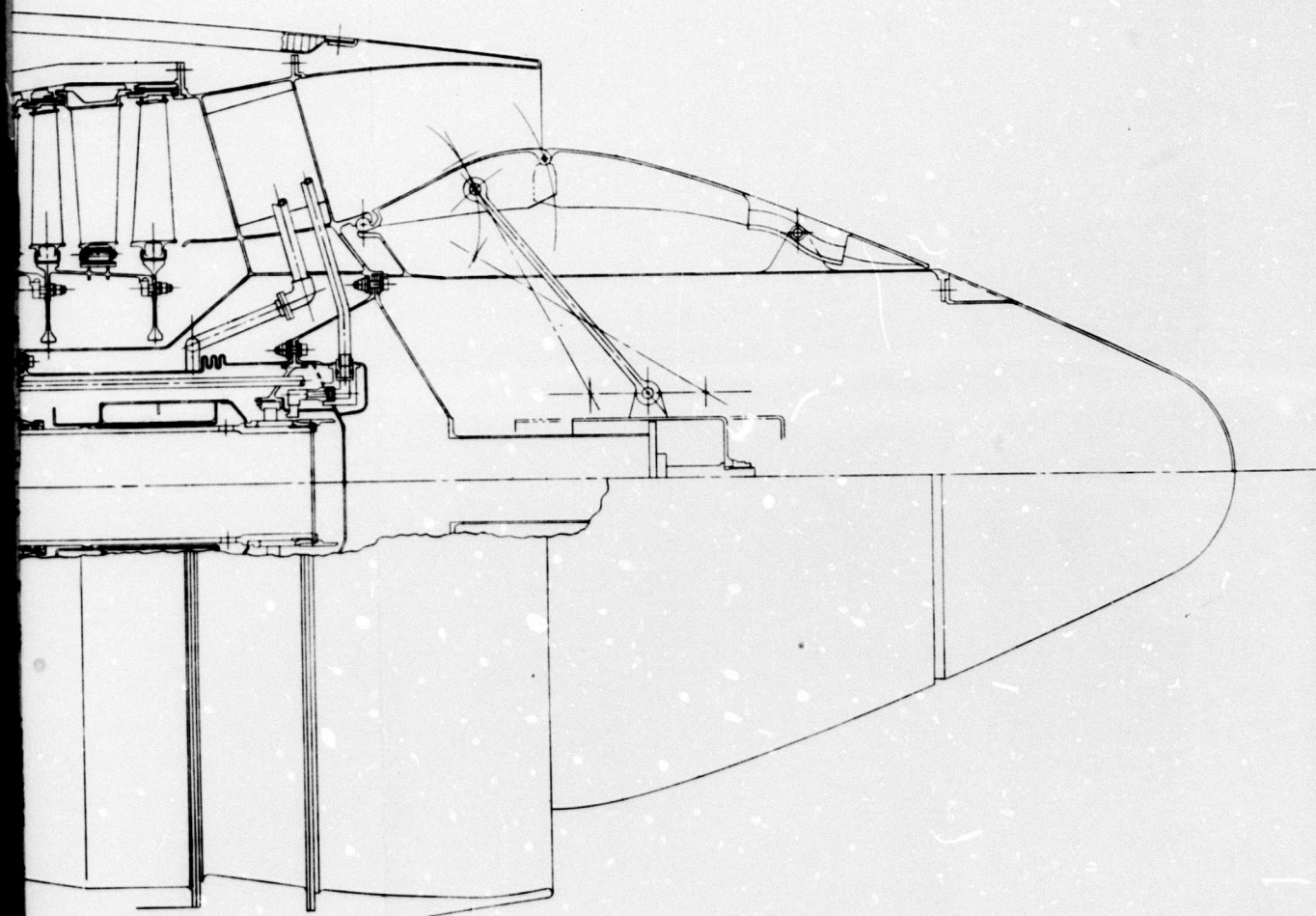
A



B



C



D

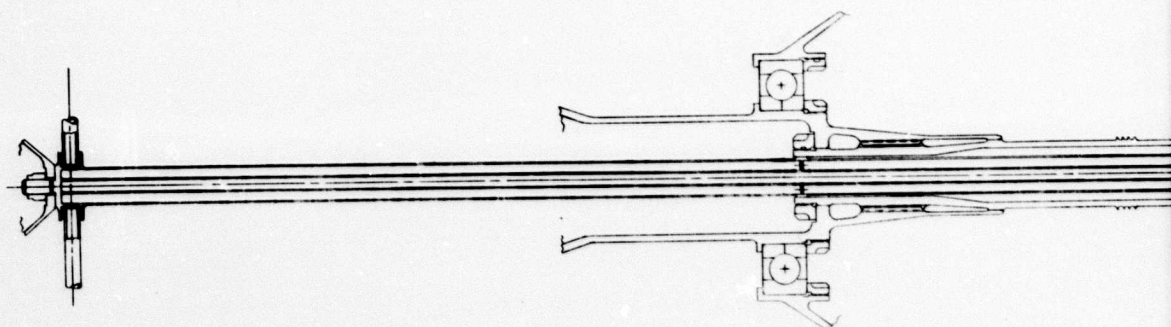


Figure 44. Alternate Method of Pressurizing Actuators.

15

1

14

1

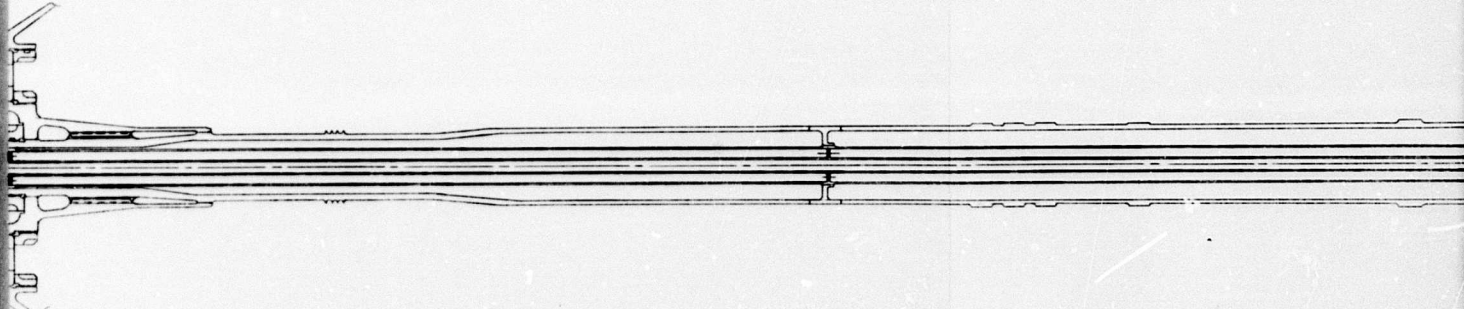
13

12

1

11

10



15

1

14

J 17A106-855 2

13

12

1

11

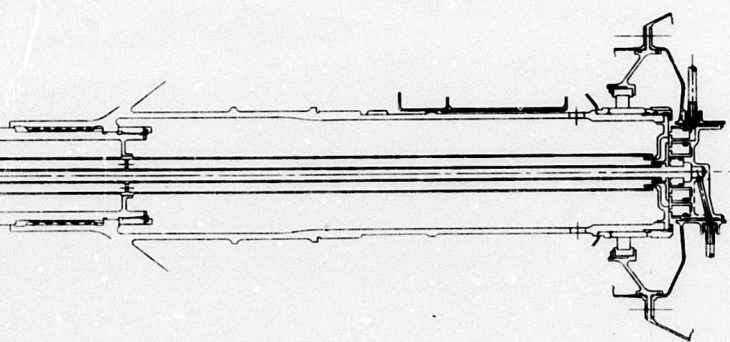
10

1

9

B

1 10 1 9 4 8 1 7 1 6 1 5 1 4



1 10 1 9 4 8 1 7 1

6

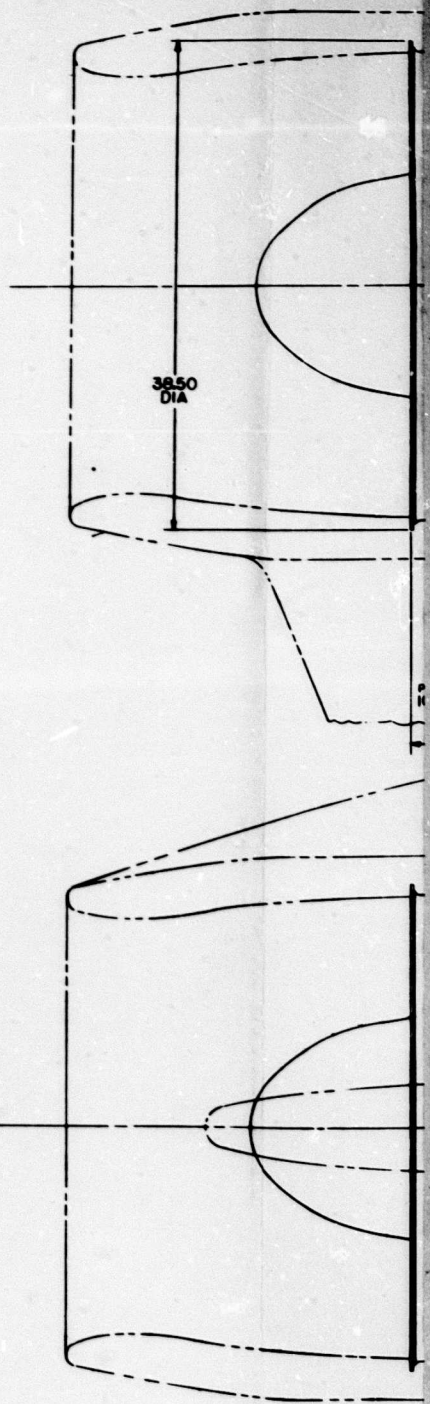
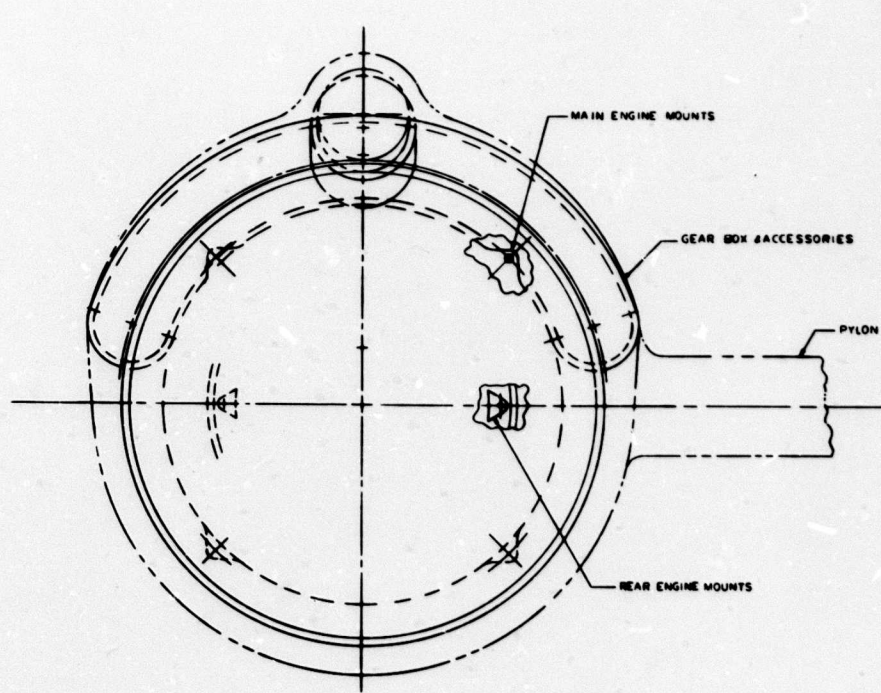
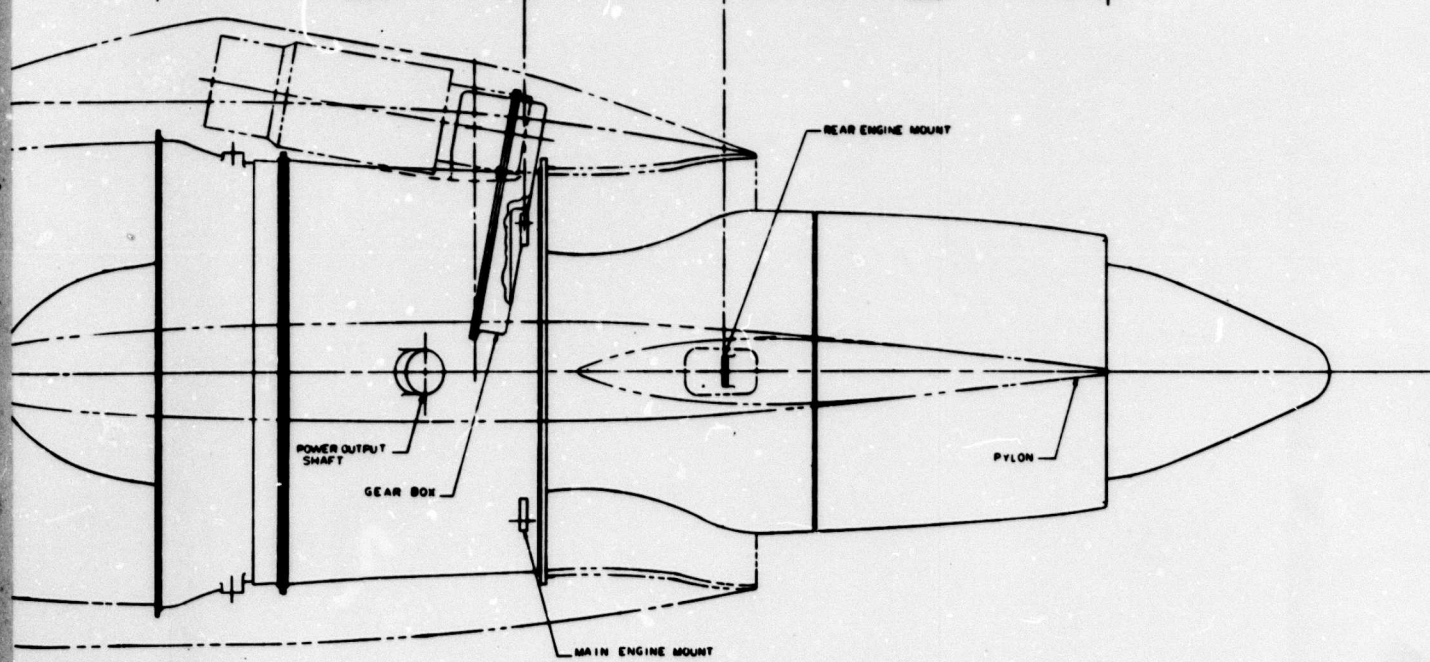
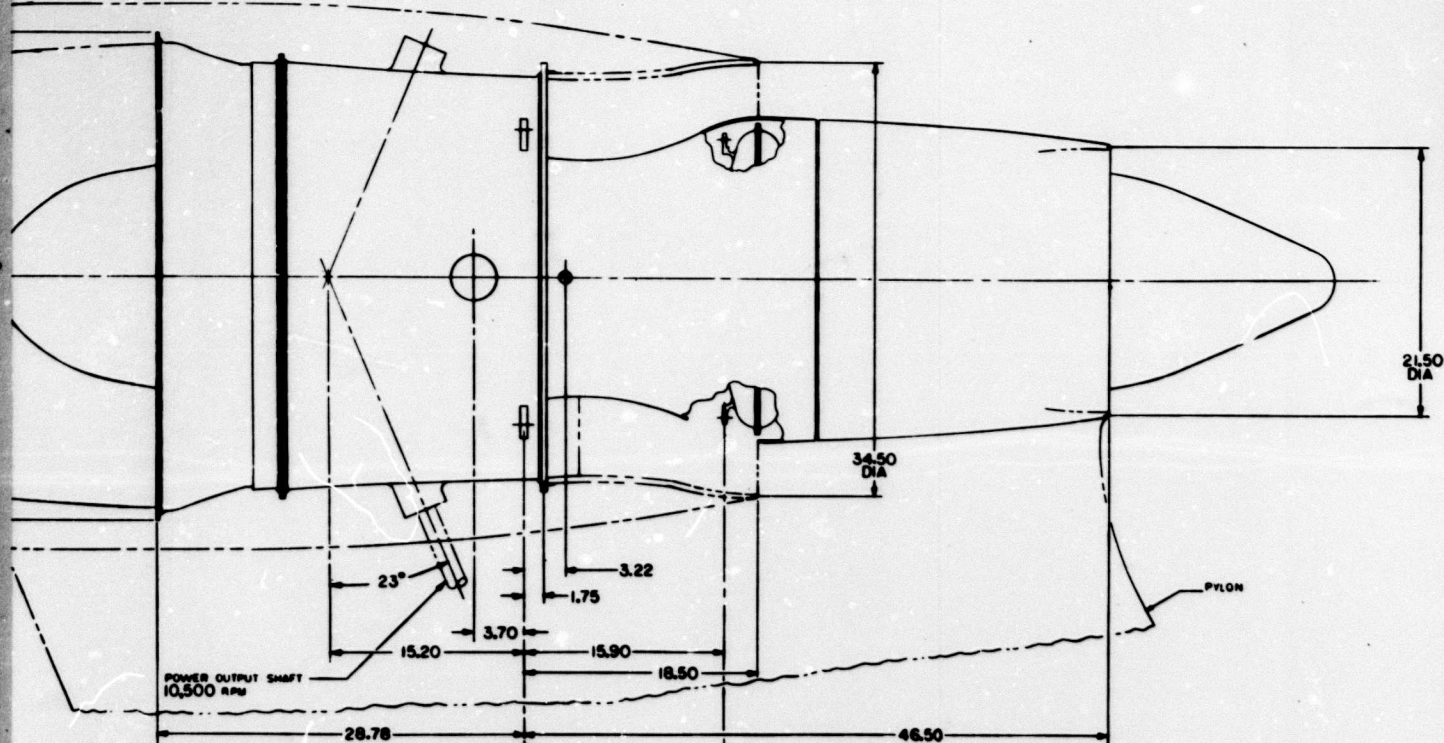


Figure 45. Preliminary Installation Drawing, Geared Engine.



B

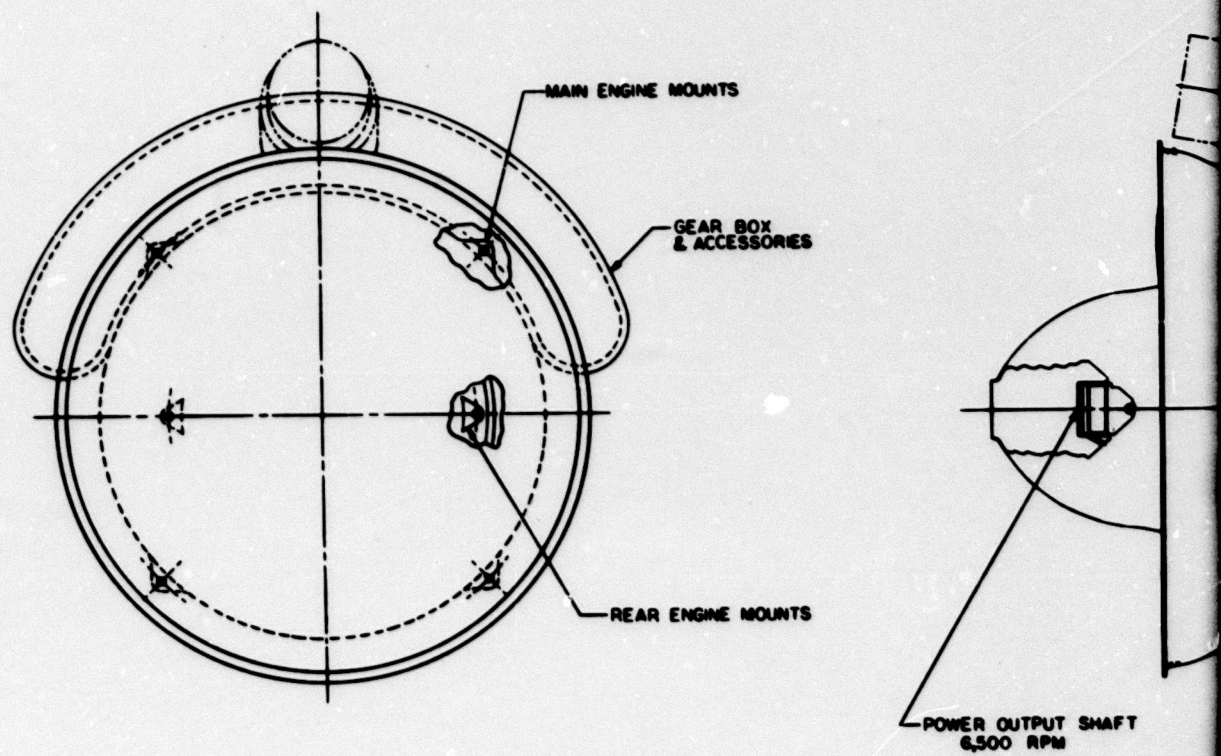
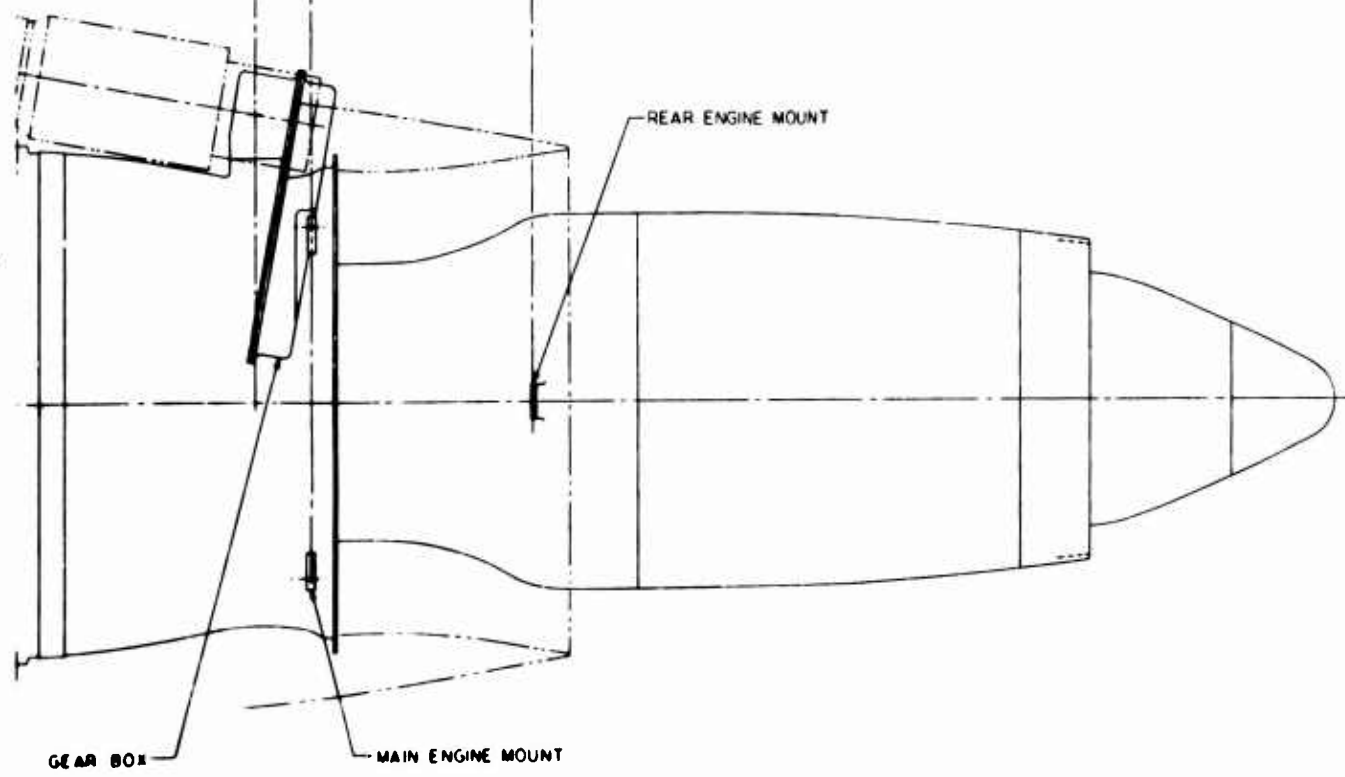
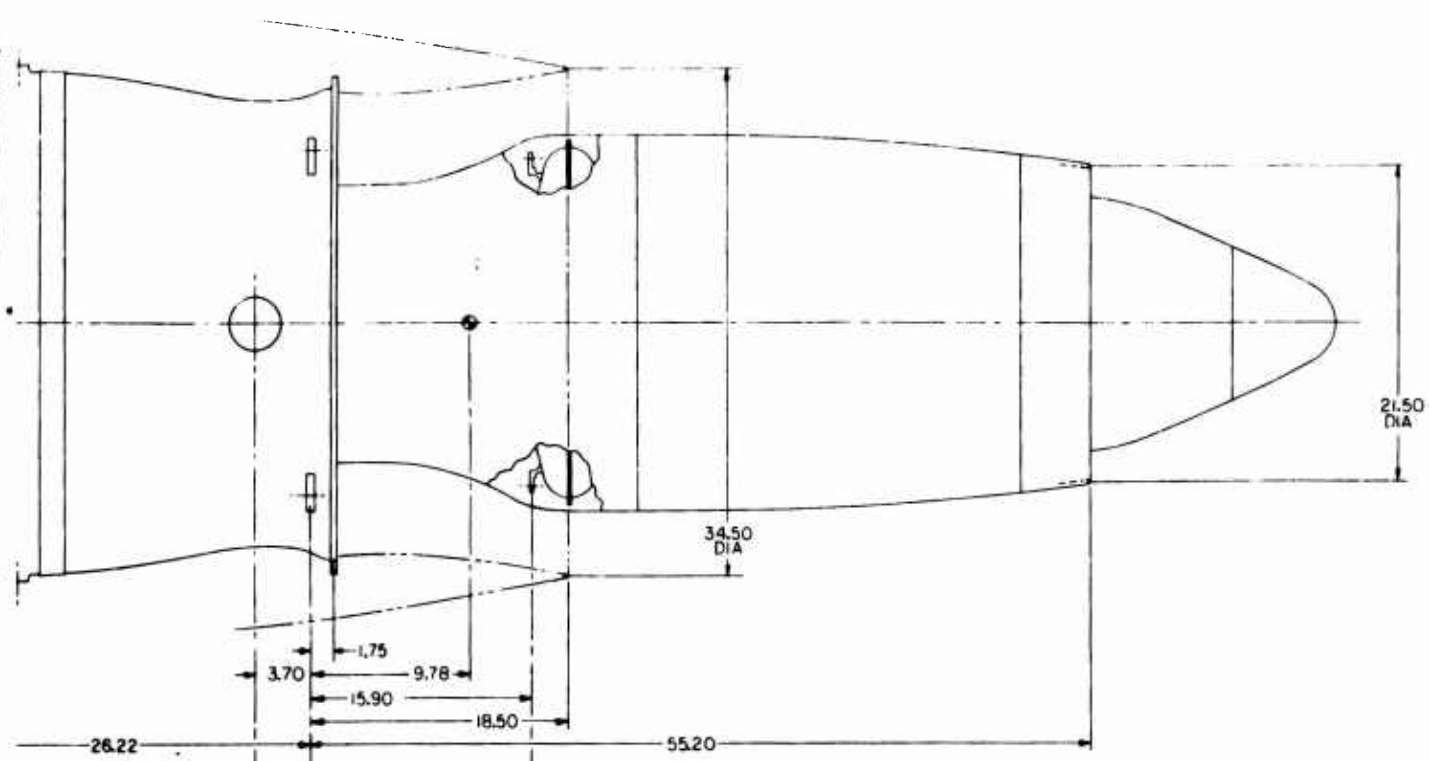


Figure 46. Preliminary Installation Drawing, Ungared Engine.



and increase the area by moving inward to open the slots. Simple hinged flaps are also shown on the inner wall of the fan nozzle to vary this area (A_{2e}). In this case it is desirable to actually spoil any residual thrust, so that again a somewhat crude design is acceptable.

Figures 45 and 46 are preliminary installation drawings for the geared and ungeared engines respectively. Figure 11 shows the shape of a typical inlet duct that is required for the ungeared engine.

Preliminary engine weight estimates have been derived by approximate computation for the parts peculiar to the convertible engine, and by scaling current engine data for the gas generator and power turbine and for the gearbox, controls, and accessories. The weights for the geared engine are tabulated below. The ungeared engine is estimated to be 83 lb lighter

Geared Engine Preliminary Weight Estimate

| | |
|---|----------------|
| Fan Rotor | 152 |
| Fan Stator | 62 |
| Power & Fan Reduction Gearbox | 190 |
| Front Frame | 68 |
| Fan Variable Nozzle | 34 |
| Gas Generator Variable Nozzle | 35 |
| Nacelle | 14 |
| Gas Generator and Power Turbine | 430 |
| External Gearbox, Controls, and Accessories | 190 |
| Total Engine Weight | 1175 lb |

This weight is an estimated weight without margin for growth due to design changes. Appropriate margins are: gas generator and power turbine - 5%, since this weight is based on a very similar, fully detailed design; remainder - 11%, since this is based on a mixture of conventional, but not detail designed, parts and unconventional parts.

Thus, weight for quotation purposes = 1280 lb.

INLET SEPARATION CONSIDERATIONS

The environment of the engine in the shaft mode will often consist of a large sand and/or dust content in the air because of the rotor downwash during vertical flight near the ground. The fan in the shaft mode presents good possibilities for providing a sand/dust separator of the centrifuging type. The essential action of such a separator is to put swirl into the air, causing centrifuging of the solid particles to the outer periphery, to extract the centrifuged particles along with some small amount of air, and, finally, to take out the swirl before passing into the engine.

The fan rotor puts in a large swirl, for instance, the exit stators have to take out about 40° of flow angularity in the shaft mode. It is believed that an efficient separator would result if part of the swirl were left in at the stator exit and removed at the compressor inlet by de-swirl vanes, which would be moved in unison with the variable fan exit stators. In the fan mode, these de-swirl vanes would be inoperative, i.e., axially oriented. The flow through the fan exit duct would retain the swirl. The flow in this duct is at least as much as would be used in an inlet separator scavange duct (about 10% of engine flow), so that good scavenging action could be expected.

It is believed that this possibility of dealing with inlet contamination is to be preferred to schemes which bring the gas generator air in behind the fan, but through an independent separator.

A preliminary trajectory analysis has been performed using a time-shared computer program developed for inlet separator design and using fan aerodynamic data for the minimum pitch mode. The results are shown in Figure 47. It appears from this preliminary data that, provided some residual swirl is left in the fan exit air, excellent separation can be expected. The rotor exit initial condition trajectory line shows that the rotor itself provides good separator action, regardless of stator residual swirl. However, any particles which remain near the hub at the stator station by somehow escaping the rotor centrifugal effect, while exhibiting much less steep radial velocity components, will nevertheless still move clear of the gas generator inlet.

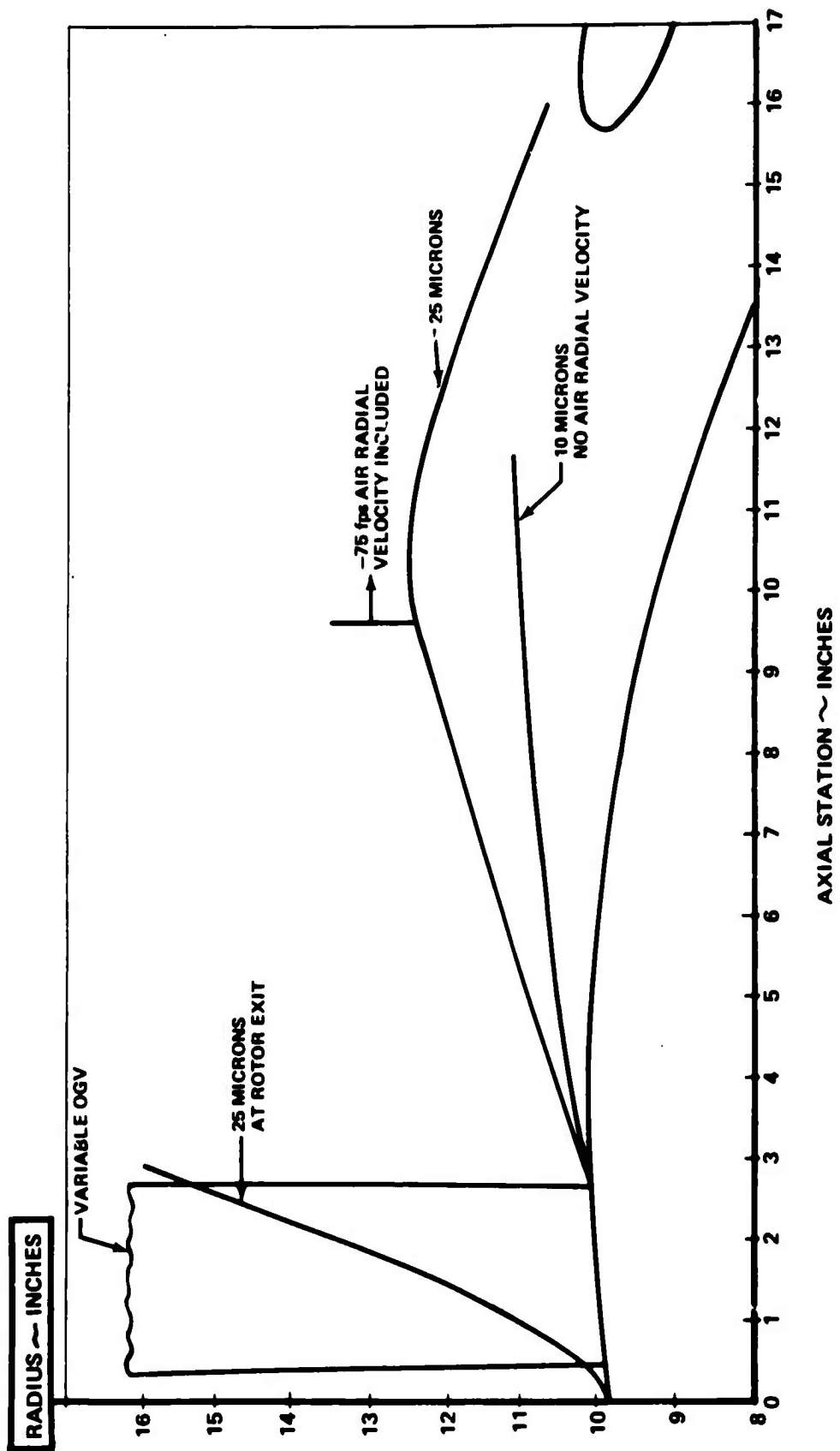


Figure 47. Sand Trajectories in Convertible Engine Fan.

RISK AREAS

The two general areas where risk can be expected are: fan aerodynamics and fan rotor mechanical design.

FAN AERODYNAMICS

The specific risk areas are:

- Accuracy of estimation of parasitic power and flow at minimum pitch.
- Ability of exit stators to cover flow angle change.
- Bypass ratio migration.

Accuracy of estimation of parasitic fan power and flow. The computation of fan power at reduced blade angles has required the adaptation of existing aerodynamic computation procedures to the different conditions of a rigid, twisted blade operating at an angle different from the design value, normally fixed. This adaptation has to take account of reduced flow both generally and locally as regards increasing blockage as the blades approach each other, especially near the tip. It is estimated that the computation procedures used will provide about 2% accuracy on flow and 8 - 10% accuracy in temperature rise prediction. Thus, the overall power prediction variation is expected to be in the order of 5 - 10%. This value appears to be acceptable.

Ability of exit stators to cover flow angle change. The estimated total angle change is $\approx 40^\circ$. This will be divided equally between the movable and fixed stators of the tandem pair. This angle is on the high side and involves some risk as regards incipient flow separation in the shaft mode, as it could affect the gas generator compressor, efficiency of the stators not, of course, being of any importance. A promising approach to minimizing this problem would be to use a nonuniform loading on the fan rotor blade in the radial direction, with pressure ratio reduced near the hub. With such a distribution, the angle-of-attack change near the hub (which is the area of interest from the compressor point of view) would be reduced.

Bypass ratio migration. The important geometric variable influencing risks from bypass ratio migration is spacing ratio, L/H_1 . In the study engine, this ratio is much above average, i. e., favorable. The bypass ratio migration case deemed to contain the most potential risk is that of high gas generator power with the fan in fine pitch, because the amount of migration will be greater than in fixed-pitch fan engines. The available experimental data has been reviewed and potential fixes for any problems have been considered. It is concluded that the risks are only moderate. A fuller discussion will be found under "Cycle Selection".

FAN MECHANICAL DESIGN

Initial consideration resulted in the following potential risk areas:

- Bearing stresses and wear on contact surfaces.
- Frictional loads on blade mechanism.
- Spreading of disks under centrifugal load.
- Aeroelastic stresses in fan blades at reduced pitch.
- Fretting of blade contact points (if any) at reduced pitch.
- Synchronization of blade angles.

After the fan mechanical design has been studied, these areas can be reduced to essentially the first two, which are interrelated. The design criteria for the bearing stresses and the kinematics of the blade mechanism are discussed under "Fan Mechanical Design". The conclusion is that a simple hardware rig test could be used to check the degree of risk involved in these two items before any appreciable amount of effort need be put into any follow-on work on the variable-pitch fan. See "Recommendations" for a description of the suggested test procedure.

CONCLUSIONS

1. An analysis of a convertible fan/shaft engine with variable-pitch fan rotor has been completed, with primary emphasis on fan aerodynamics, fan rotor mechanical design, and engine/control/rotor transition control dynamics.
2. Aerodynamic analysis of the fan shows that the fan power can be reduced to about 400 HP where 3100 HP is available from the low-pressure turbine. A tandem variable/fixed exit stator combination is required to handle the flow angle excursion leaving the rotor.
3. A novel method of fan blade retention which permits blade pitch change and synchronizing has been devised.
4. An engine/control/rotor system has been synthesized which provides satisfactory control and transition mode dynamic behavior.
5. The engine system requires a variable fan exhaust exit area. A variable gas generator exhaust area is desirable for optimum performance.
6. The gas generator is sized by the fan mode for the 400 Kt, sea level, thrust requirements. In addition to the 2000 HP required for the rotary-wing mode takeoff, there is a surplus power of 26% at 80% fan speed and of 44% at 100% fan speed. The greater surplus at 100% speed results from the increased gas generator supercharge and low-pressure turbine power, which more than compensate for the increased fan power required.
7. Although not investigated in detail, a promising method of integrating a centrifugal type sand separator into the fan and fan exit duct of the engine, for shaft mode operation only, has been devised.

RECOMMENDATIONS

In future work on this concept, the following areas requiring more detailed investigation were revealed by the subject study:

1. A simple rig test could be used to assess the probable characteristics of the variable-pitch mechanism. (See separate description below.)
2. A re-programming of the fan aerodynamic computation logic is required. This new program would be designed to handle variable-pitch fan aerodynamic design computations efficiently and avoid the problems which arose when using a fixed-pitch fan computer program.
3. Availability of this computer capability would permit a more refined engine performance optimization to be carried out. For instance, the best choice of shaft mode fan pressure ratio (controlled by exhaust area since fan speed is constant) and flow for shaft power optimization should be determined. Further investigation of fan/gas generator flow matching should also be made, once recommendation 2 above has been implemented, together with a more favorable radial pressure distribution in the fan.
4. Various sequences and combinations of transition mode control inputs should be tried, using the already developed Dynasar-type dynamic simulation. This work should be done in collaboration with airframe contractors.

SUGGESTED TEST OF VARIABLE PITCH PRINCIPLE

Simulated testing of the rolling motion between the blade bearing plate and the disk would be desirable to provide information that would facilitate development of the fan rotor. Figure 48 is a sketch of a simple rig for such testing. Two double-taper roller bearings are mounted with their axes horizontal in a housing to simulate the freedom for rotation between disks. Special inserts placed at the bottom of the inner races simulate the disk bearing surfaces. They are held in position by the corresponding bearing plate, which is loaded from below through a vertical spindle. The load is provided by tension in a loaded cable, which is torsionally flexible. Rotation of the spindle about its axis simulates actuation of the blade. The torque required to rotate the spindle may be corrected by the torque required to rotate the bearings to determine the friction on the loaded surfaces. The torque required to rotate the bearings may be established by measuring the bearing friction independently. The value of a horizontal load applied to the spindle to cause both roller bearings to rotate in the same direction, without any rotation of the spindle, is a measure of bearing friction.

The testing would be aimed at selecting a suitable combination of materials and coatings for the contacting surfaces and the optimum design contact stress to avoid excessive wear and friction. Although the relative motion is predominantly rolling, rotation about the point of contact produces some sliding which may cause "galling" wear with repeated cycles. The amount of sliding depends on the design contact stress which determines the diameter of the area in contact. Hence the design stress selected may affect both wear and friction.

The nickel alloy disk would be preoxidized; a thin, tight layer of oxide acts as a barrier to pressure bonding, which is the cause of "galling" wear. The bearing plate would be of L605, a cobalt-based alloy, and also would be preoxidized. Both surfaces would be coated with a dry film lubricant such as molybdenum disulphide or tungsten diselenide. Should the feasibility of eliminating the bearing plates from the titanium blade be indicated, a titanium plate with a plasma coat of copper-nickel-indium alloy, developed by General Electric to minimize fretting on titanium mating surfaces, would be tried.

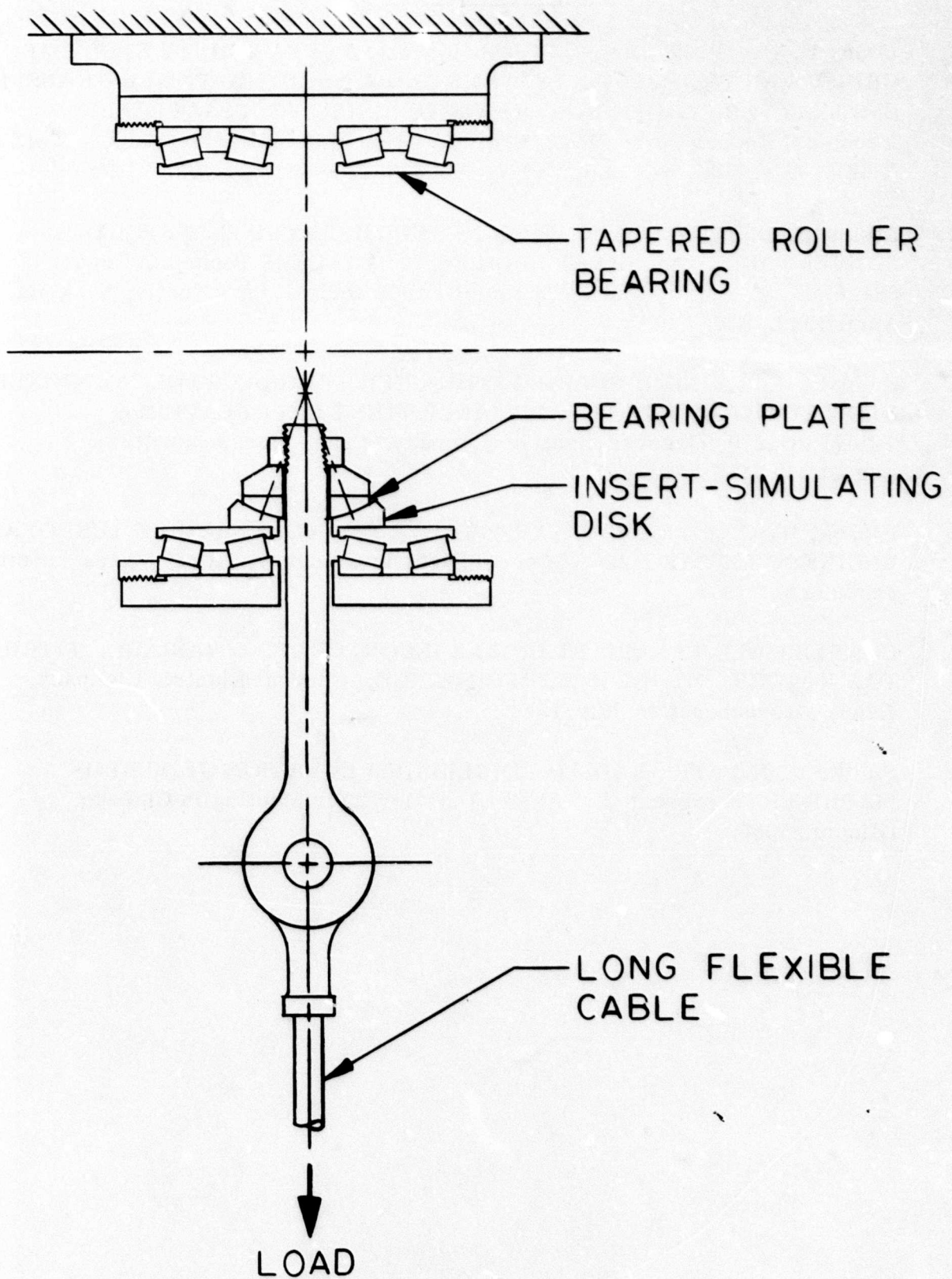


Figure 48. Rig Test, Pitch Mechanism.

LITERATURE CITED

1. **Dean, F. H., Preger, P. C., Schneider, J. J., FEASIBILITY STUDY OF CRUISE FAN PROPULSION SYSTEMS AND ASSOCIATED POWER TRANSFER SYSTEMS FOR COMPOUND COMPOSITE AIRCRAFT, USAAVLABS Technical Report 67-28, U. S. Army Aviation Materiel Laboratories, Fort Eustis, Virginia, September 1967, AD663831.**
2. **Atkinson, R. P., Raymond, C. C., PRELIMINARY DESIGN STUDY OF CONVERTIBLE FAN/SHAFT ENGINES; USAAVLABS Technical Report 68-26, U. S. Army Aviation Materiel Laboratories, Fort Eustis, Virginia, April 1968, AD673148.**
3. **Randall, J. R., TIME-SHARING COMPUTER PROGRAMS FOR NON-MIXED FLOW FORWARD FAN PERFORMANCE POINT CALCULATIONS; TM67FPD1579, General Electric Company, Lynn, Massachusetts, August 31, 1967.**
4. **Hickok, R. C., FEASIBILITY STUDY OF TWO CONVERTIBLE TURBOFAN ENGINES; TM68AEG1426, General Electric Company, Lynn, Massachusetts, January 25, 1968.**
5. **CONVERTIBLE FAN/SHAFT ENGINE INCORPORATING VARIABLE PITCH FAN ROTORS, PLAN FOR PERFORMANCE; General Electric Company, Lynn, Massachusetts, July 1968.**
6. **Smith, L. H., THE RADIAL-EQUILIBRIUM EQUATION OF TURBO-MACHINERY; presented at ASME Annual Winter Meeting in Chicago, Illinois, 1965.**

APPENDIX
CONVERTIBLE FAN ENGINE
PRELIMINARY PERFORMANCE BULLETIN

| Mode | Alt Shaft | Mach No. or Vel | Amb Temp | 'SHP G | SFC G | T ₄ | T ₈ | P ₈ |
|------|--------------|--------------------|-------------|--------|--------|----------------|----------------|----------------|
| | 0 | 0 | 59° F | 3713 • | 506 | 2620 | 1396 | 17.2 |
| | | | | 2853 | 519 | 2400 | 1285 | 16.6 |
| | | | | 2152 | 558 | 2250 | 1222 | 16.2 |
| | | | | 1500 | 636 | 2100 | 1166 | 15.8 |
| | | | | 3884 • | 504 | 2657 | 1416 | 17.3 |
| | | | | 2886 | 516 | 2400 | 1284 | 16.6 |
| | | | | 2180 | 553 | 2250 | 1221 | 16.2 |
| | | | | 1522 | 630 | 2100 | 1165 | 15.8 |
| | | | | 4043 • | 502 | 2692 | 1434 | 17.4 |
| | | | | 2918 | 513 | 2400 | 1283 | 16.6 |
| | | | | 2208 | 549 | 2250 | 1220 | 16.2 |
| | | | | 1543 | 624 | 2100 | 1164 | 15.8 |
| | | | | 4089 | 502 | 2700 | 1439 | 17.5 |
| | | | | 2927 | 512 | 2400 | 1283 | 16.6 |
| | | | | 2216 | 547 | 2250 | 1219 | 16.2 |
| | | | | 1550 | 632 | 2100 | 1163 | 15.8 |
| | | | | 4105 | 501 | 2700 | 1439 | 17.5 |
| | | | | 2938 | 511 | 2400 | 1282 | 16.7 |
| | | | | 2225 | 546 | 2250 | 1219 | 16.2 |
| | | | | 1556 | 620 | 2100 | 1163 | 15.9 |
| | | | | 4116 | 485 | 2700 | 1432 | 17.7 |
| | | | | 3133 | 492 | 2400 | 1276 | 16.6 |
| | | | | 2394 | 521 | 2250 | 1212 | 16.3 |
| | | | | 1685 | 586 | 2100 | 1156 | 15.9 |
| | | | | 3383 • | 516 | 2687 | 1386 | 17.1 |
| | | | | 3435 • | 516 | 2674 | 1455 | 16.9 |
| | | | | 0 | 103° F | | | |
| | | | | | 95° F | | | |

| Mode | Alt | Mach No. or Vel | Amb Temp | FN_G/SHP_G | SFC _G | T ₄ | T ₈ | P ₈ |
|-------|------|--------------------|-------------|--------------|------------------|----------------|----------------|----------------|
| Shaft | 4000 | 0 | 95° F | 2936.0 | 516 | 2675 | 1445 | 14.6 |
| | 6000 | 0 | 95° F | 2751.0 | 517 | 2676 | 1447 | 13.6 |
| | | | | 2528 | 520 | 2600 | 1407 | 13.4 |
| | | | | 2154 | 537 | 2500 | 1360 | 13.2 |
| | | | | 1802 | 561 | 2400 | 1318 | 13.0 |
| | | | | 1628 | 578 | 2350 | 1298 | 12.9 |
| | | | | 2549 | 518 | 2678 | 1447 | 12.5 |
| | | | | 2769 | 499 | 2567 | 1352 | 12.0 |
| | | | | 2764 | 499 | 2564 | 1350 | 12.0 |
| | | | | 2729 | 499 | 2550 | 1342 | 12.0 |
| | | | | 2422 | 501 | 2587 | 1358 | 10.2 |
| | | | | 2365 | 498 | 2550 | 1336 | 10.0 |
| | | | | 1868 | 497 | 2299 | 1204 | 9.6 |
| | | | | 100 | 59° F | 395 | 2700 | 1456 |
| | | | | | 5639 | | | 20.7 |
| | | | | | 5261 | 382 | 2600 | 1403 |
| | | | | | 4210 | 366 | 2400 | 1310 |
| | | | | | 34: | 359 | 2250 | 1249 |
| | | | | | 274 | 356 | 2100 | 1191 |
| | | | | | 4519 | 500 | 2700 | 1454 |
| | | | | | 4168 | 489 | 2600 | 1400 |
| | | | | | 3232 | 482 | 2400 | 1308 |
| | | | | | 2564 | 497 | 2250 | 1247 |
| | | | | | 1975 | 500 | 2100 | 1168 |
| | | | | | 4459 | 508 | 2700 | 1453 |
| | | | | | 4109 | 497 | 2600 | 1400 |
| | | | | | 3178 | 491 | 2400 | 1307 |
| | | | | | 2517 | 497 | 2250 | 1246 |
| | | | | | 1933 | 512 | 2100 | 1187 |

| Mode | A!! or Vel | Mach No. | Amb Temp | FN _G /SHP _G | SFC _G | T ₄ | T ₃ | P ₈ |
|------------|---------------|----------|-------------|-----------------------------------|------------------|----------------|----------------|----------------|
| Fan | 0 | 160 Kts | 59° F | 4401 | .516 | 2700 | 1453 | 21.0 |
| | | 4051 | | .505 | 2600 | 1400 | 20.3 | |
| | | 3125 | | .500 | 2400 | 1307 | 18.6 | |
| | | 2470 | | .507 | 2250 | 1246 | 17.6 | |
| | | 3500 | | .711 | 2700 | 1442 | 22.6 | |
| | | 2774 | | .699 | 2700 | 1433 | 16.8 | |
| | | 2568 | | .685 | 2600 | 1376 | 16.1 | |
| | | 1966 | | .691 | 2400 | 1274 | 14.3 | |
| | | 1516 | | .719 | 2250 | 1205 | 13.2 | |
| | | 1121 | | .770 | 2100 | 1141 | 12.4 | |
| | | 1867 | | .671 | 2550 | 1341 | 11.3 | |
| | | 1662 | | .652 | 2400 | 1257 | 10.5 | |
| | | 1327 | | .661 | 2250 | 1185 | 9.6 | |
| | | 1004 | | .694 | 2100 | 1117 | 8.8 | |
| | | 1229 | | .676 | 2400 | 1250 | 7.7 | |
| | | 20000 | 6 | | | | | |
| | | 30000 | 400 Kts | | | | | |
| Transition | 0 | 140 Kts | 59° F | 3785 | .580 | 2700 | 1461 | 20.5 |
| | | 3363 | | .587 | 2600 | 1410 | 19.8 | |
| | | 2428 | | .631 | 2400 | 1318 | 18.4 | |
| | | 1673 | | .734 | 2250 | 1262 | 17.5 | |
| | | 888 | | 1.091 | 2100 | 1219 | 16.8 | |
| | | 3734 | | .589 | 2700 | 1461 | 20.6 | |
| | | 3314 | | .597 | 2600 | 1410 | 19.9 | |
| | | 2363 | | .644 | 2400 | 1317 | 18.4 | |
| | | 1640 | | .750 | 2250 | 1262 | 17.5 | |
| | | 876 | | 1.107 | 2100 | 1218 | 16.8 | |

| Mode | A ₁₁ | A ₁₁ or V _d | Mach No. | Amb Temp | R _N _G /SHP _G | sFC _G | T ₄ | T ₈ | T ₉ | P ₈ |
|-------------|-----------------|--------------------------------------|----------|-------------|---|------------------|----------------|----------------|----------------|----------------|
| Transitions | 0 | 160 kts | 59° F | | 3695 | 598 | 2700 | 1460 | 20.6 | |
| | | | | | 3267 | 607 | 2800 | 1460 | 19.9 | |
| | | | | | 2940 | 658 | 2400 | 1317 | 18.4 | |
| | | | | | 1907 | 766 | 2250 | 1261 | 17.5 | |
| | | | | | 986 | 1123 | 2100 | 1216 | 16.6 | |

- Operation at these conditions was limited by fan inlet flow rather than by maximum T₄ due to the selected blade closure. This could be altered in a follow-on study by varying A₂₈, which controls the fan operating line. At this time, insufficient off-design characteristics are available to permit extensive migration on the fan map. Little change in staff mode performance is expected to result from this fan map modification.

Unclassified

Security Classification

DOCUMENT CONTROL DATA - R & D

(Security classification of title, body of abstract and indexing annotation must be entered when the overall report is classified)

| | | |
|---|--|--|
| 1. ORIGINATING ACTIVITY (Corporate author) General Electric Company 1000 Western Avenue West Lynn, Massachusetts 01905 | | 2a. REPORT SECURITY CLASSIFICATION Unclassified |
| 3. REPORT TITLE CONVERTIBLE FAN/SHAFT ENGINES INCORPORATING VARIABLE-PITCH FAN ROTORS | | 2b. GROUP N/A |
| 4. DESCRIPTIVE NOTES (Type of report and inclusive dates) Final Report | | |
| 5. AUTHOR(S) (First name, middle initial, last name) Denis P. Edkins | | |
| 6. REPORT DATE June 1969 | 7a. TOTAL NO. OF PAGES 116 | 7b. NO. OF REFS 6 |
| 8a. CONTRACT OR GRANT NO. DAA J02-68-C-0054 | 9a. ORIGINATOR'S REPORT NUMBER(S) USAABLabs Technical Report 69-36 | |
| 8b. PROJECT NO. c. Task IG162203D14415 | 9b. OTHER REPORT NO(S) (Any other numbers that may be assigned this report) -- | |
| 10. DISTRIBUTION STATEMENT This document is subject to special export controls and each transmittal to foreign governments or foreign nationals may be made only with prior approval of US Army Aviation Materiel Laboratories, Fort Eustis, Virginia 23604. | | |
| 11. SUPPLEMENTARY NOTES None | 12. SPONSORING MILITARY ACTIVITY U. S. Army Aviation Materiel Laboratories Fort Eustis, Virginia | |
| 13. ABSTRACT This report presents the results of an analytic study of a convertible turbofan/turboshaft engine embodying a variable-pitch fan rotor. By moving the fan blades into minimum pitch, their power absorption is reduced to about 15% of the power available from the low pressure turbine; thus, the remaining power is available as external shaft power. The engine was sized to produce 3500 lb thrust at 400 knots S. L. and then had 50% excess power over the requirement for 2000 HP at 95°F 6000 ft altitude. The bypass ratio changed from 5.5 in the fan mode to approximately 0.1 in the shaft mode. Variable gas generator and fan exhaust nozzle areas were required to optimize performance. A preliminary dynamic analysis of representative engine/control/rotary-wing systems was made and indicated satisfactory control characteristics. Two preliminary design engine configurations were studied, one with a shaft drive emerging from the side of the engine and the other with front or rear direct drive. A novel method of variable-pitch fan blade attachment was devised. Estimated performance and weight of the engine are presented. (1) ↘ | | |

DD FORM 1473
1 NOV 66

REPLACES DD FORM 1473, 1 JAN 64, WHICH IS
OBsolete FOR ARMY USE.

Unclassified

Security Classification

Unclassified

Security Classification

| 14. KEY WORDS | LINK A | | LINK B | | LINK C | |
|--|--------|----|--------|----|--------|----|
| | ROLE | WT | ROLE | WT | ROLE | WT |
| Composite Convertible Fan/Shaft Helicopter Rotary Wing Variable-Pitch VTOL | | | | | | |

Unclassified

Security Classification